

# NEUR 608: NEUROIMAGING DATA SCIENCE

BORIS BERNHARDT, PHD

MONTREAL NEUROLOGICAL INSTITUTE

MCGILL UNIVERSITY

<http://mica-mni.github.io>

 @BorisBernhardt

## LAST WEEK RECAP: FINAL PAPER

START THINKING ABOUT IT NOW

DISCUSS YOUR IDEAS WITH YOUR COLLEAGUES AND WITH US

PREPARE YOUR PAPER DRAFT (~10 PAGES)

SUBMIT THE FULL VERSION BY MONDAY OCTOBER 26TH

WE GIVE FEEDBACK BY FRIDAY NOVEMBER 6TH

SUBMIT THE FINAL VERSION MONDAY NOVEMBER 20TH

PRESENTATION AND DISCUSSION OF THE WORK ON LAST DAY OF CLASS  
(NOV. 27TH: 8 MINS TALK + 4 MINS QUESTIONS)

# GRADING

CLASS ATTENDANCE (EMAIL US IF YOU CANNOT MAKE IT)

SUMMARY ASSIGNMENTS

PARTICIPATION

RESEARCH PAPER

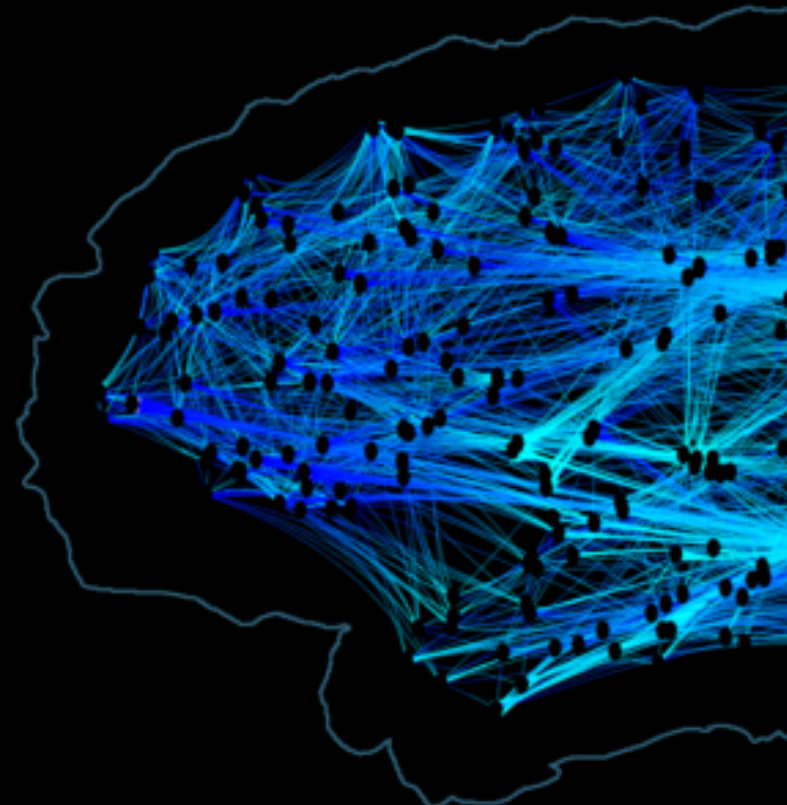
PRESENTATION

# MATERIALS

WE WILL EMAIL AROUND CHANGES AT LEAST ONE WEEK  
AHEAD OF THE NEXT CLASS

PAPERS + SLIDES WILL BE ON GITHUB  
<https://github.com/neuroimagingdatascience/Fall2020>

OPTIONAL REVIEWS  
COMPLEMENT THE RESEARCH ARTICLES



## WEEK 02: IN VIVO CONNECTOMICS

BORIS BERNHARDT, PHD

MONTREAL NEUROLOGICAL INSTITUTE

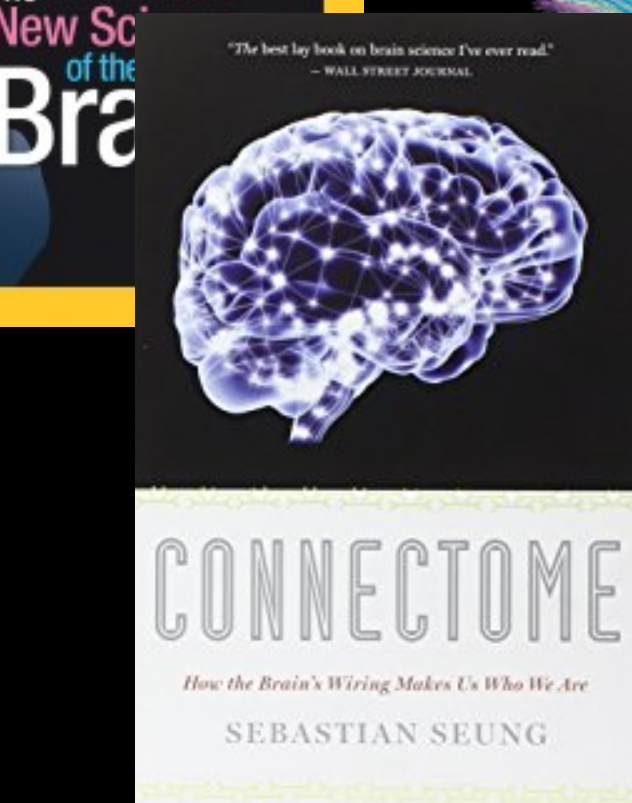
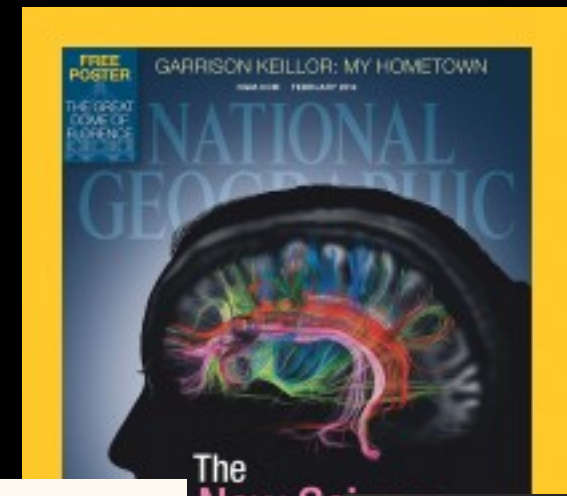
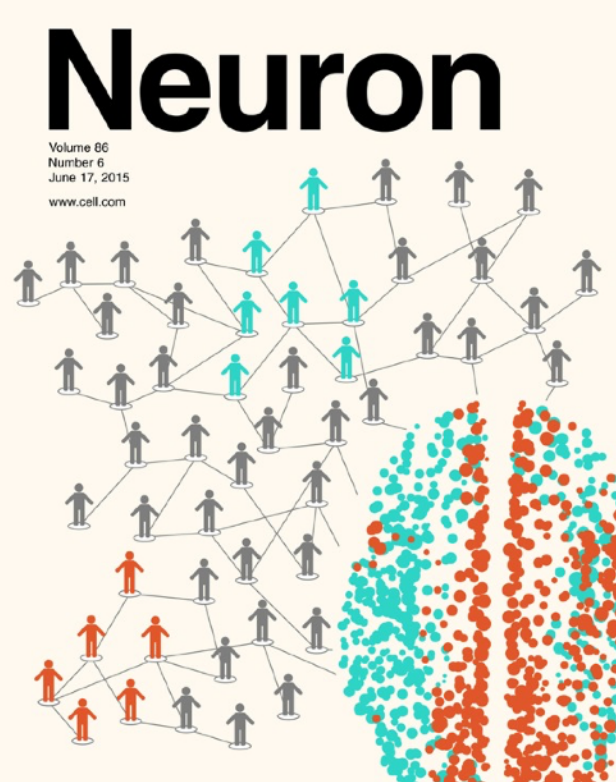
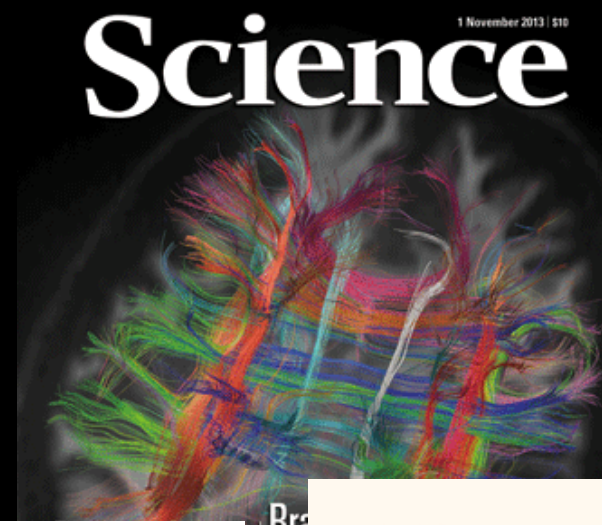
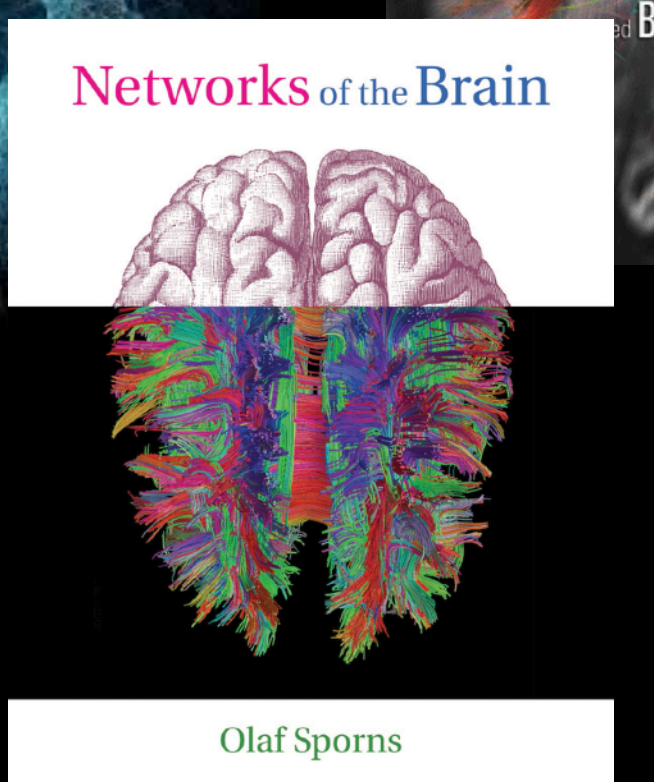
MCGILL UNIVERSITY

<http://mica-mni.github.io>

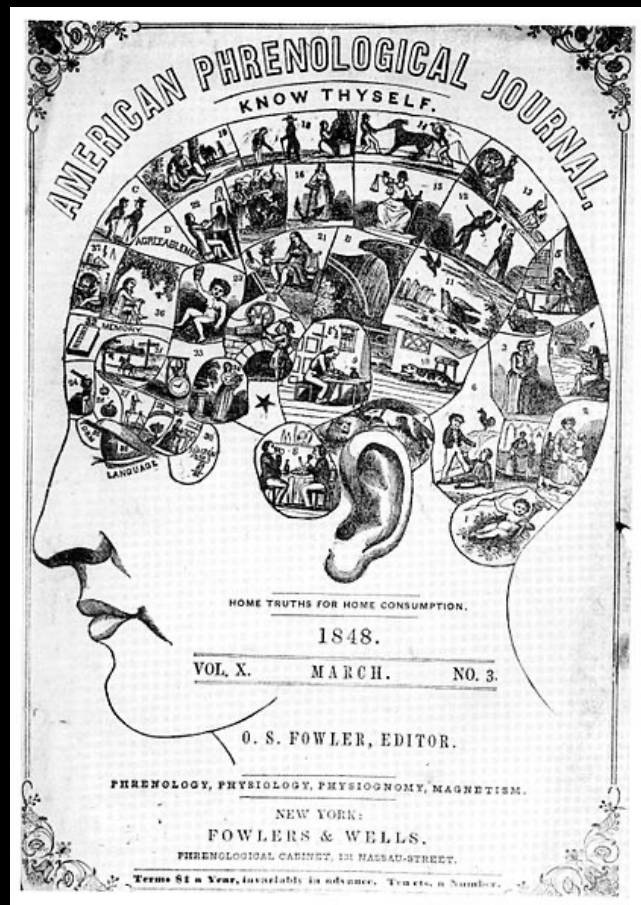
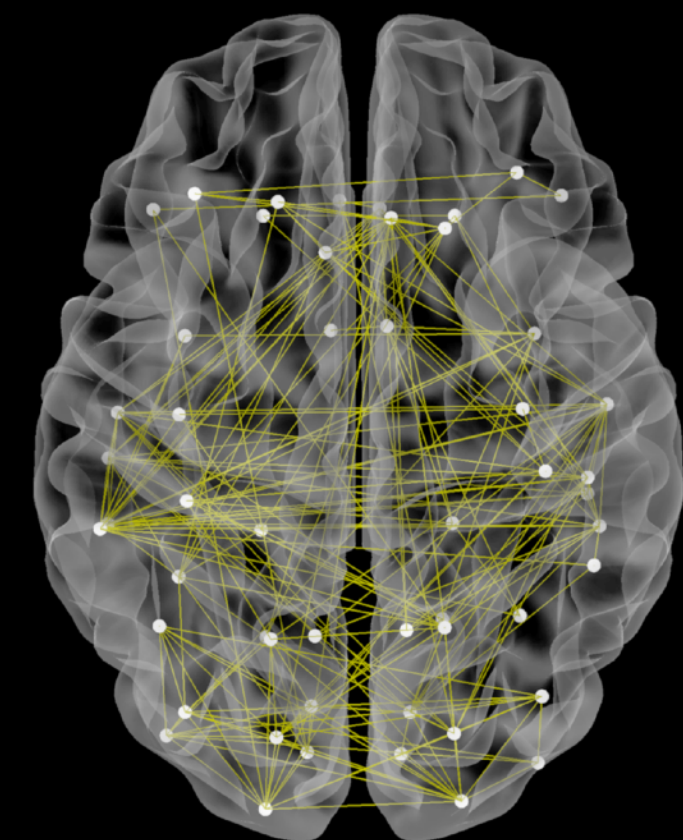
 @BorisBernhardt



# THE PREMISE

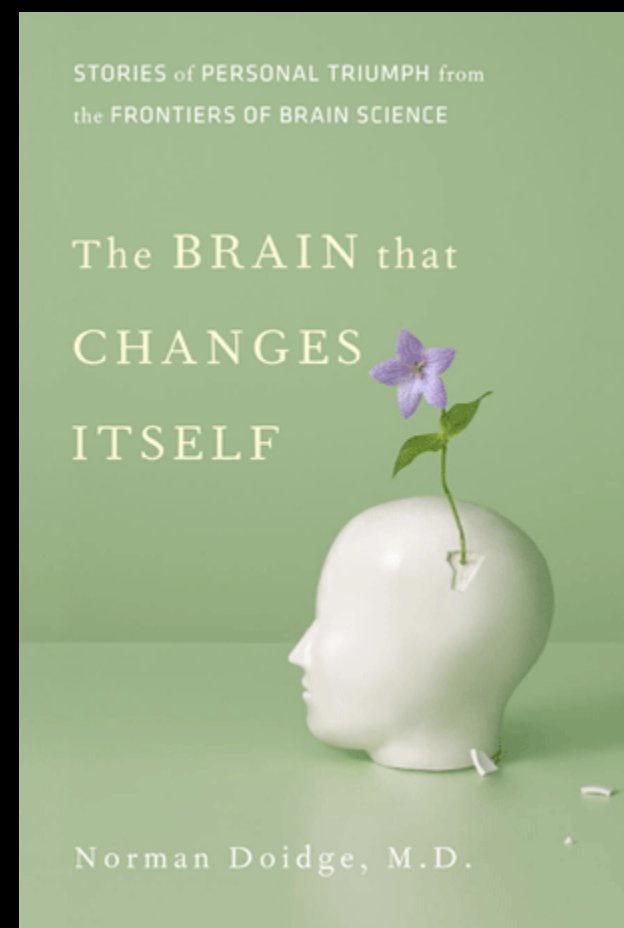


# THE PREMISE

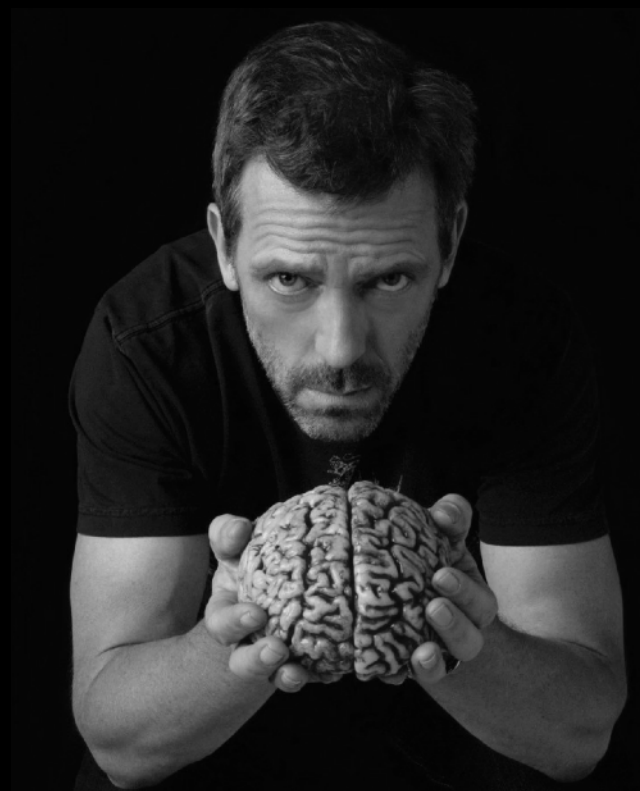


BRAIN ORGANIZATION

INDIVIDUAL DIFFERENCES



PLASTICITY



BRAIN DISORDERS

CONNECTIVITY

# (ANIMAL) CONNECTIVITY

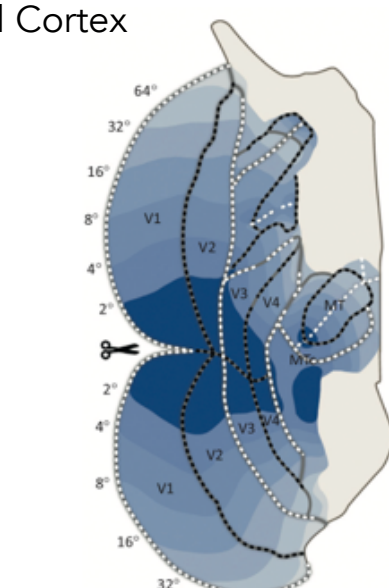
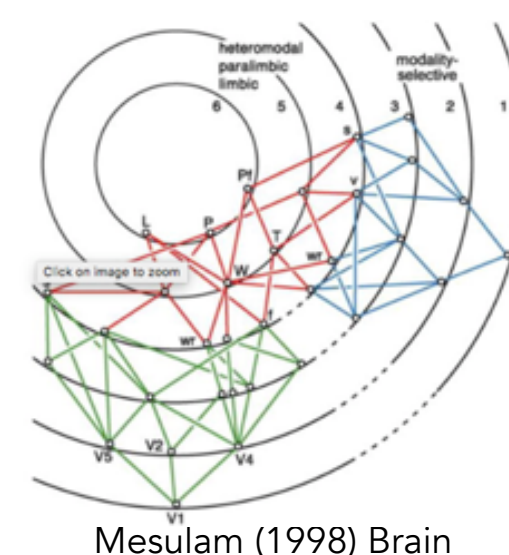
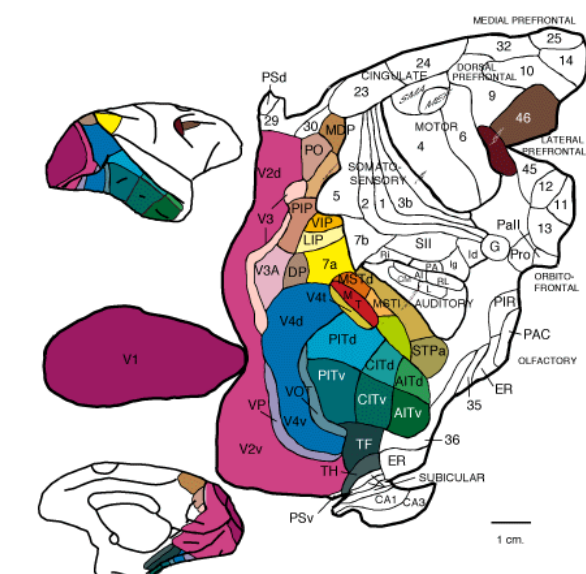
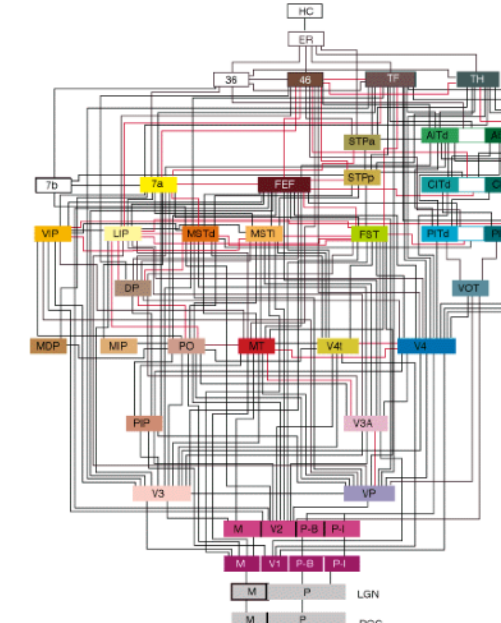
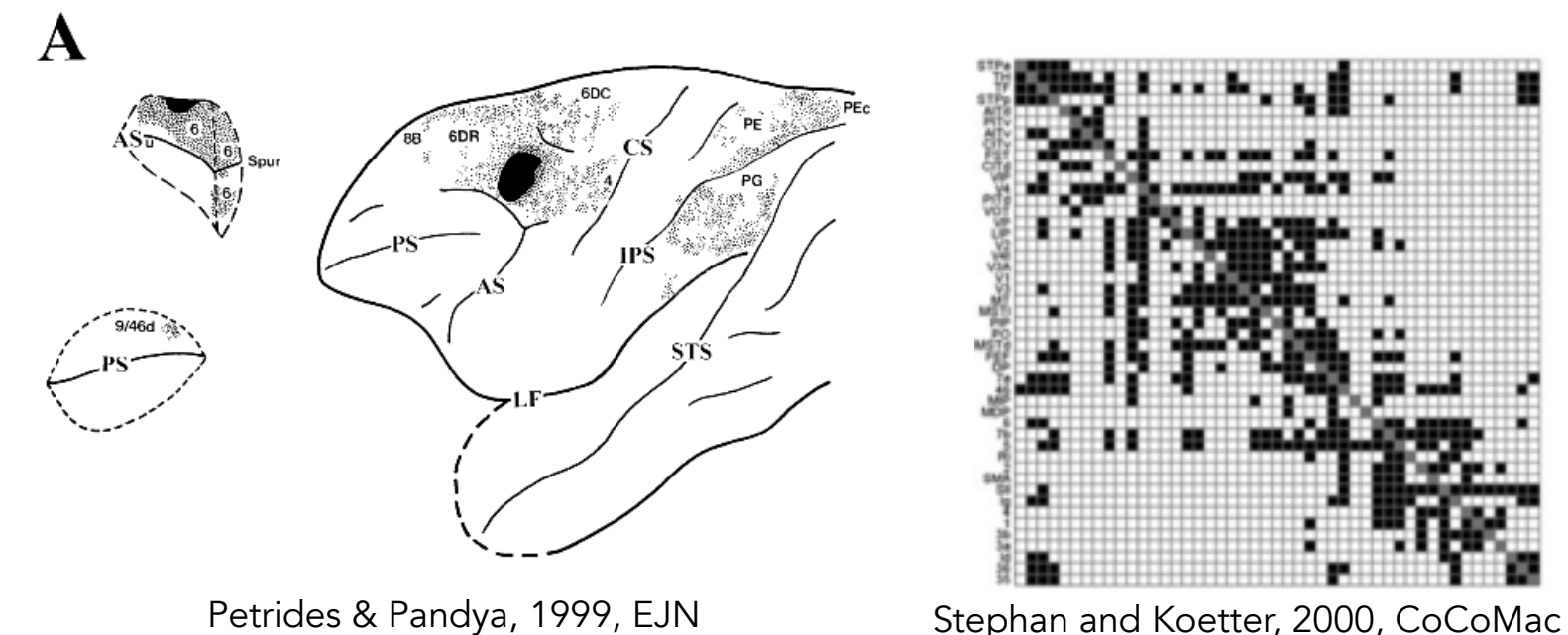
## ANATOMICAL CONNECTIONS: THE WIRING BETWEEN REGIONS

## CLASSICALLY DERIVED FROM TRACT-TRACER STUDIES

## INVASIVE: ONLY IN ANIMALS

#### **LABORIOUS & TIME CONSUMING**

# ACROSS SUBJECT AVERAGING AND ANATOMICAL CORRESPONDENCE ASSESSMENT CHALLENGING



Mesulam (1998) Brain

Rosa 2002 Braz J Med Biol Res

## HUMAN IN-VIVO CONNECTIVITY

MRI KEY MODALITY  
TO APPROXIMATE BRAIN CONNECTIVITY

NON-INVASIVE

HIGH-RESOLUTION

WHOLE-BRAIN

3-DIMENSIONAL

FUNCTIONAL & STRUCTURAL CONNECTIVITY



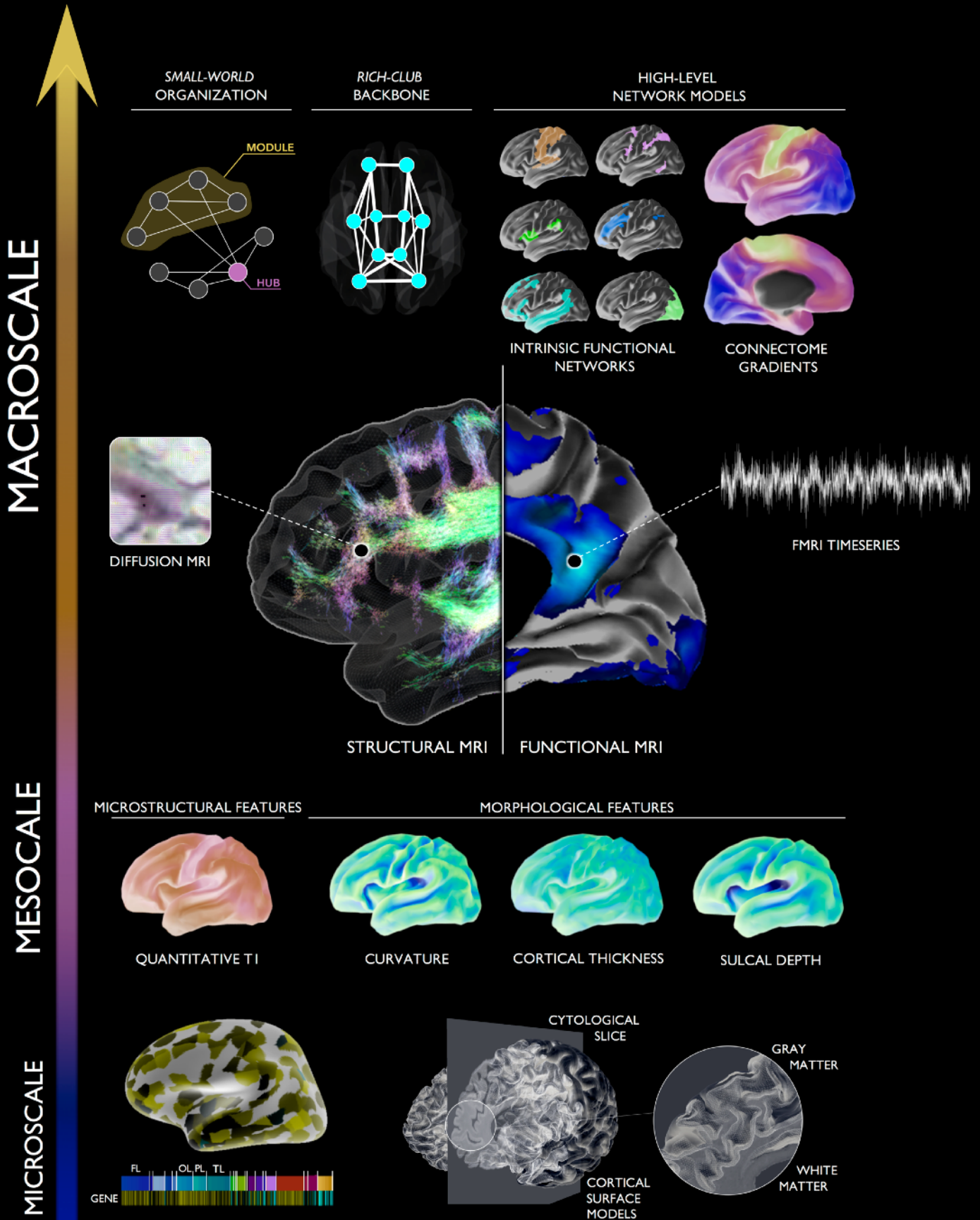
# CONNECTIVITY AT MULTIPLE SCALES

FUNCTIONAL  
CONNECTIVITY

WHITE MATTER  
CONNECTIVITY

MORPHOLOGICAL  
COORDINATION

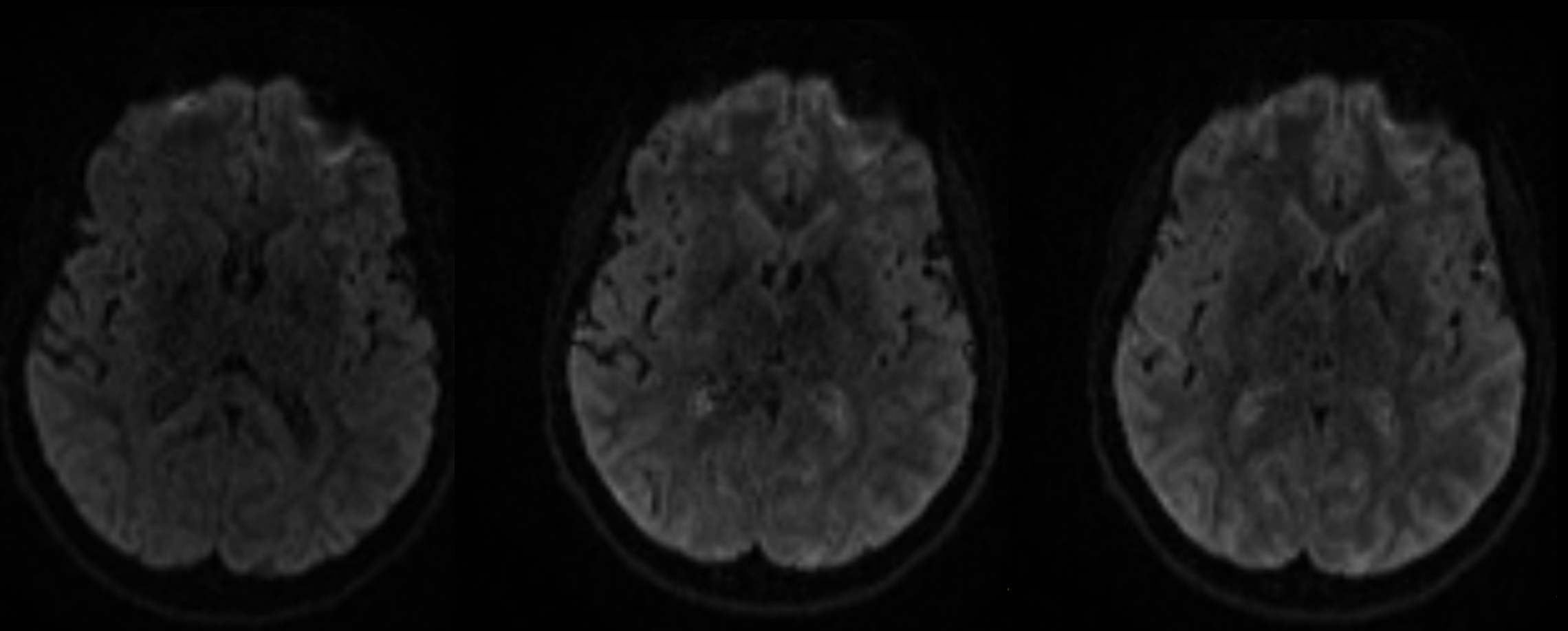
MICROSTRUCTURAL  
COORDINATION





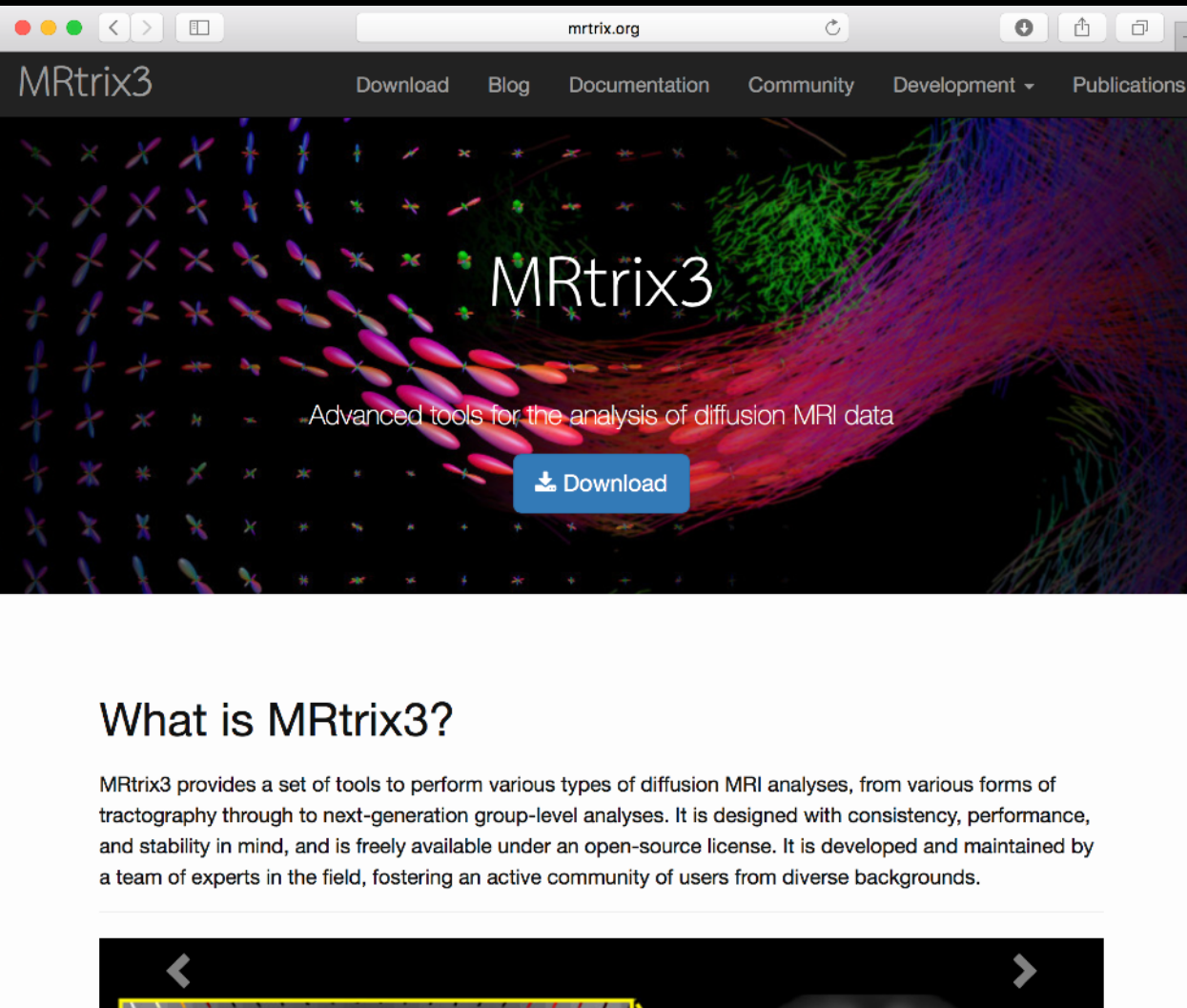
CONNECTIVITY FROM DIFFUSION MRI

# RAW DIFFUSION-MRI DATA



# GOOD AND OPEN SOFTWARE

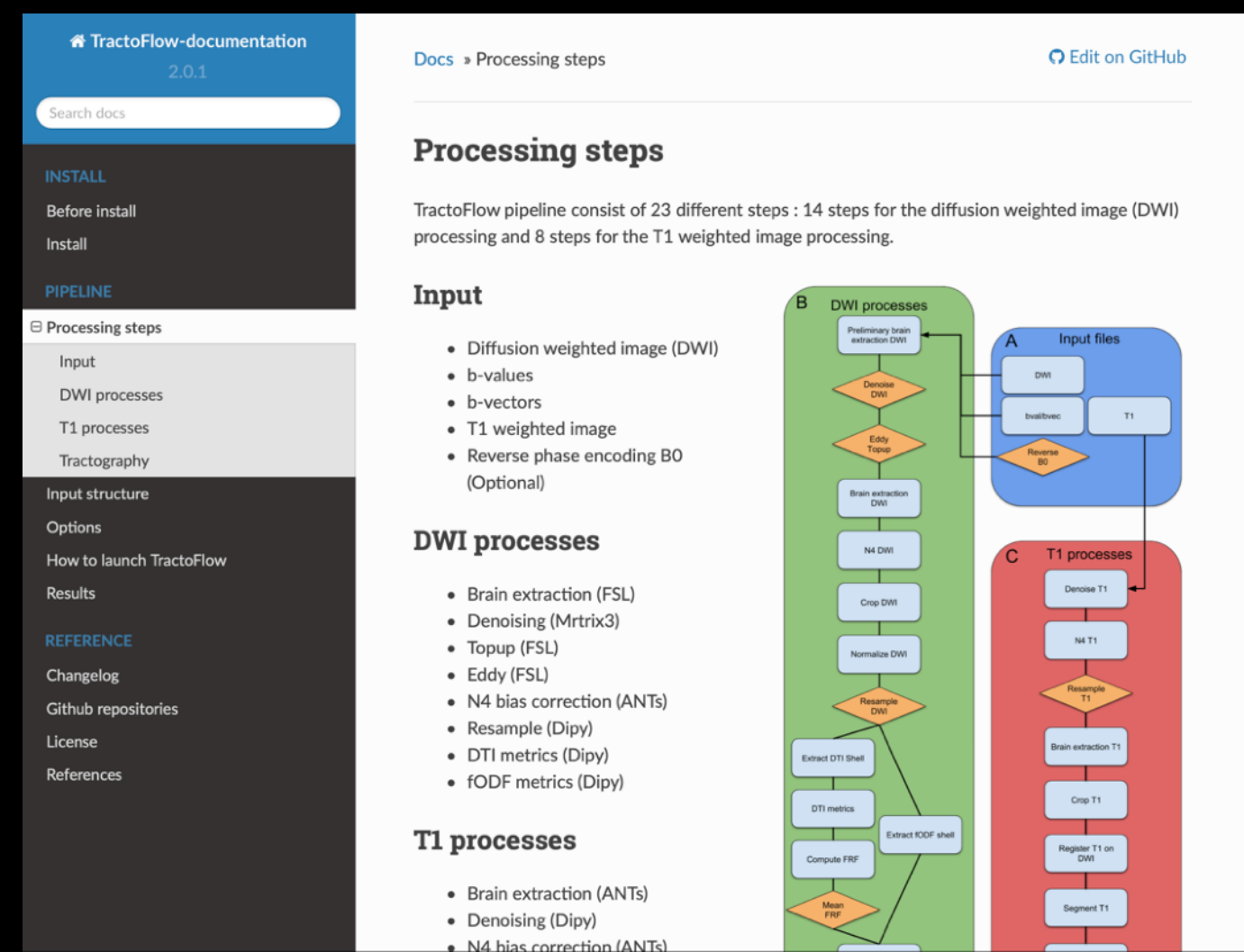
mrtrix



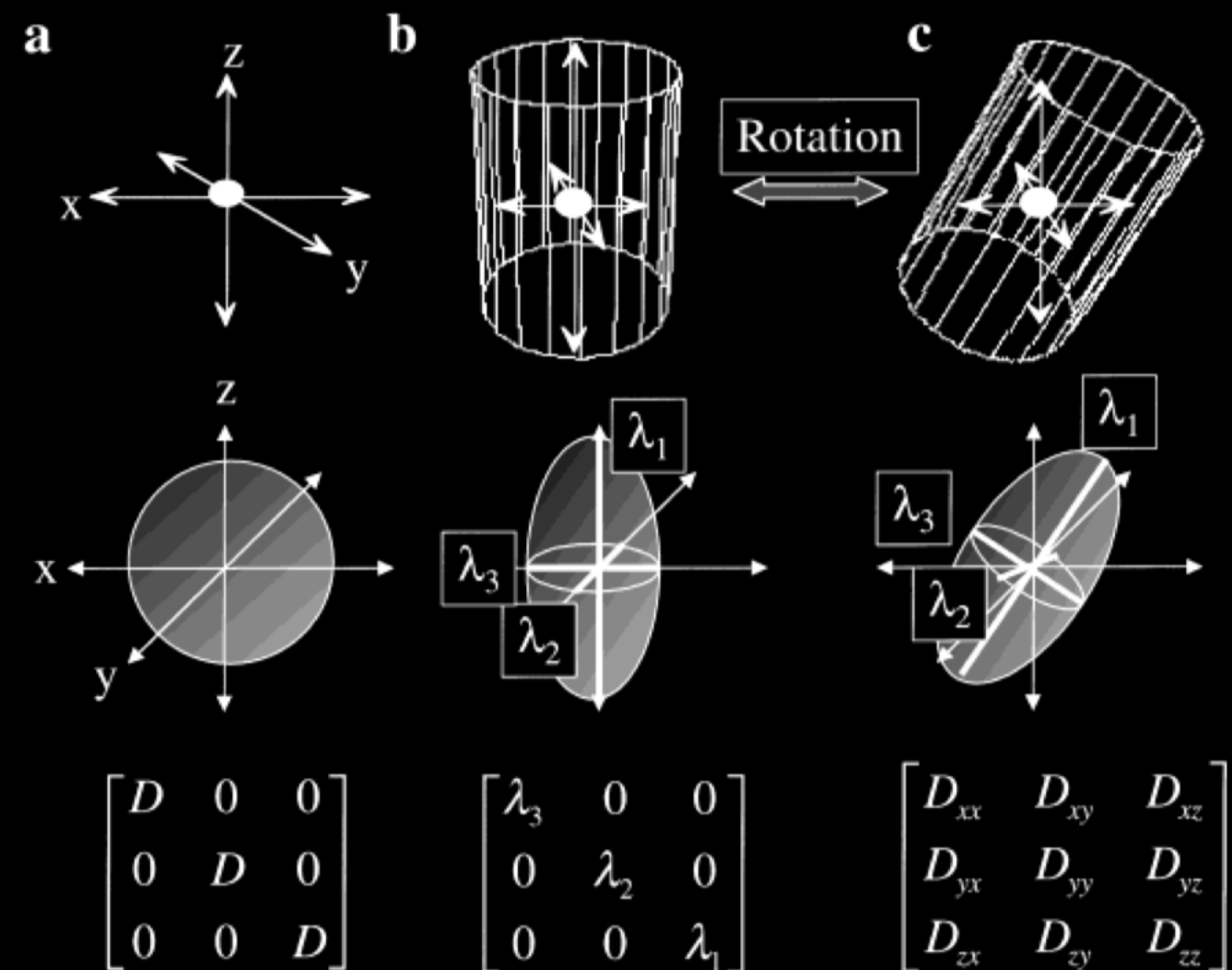
## What is MRtrix3?

MRtrix3 provides a set of tools to perform various types of diffusion MRI analyses, from various forms of tractography through to next-generation group-level analyses. It is designed with consistency, performance, and stability in mind, and is freely available under an open-source license. It is developed and maintained by a team of experts in the field, fostering an active community of users from diverse backgrounds.

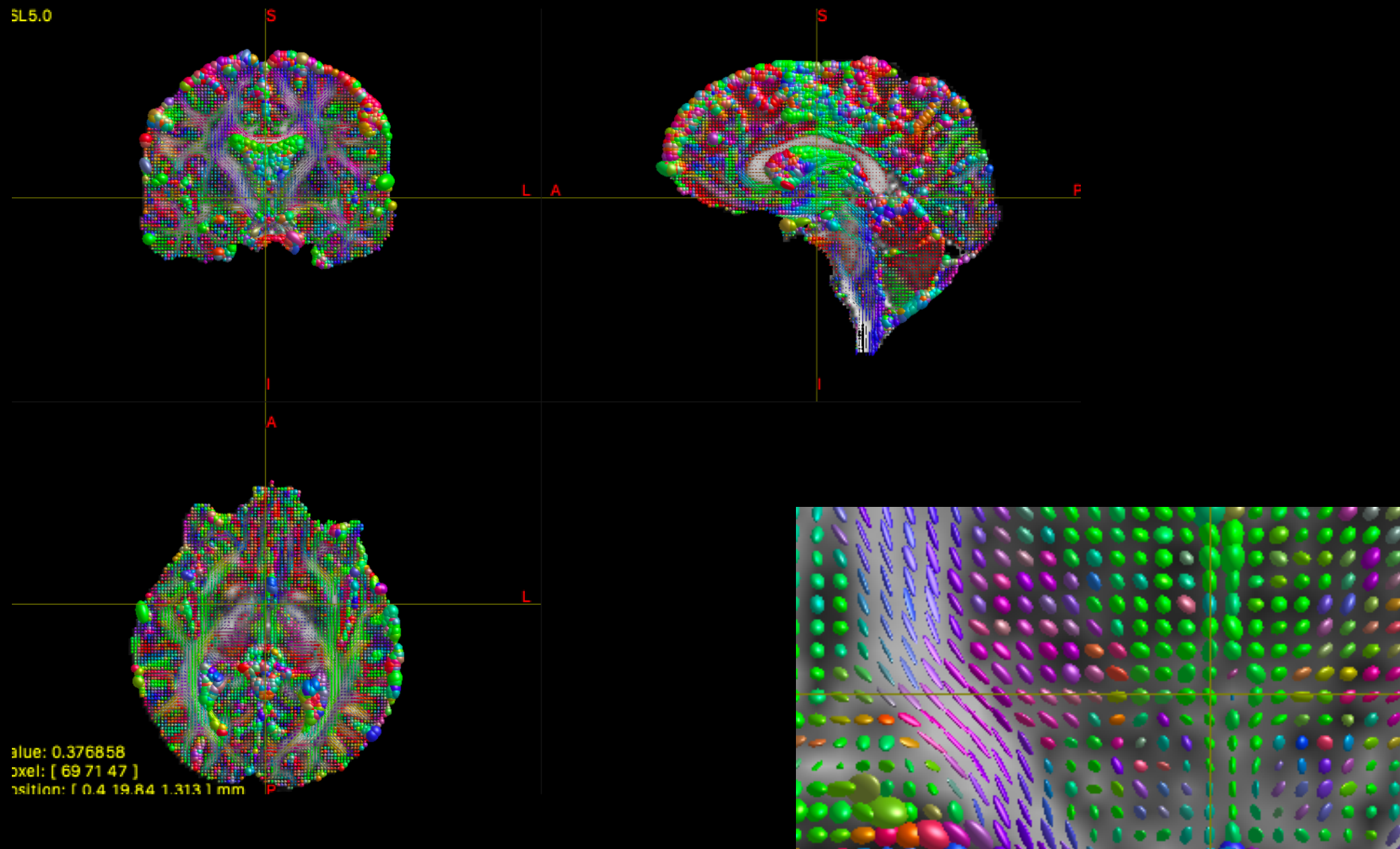
tractoflow



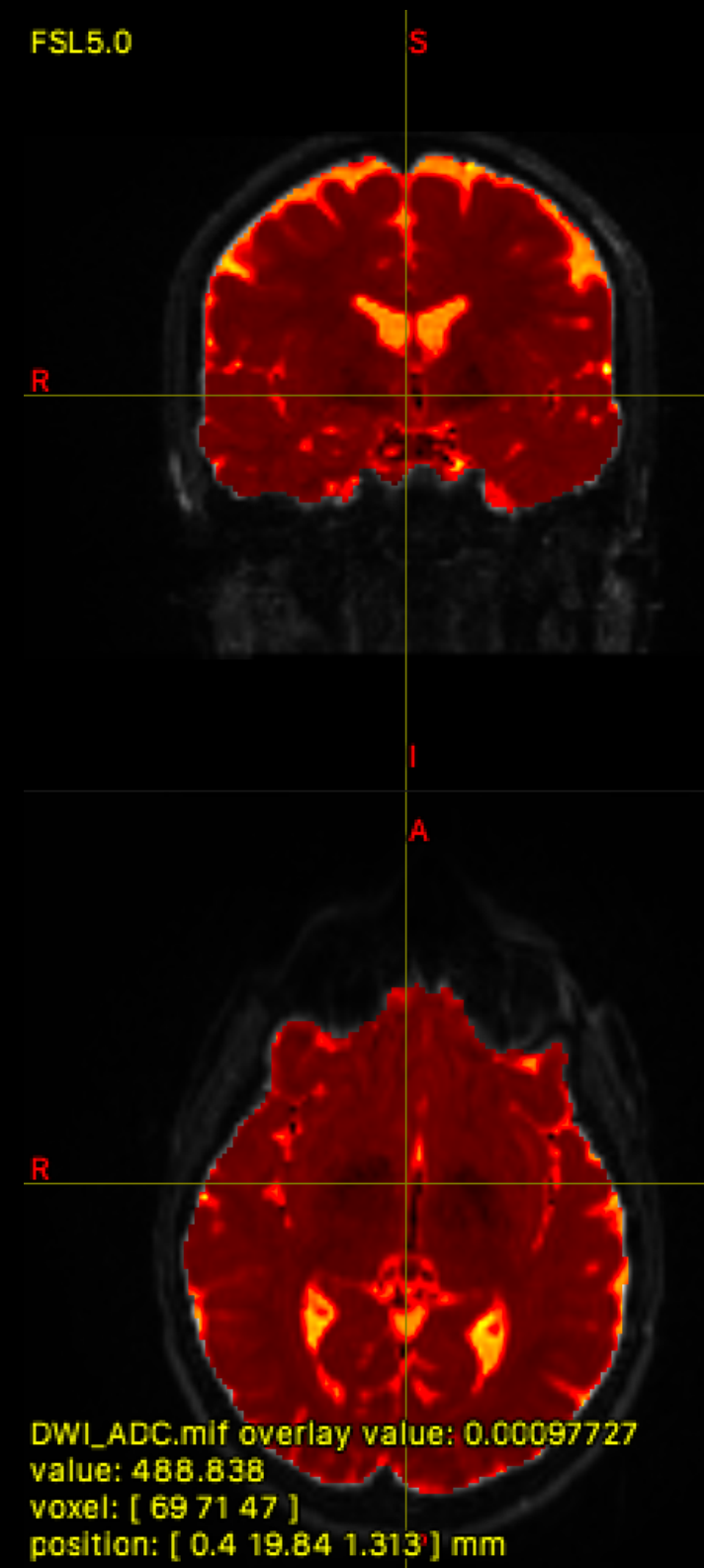
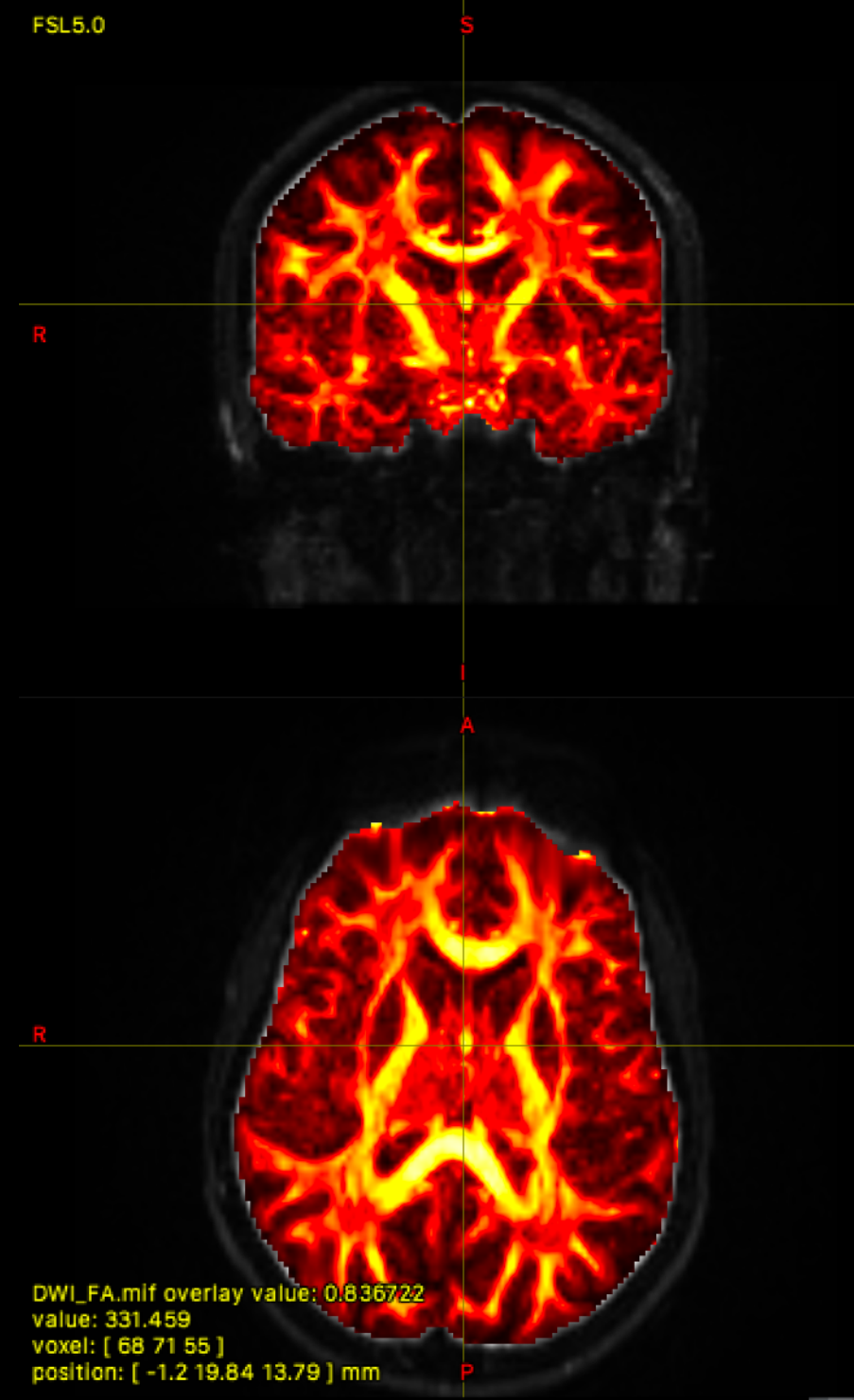
# DIFFUSION MRI TENSOR MODEL



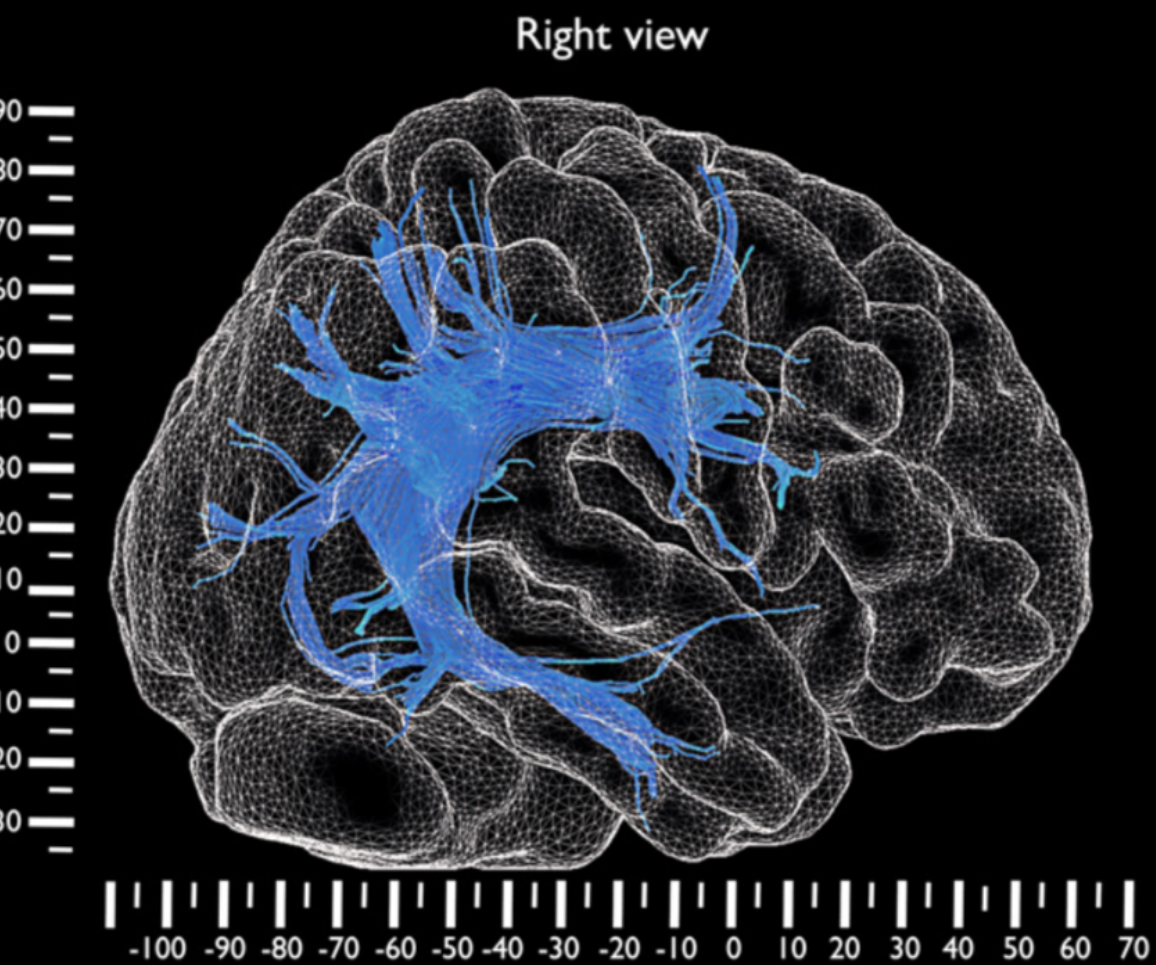
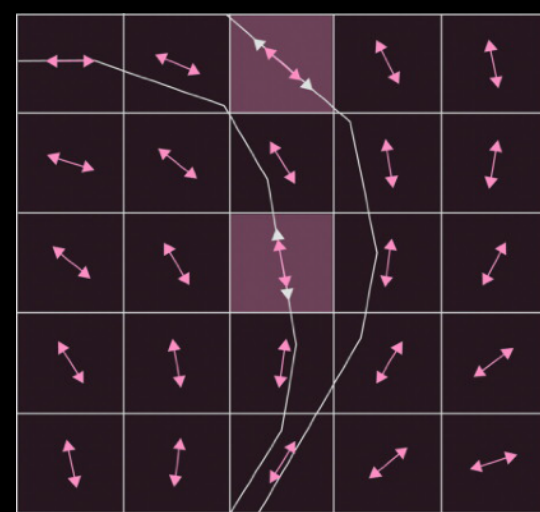
# TENSORS



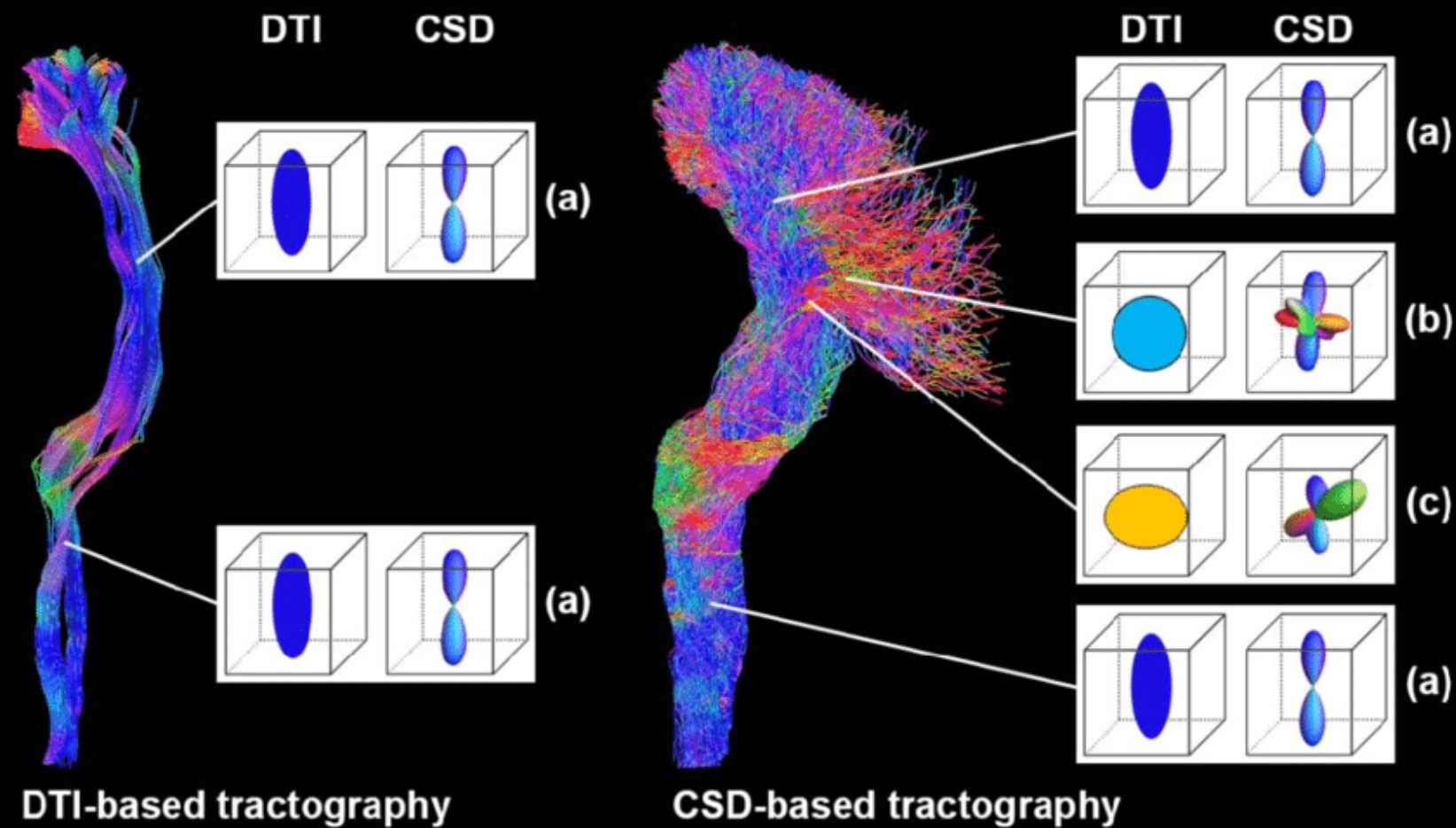
## FA AND ADC



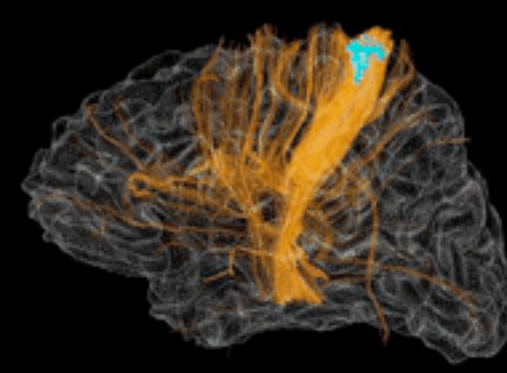
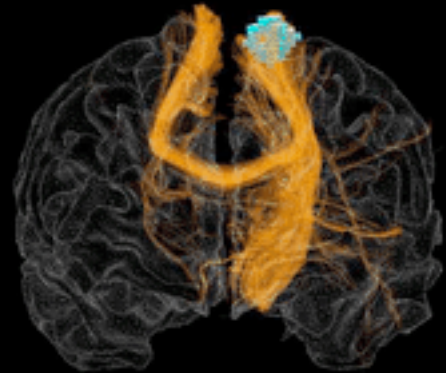
# DETERMINISTIC TRACTOGRAPHY



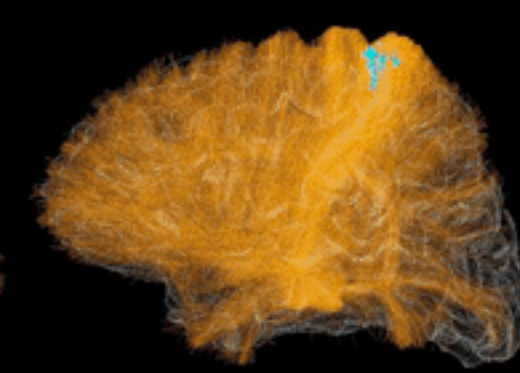
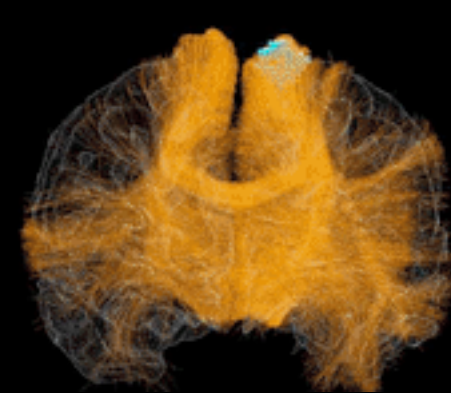
## DIFFUSION MRI: MORE COMPLEX MODELS



Deterministic streamline tractography



Probabilistic streamline tractography



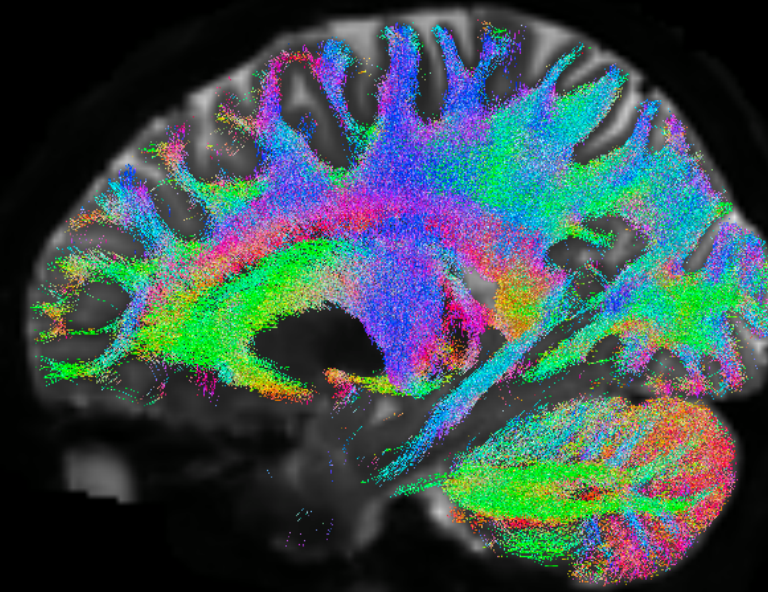
# DIFFUSION MRI

TRACKS PATHWAYS  
OF UNHINDERED WATER DIFFUSION  
TO ESTIMATE SC

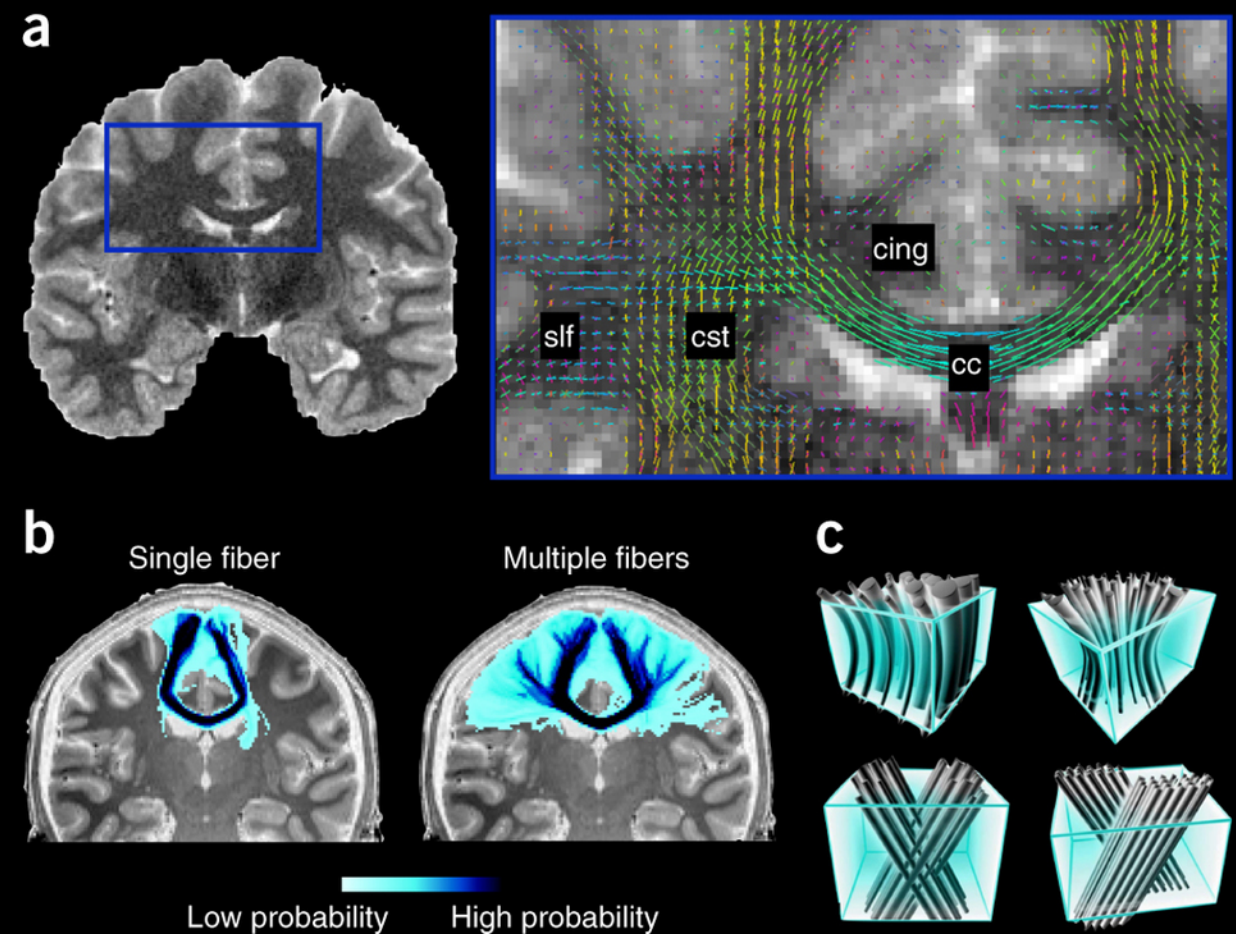
TRACKING & DIFFUSION PARAMETER  
ESTIMATION FOR MICROSTRUCTURAL  
INFERENCE

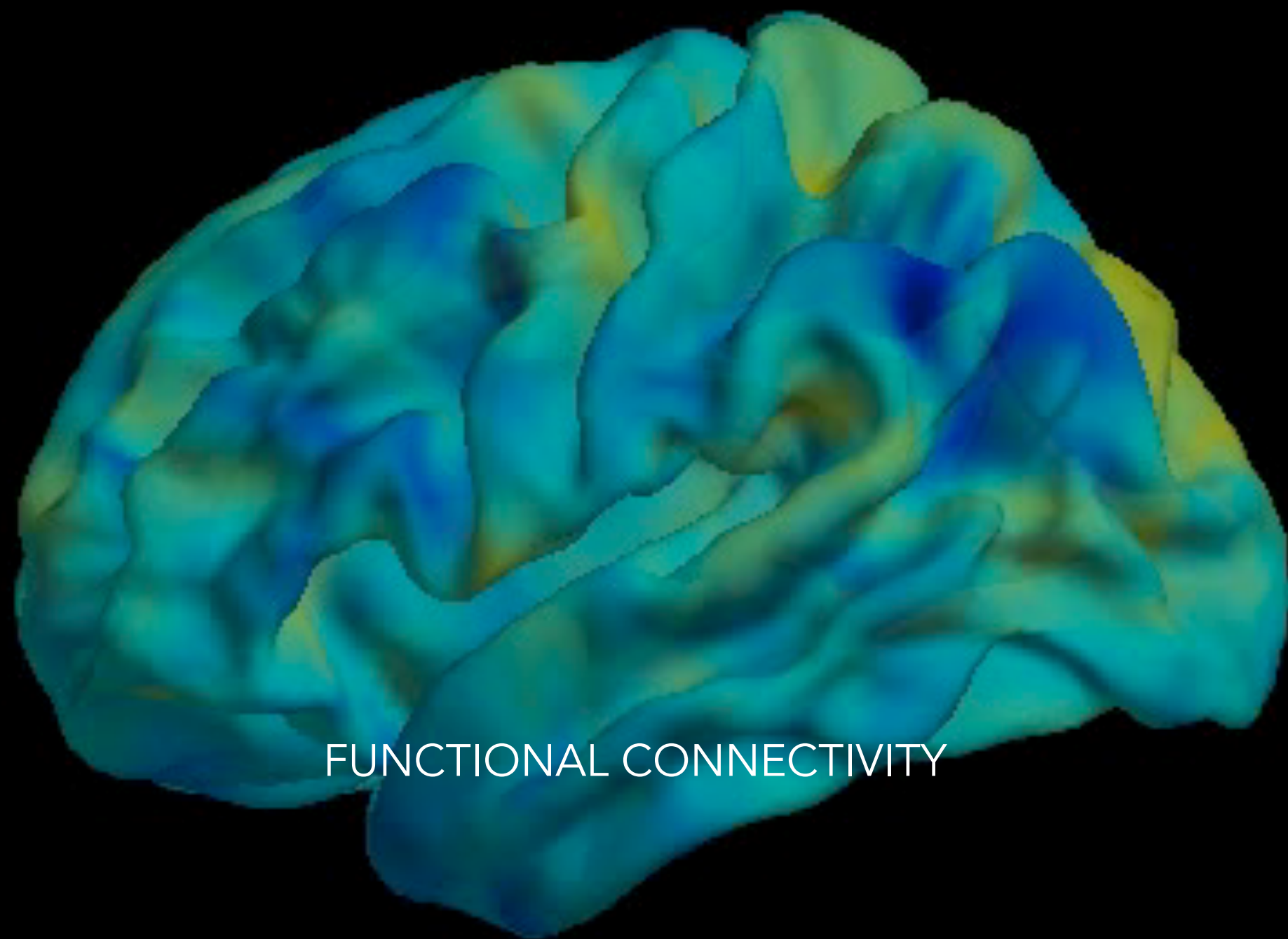
CONTINUOUS IMPROVEMENTS  
IN ACQUISITION AND MODELING

CHALLENGES REMAIN:  
FIBRE CROSSING,  
INTRACORTICAL TERMINATIONS,  
DISTANCE BIAS,  
VALIDITY IN PATHOLOGICAL  
REGIONS



SINGLE SUBJECT (HCP)

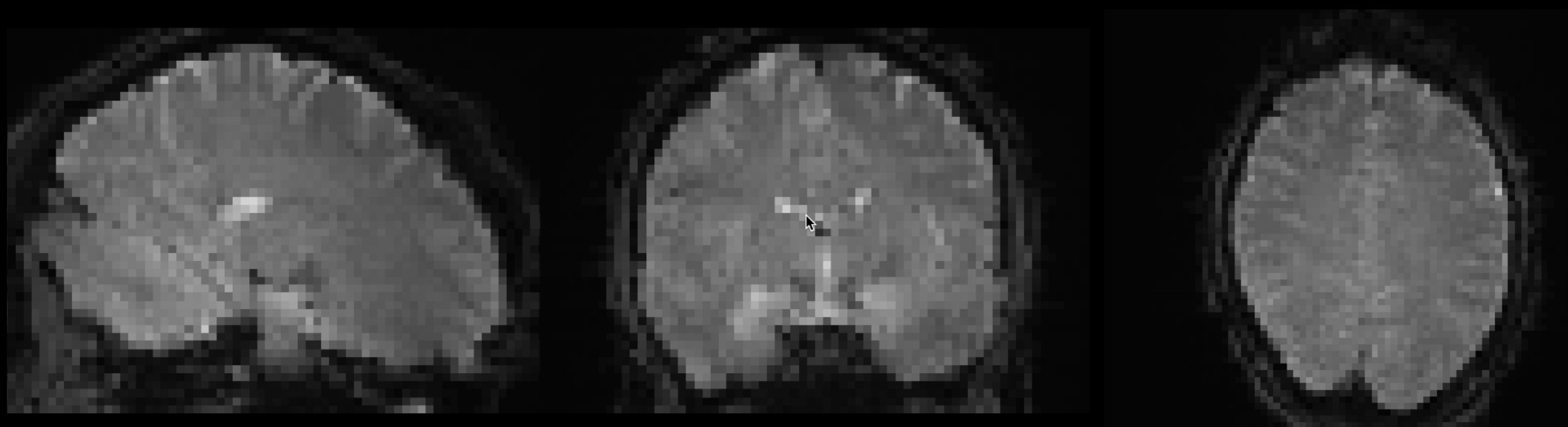




FUNCTIONAL CONNECTIVITY



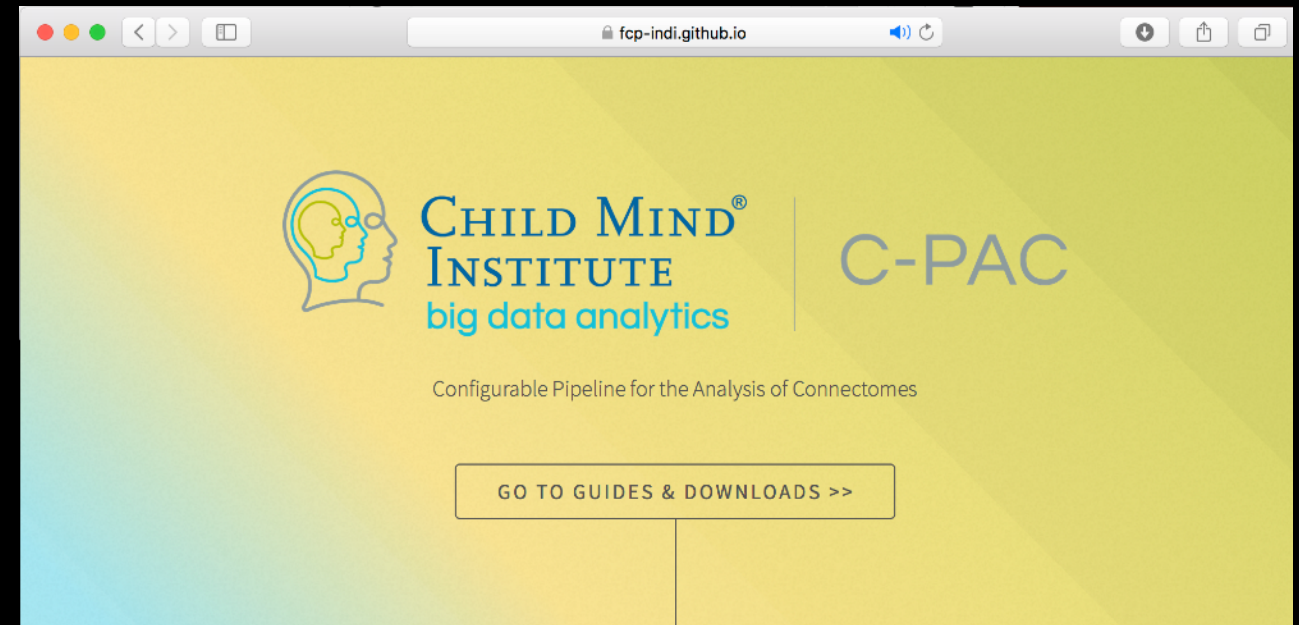
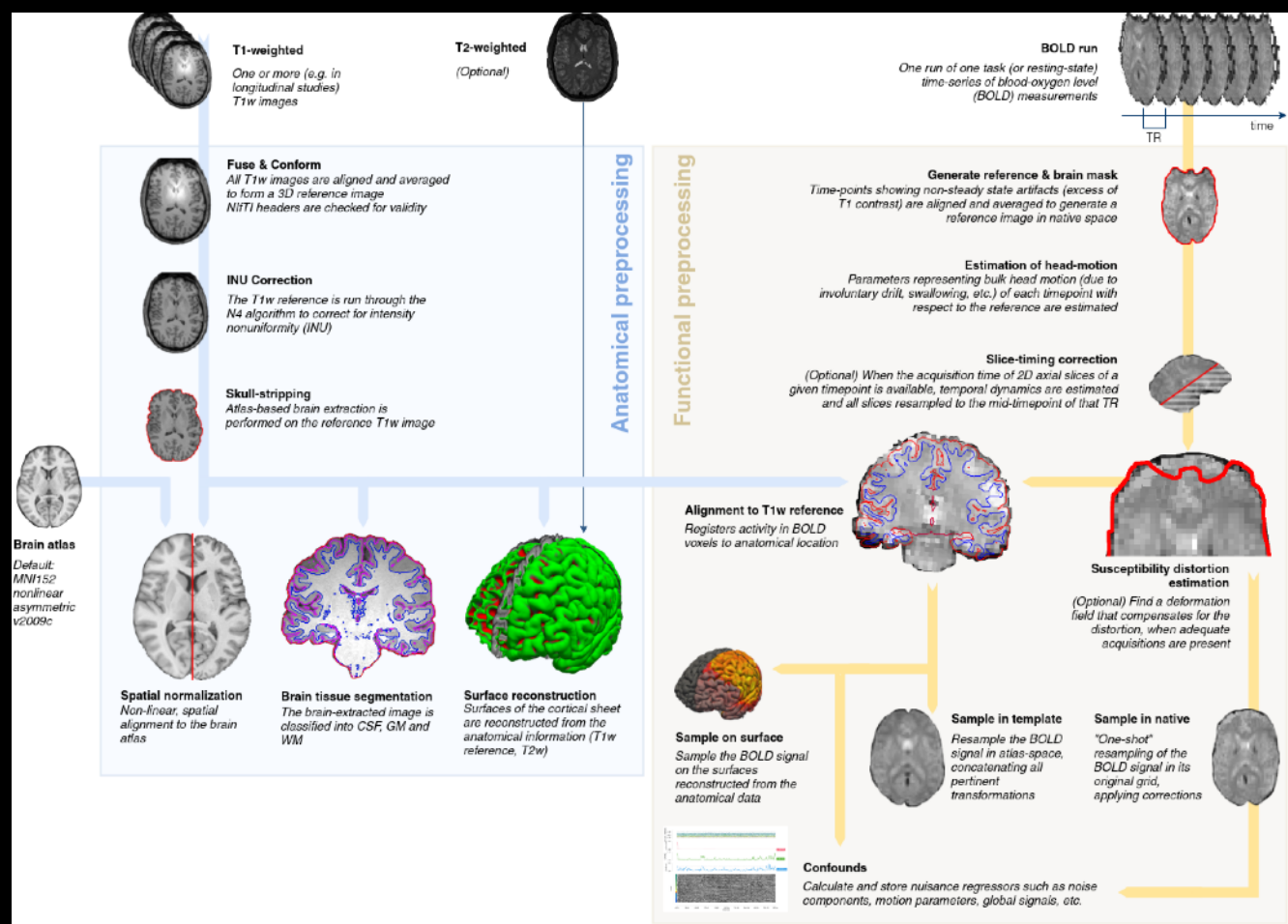
# RAW RESTING-STATE FMRI DATA



# GOOD AND OPEN SOFTWARE

[fmriprep.readthedocs.io](https://fmriprep.readthedocs.io)  
Esteban et al (2019) Nat Methods

[fcp-indi.github.io](https://fcp-indi.github.io)  
Sikka et al (2014) frontIInf

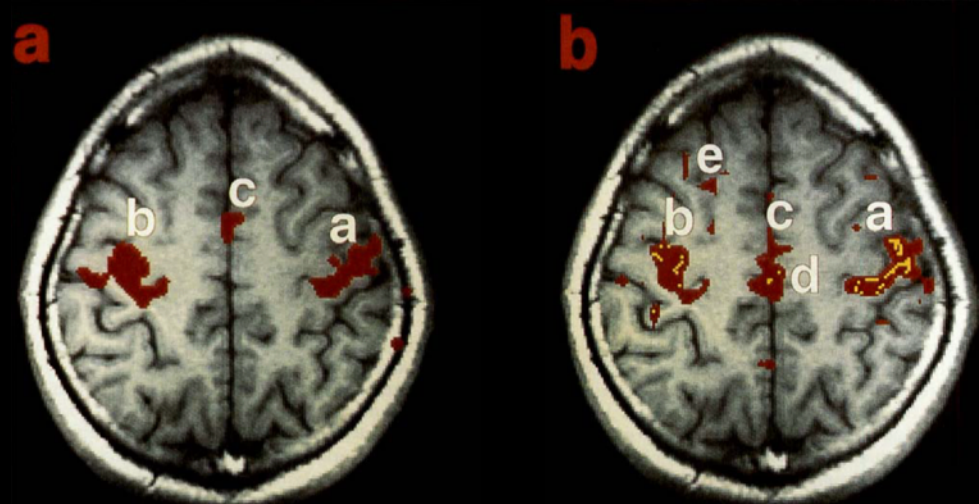


Guides & Downloads

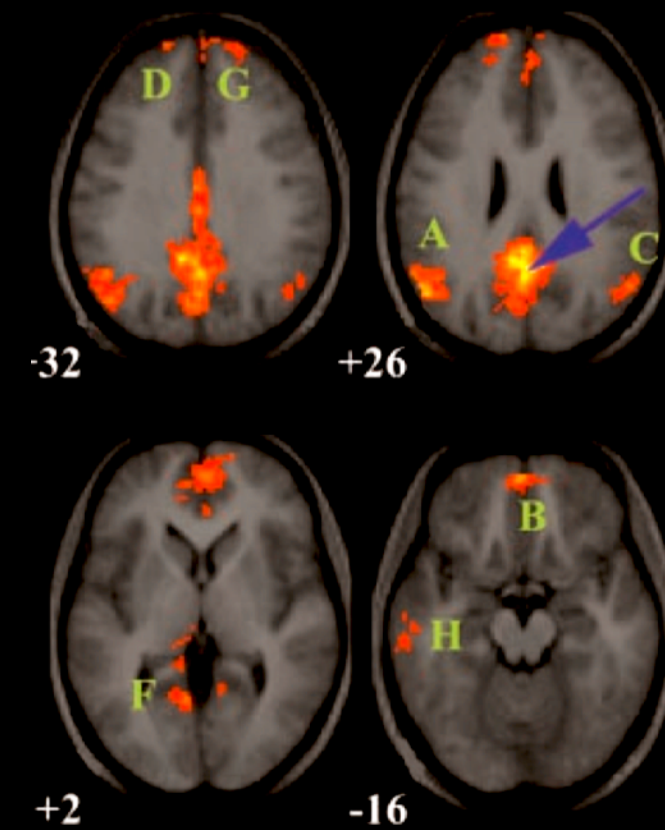


git

# HOW TO DEFINE A SEED? FROM TASK-BASED ACTIVATIONS/DEACTIVATIONS



Biswal | 1995 MRM



Grecius et al. 2003 PNAS

# HOW TO DEFINE A SEED? FROM TASK-BASED ACTIVATIONS/DEACTIVATIONS

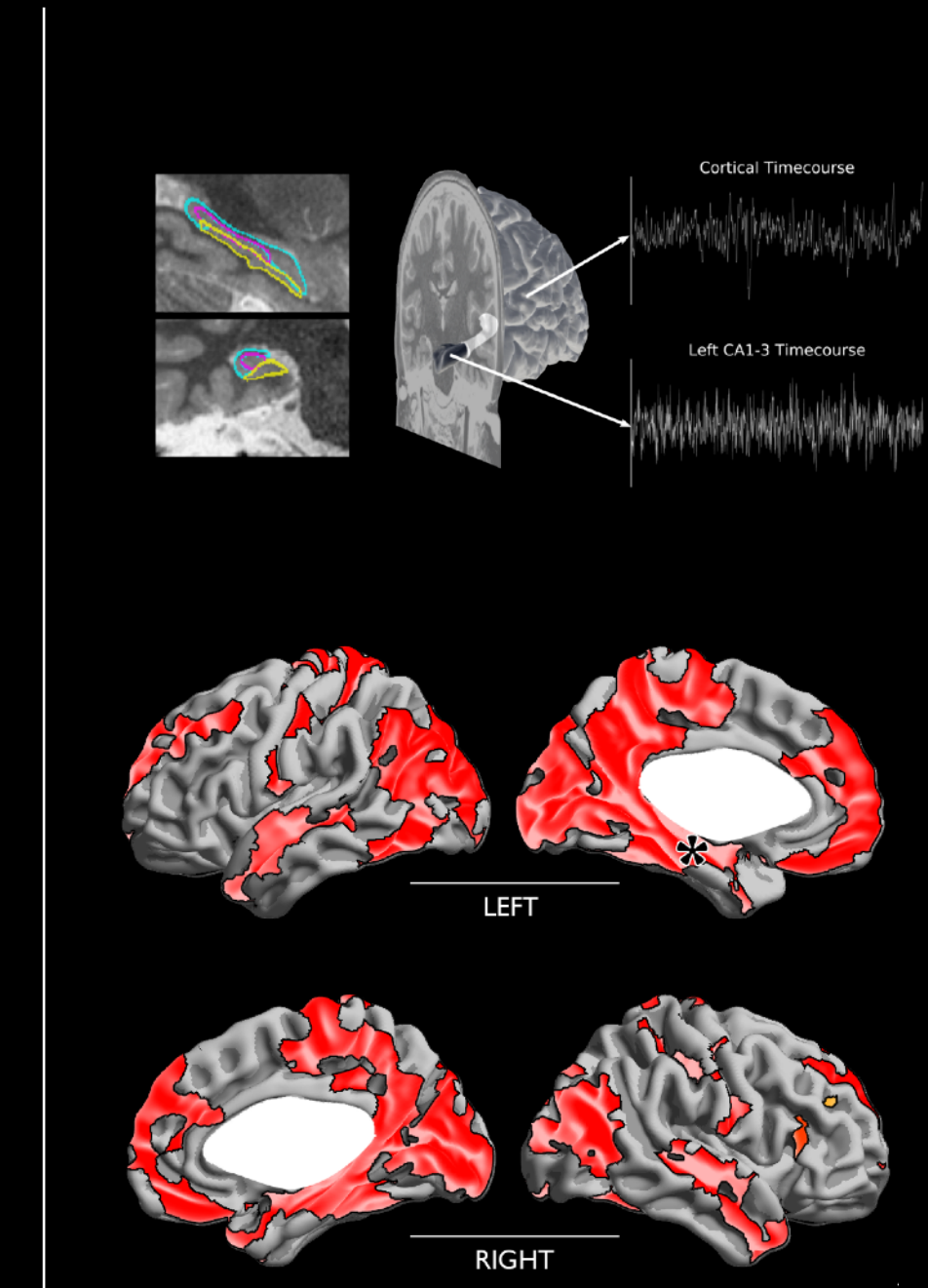
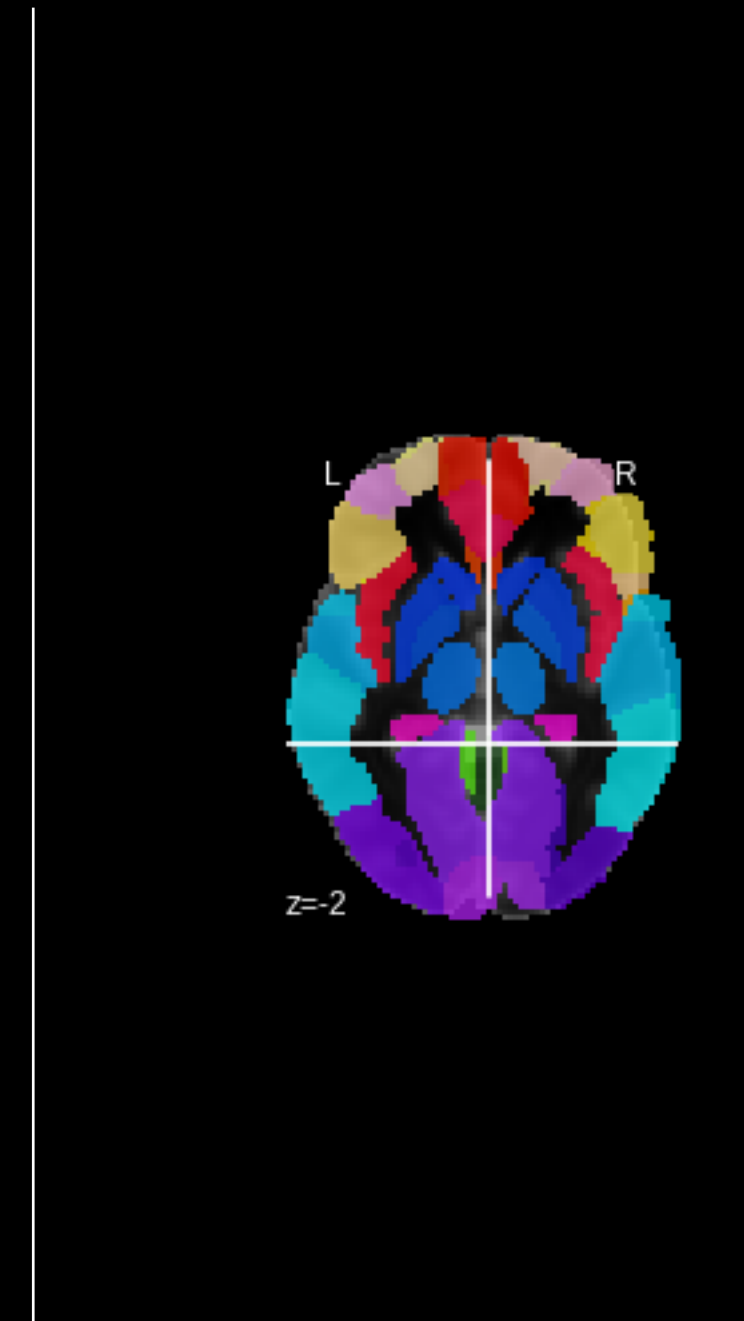
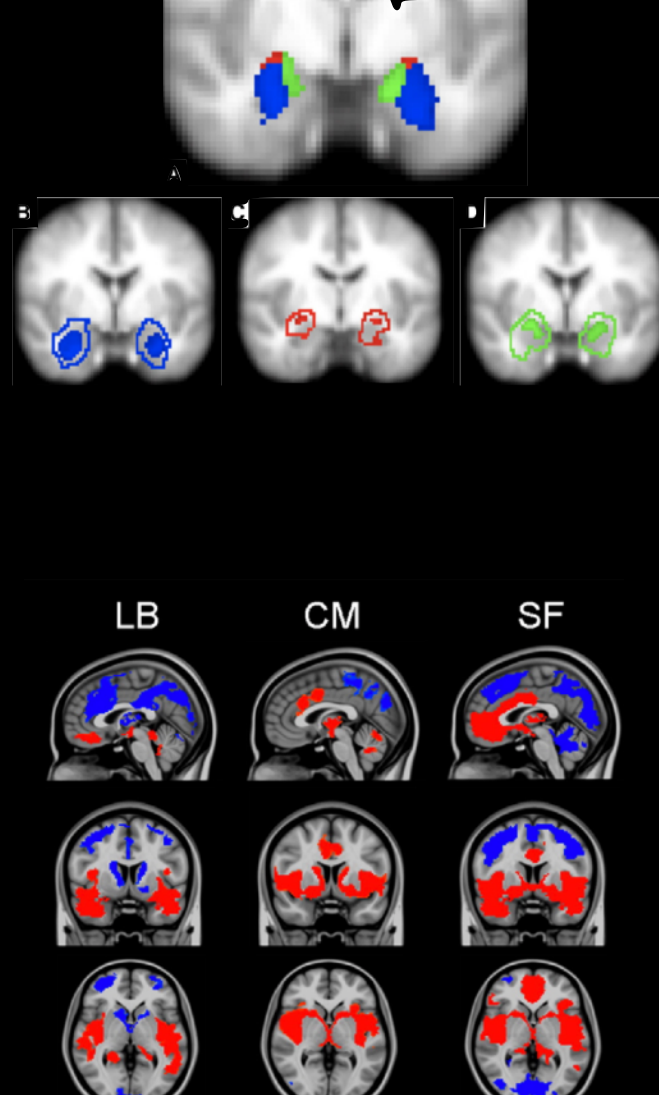
The screenshot shows the homepage of brainmap.org. At the top, there's a navigation bar with links for home, taxonomy, software, tools, publications, collaborations, credits, and contact. Below the navigation is a section titled "What is BrainMap?" which provides a brief overview of the project. To the right of this is a "BrainMap Forums" section with a link to the forum. Further down is a "Quick Author Search" form where users can enter an author's last name to check if their paper is in the database. At the bottom of this sidebar is an "Activation Coordinate Experiment-wise Search (ACES)" section with a file upload input labeled "Choose File" and "no file selected".

The screenshot shows the homepage of neurosynth.org. The main title is "neurosynth.org" in large, bold letters. Below the title, a subtitle reads: "Neurosynth is a platform for large-scale, automated synthesis of functional magnetic resonance imaging (fMRI) data." It also states: "It takes thousands of published articles reporting the results of fMRI studies, chews on them for a bit, and then spits out images that look like this:" Below this text are two brain maps. The left map is a coronal view with red clusters of activity in the left hemisphere. The right map is a sagittal view with red clusters in the right hemisphere. Both maps have coordinate axes labeled: D (dorsal), V (ventral), A (anterior), and P (posterior). Below the maps, a caption reads: "An automated meta-analysis of 1091 studies of working memory".

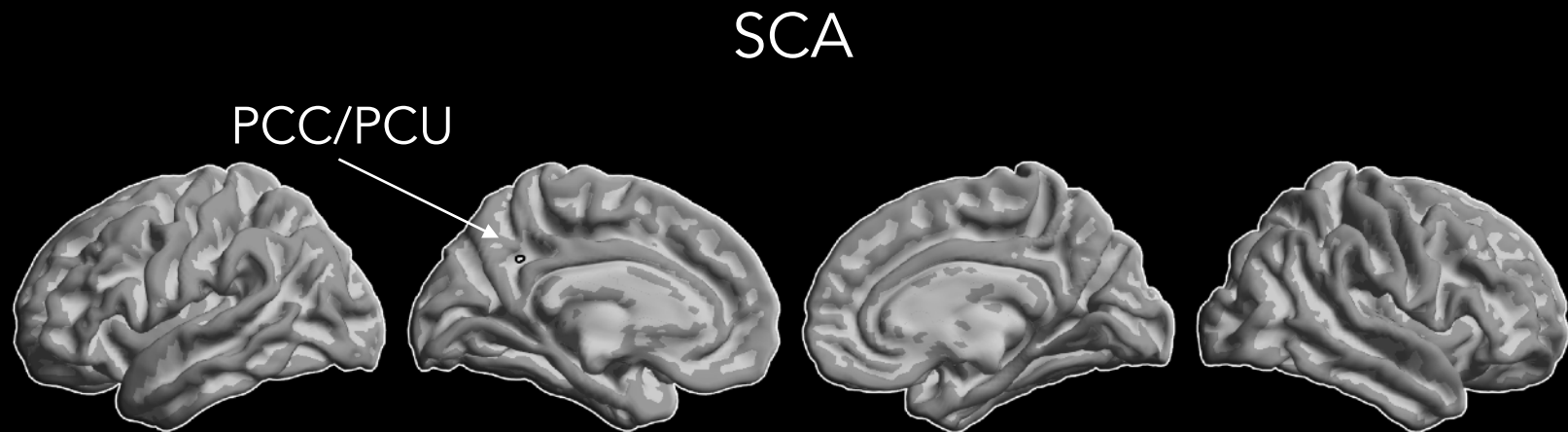
<http://www.brainmap.org/>  
Fox & Lancaster 2002  
Laird, Lancaster, Fox 2005

<http://neurosynth.org>  
Yarkoni et al. 2011 Nat Methods

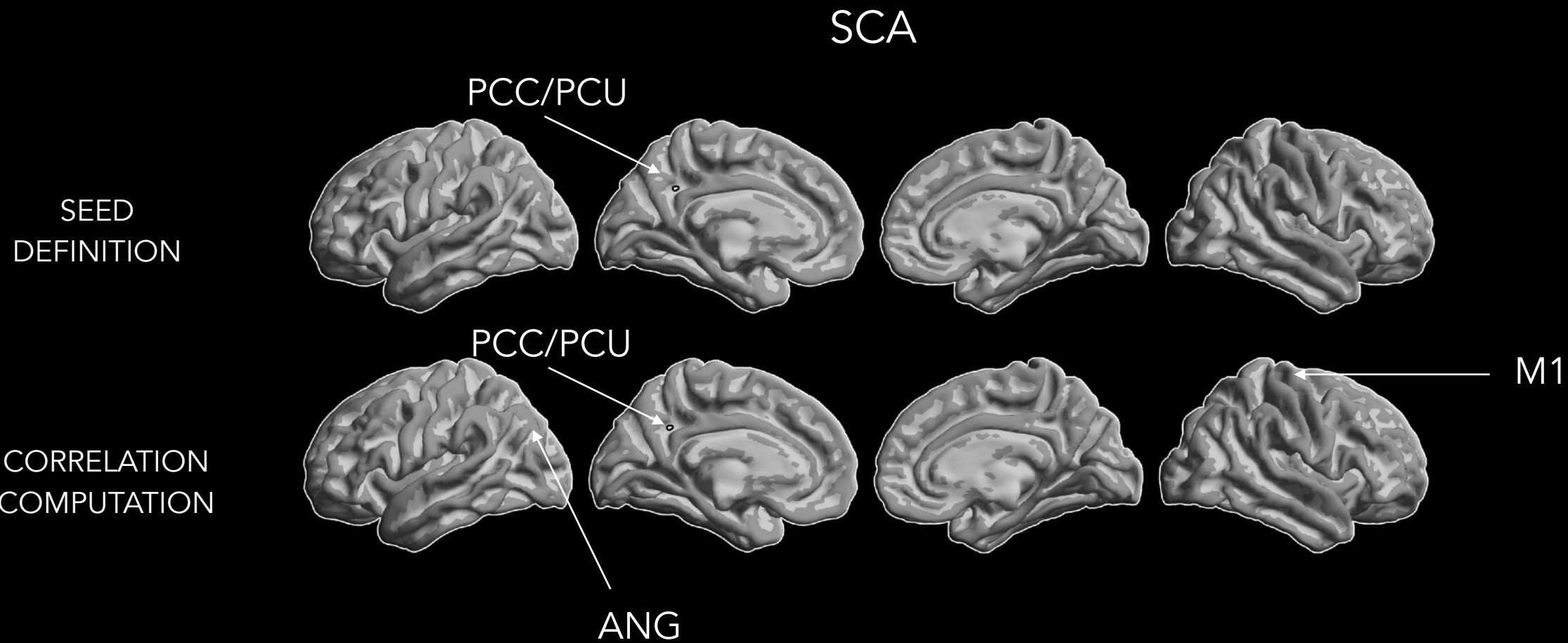
# HOW TO **DEFINE** A SEED? FROM ANATOMICALLY DEFINED REGIONS



SEED  
DEFINITION



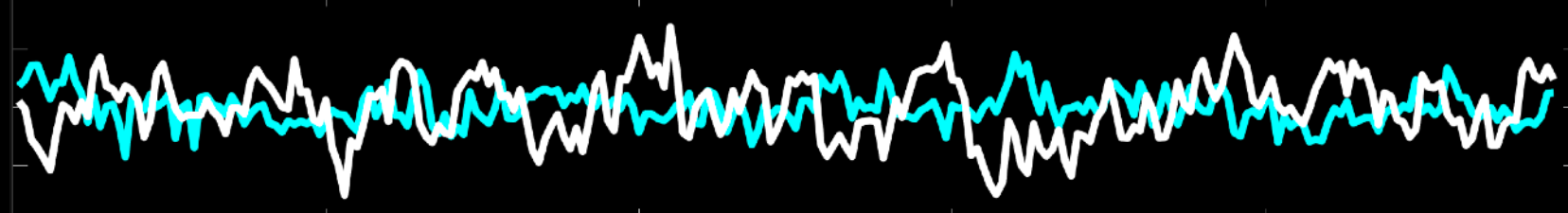
→ CODING

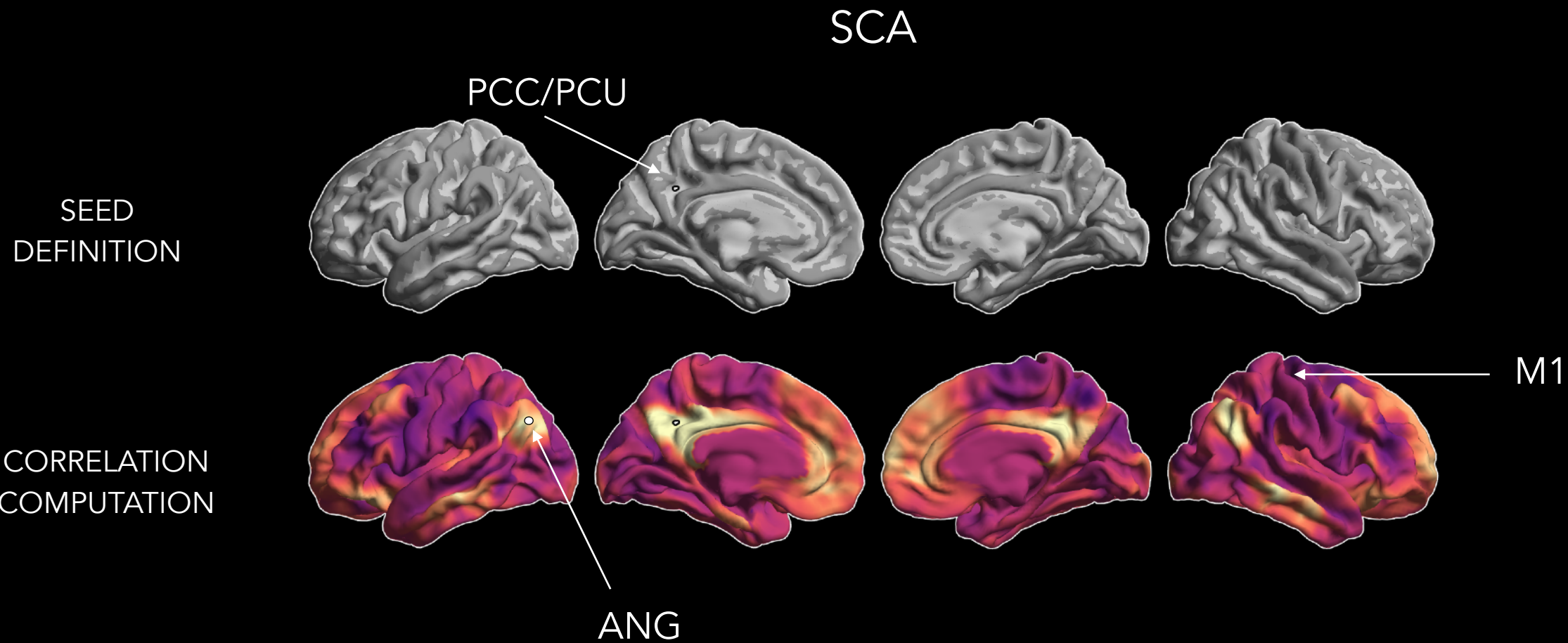


PCC/PCU vs ANG



PCC/PCU vs M1

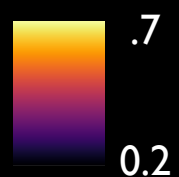
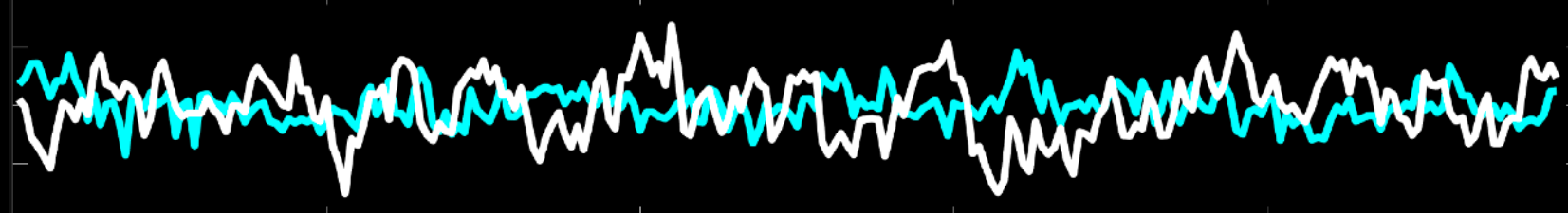




PCC/PCU vs ANG

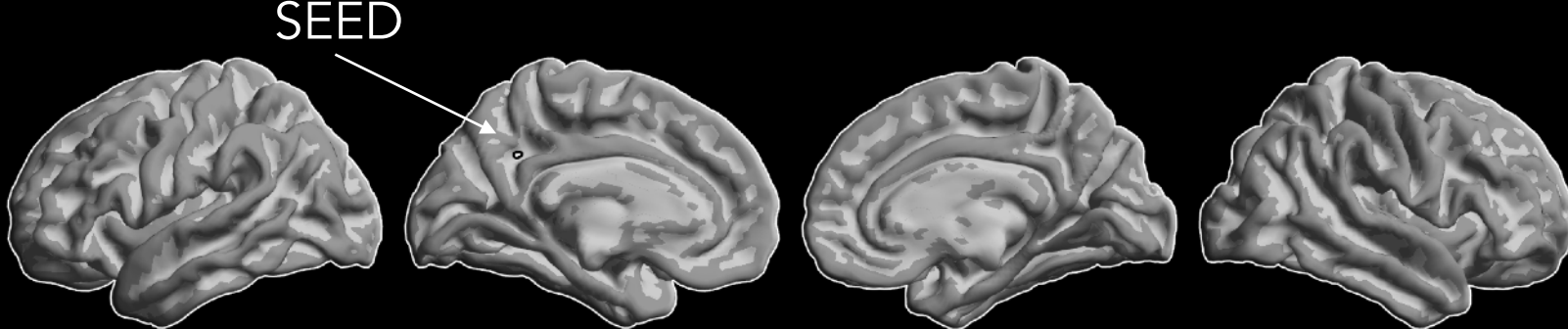


PCC/PCU vs M1

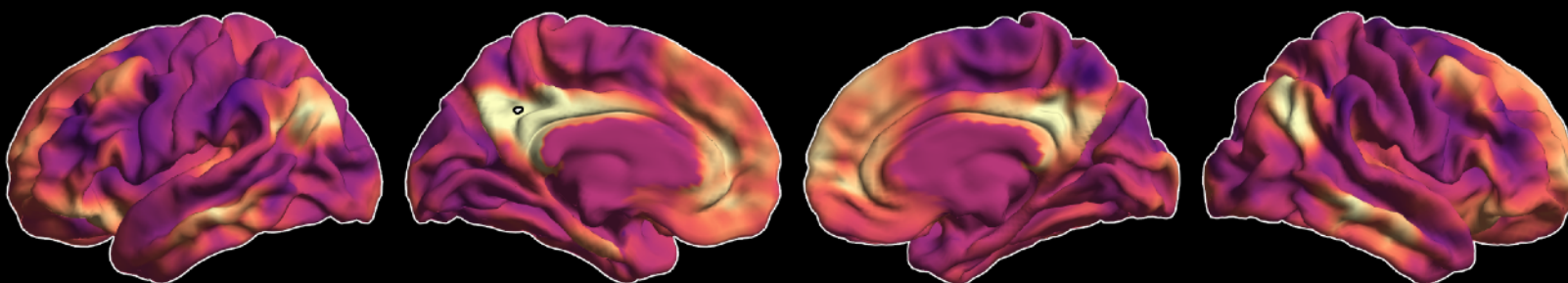


SCA

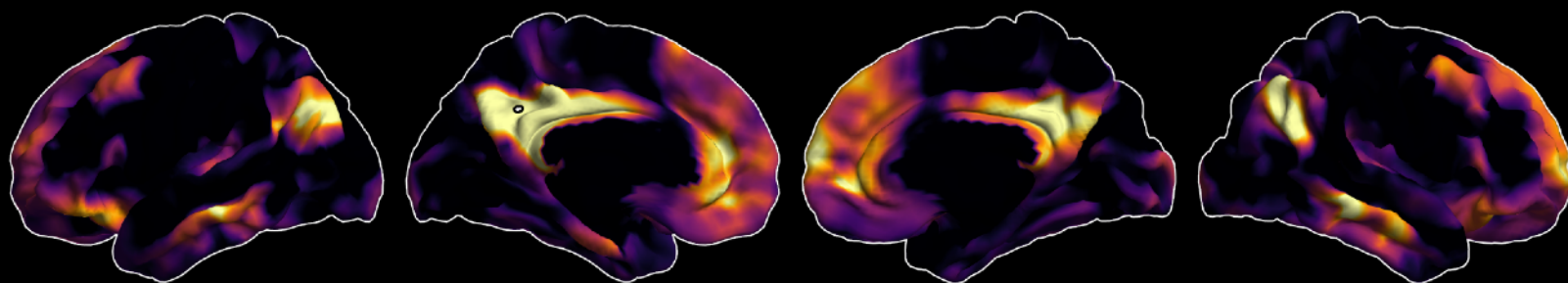
SEED  
DEFINITION



CORRELATION  
COMPUTATION

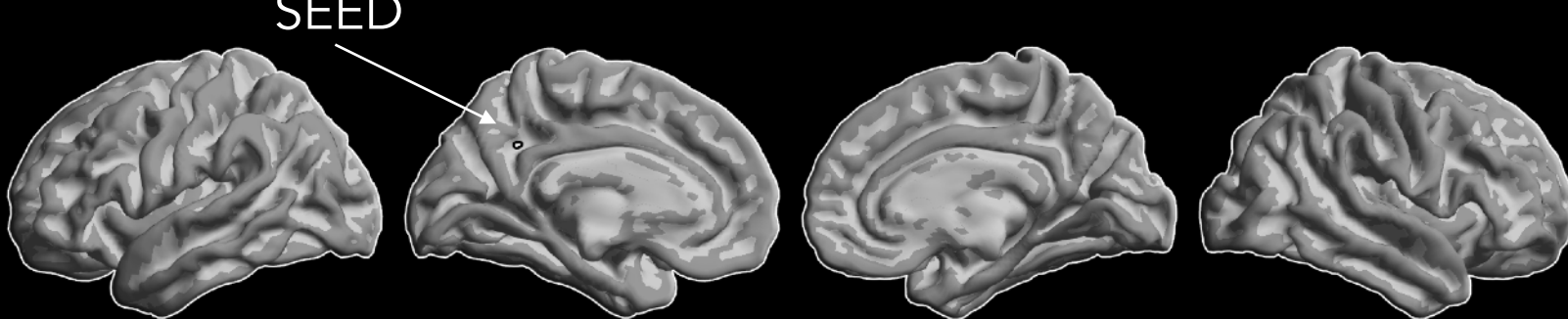


FISHER-R-TO-Z  
SUBJECT 1

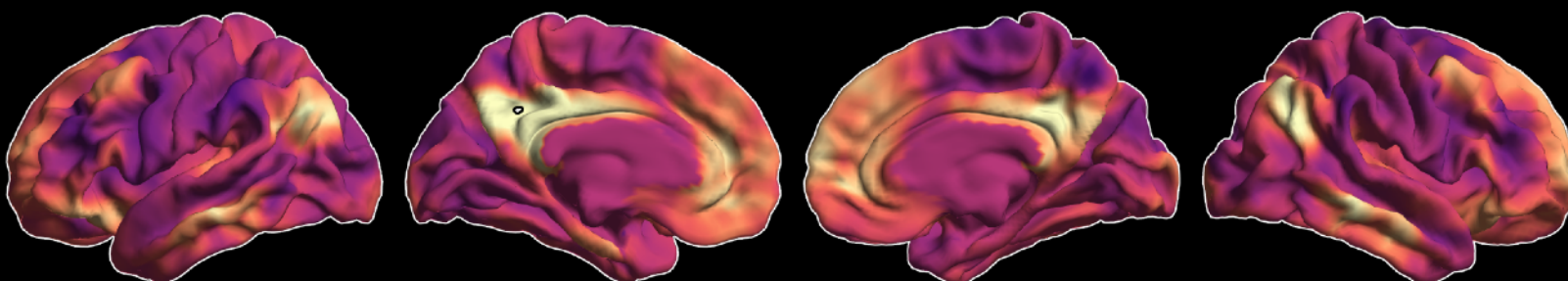


SCA

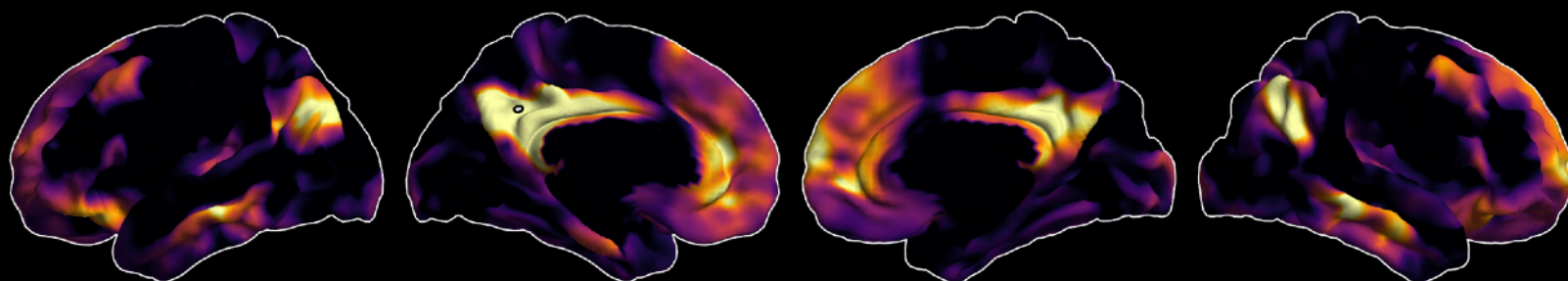
SEED  
DEFINITION



CORRELATION  
COMPUTATION

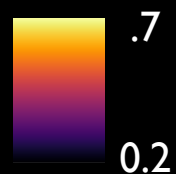
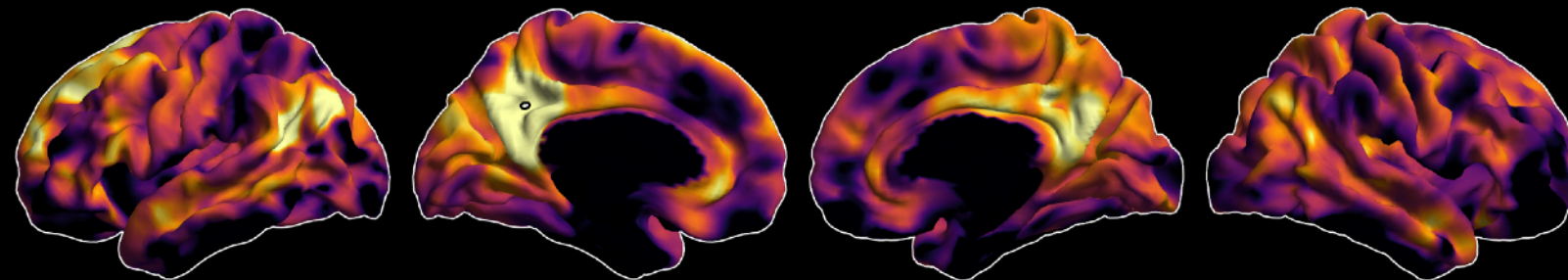


ZSUBJECT 1



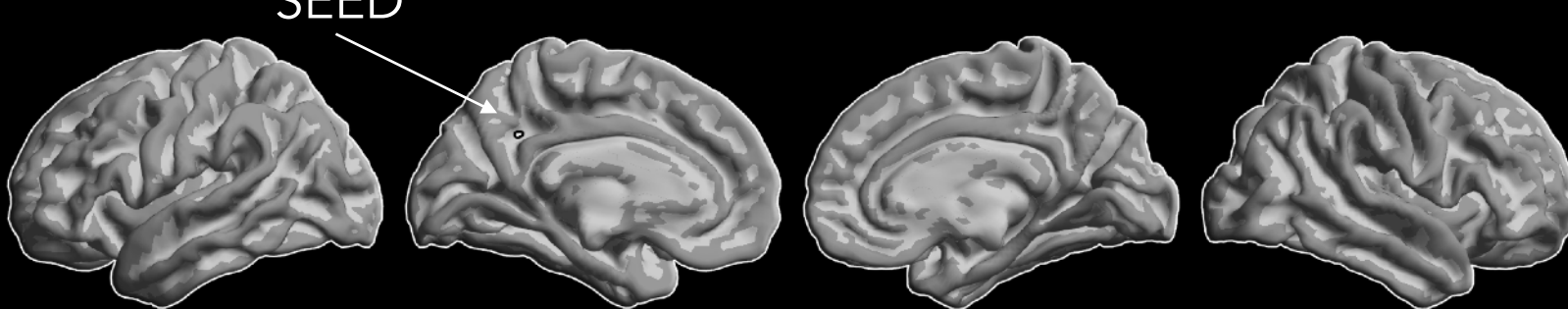
...

ZSUBJECT n

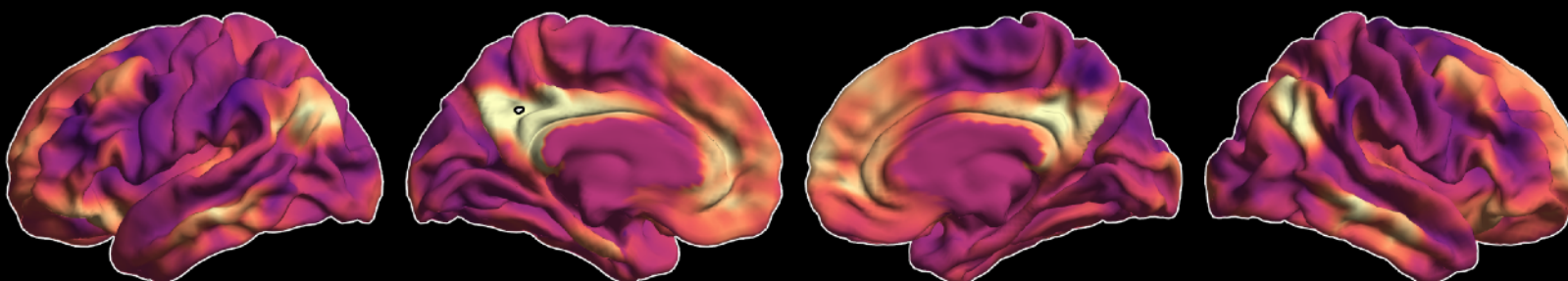


SCA

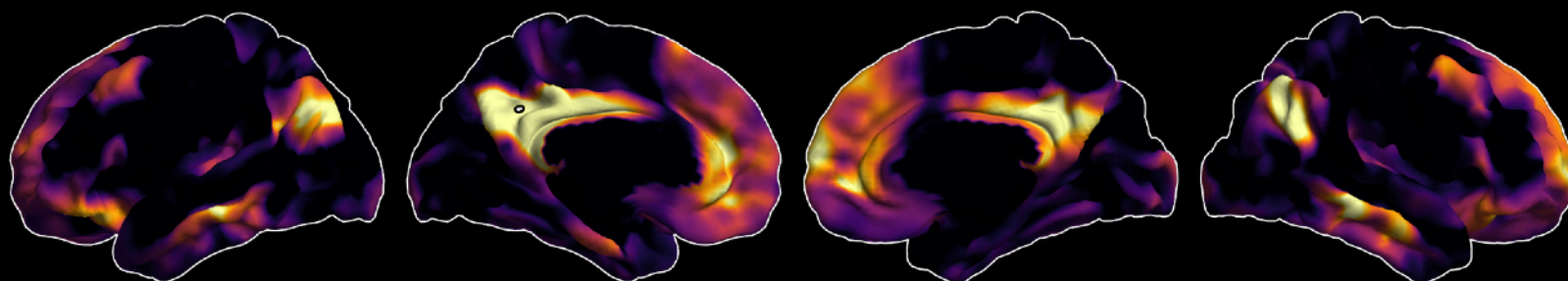
SEED  
DEFINITION



CORRELATION  
COMPUTATION

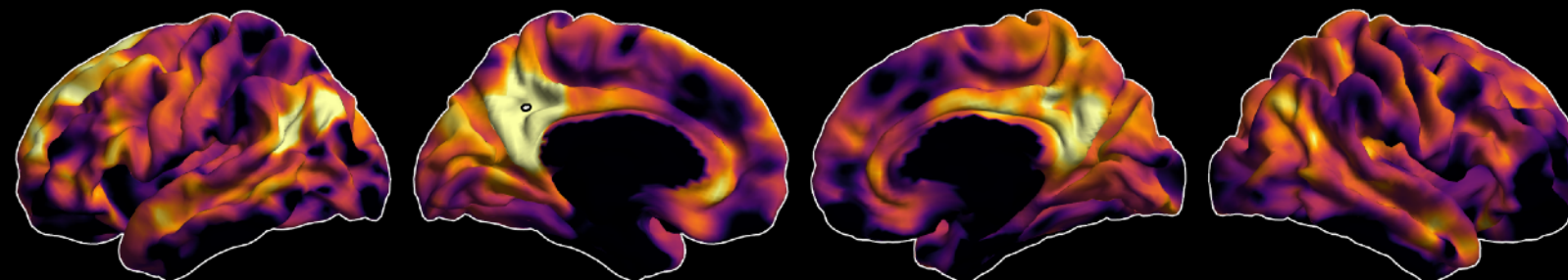


ZSUBJECT 1



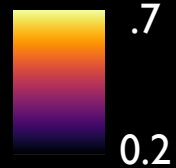
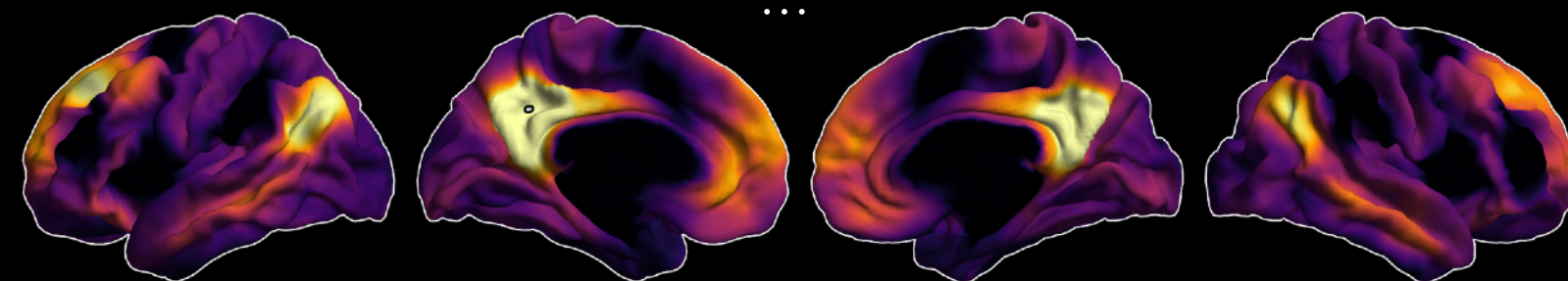
...

ZSUBJECT n

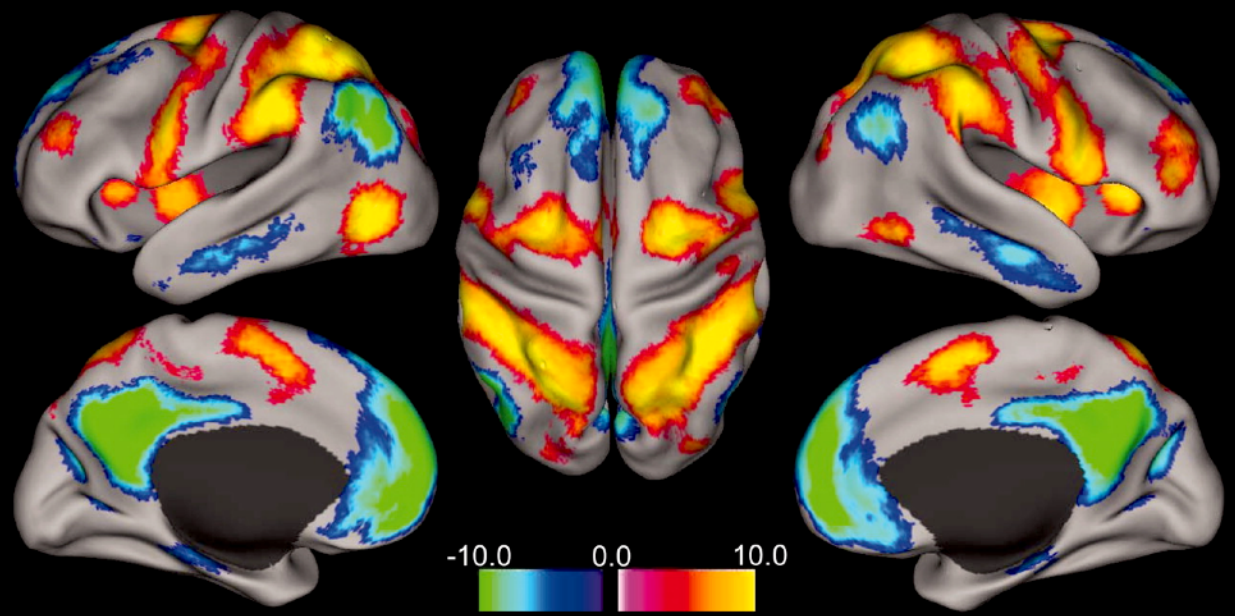
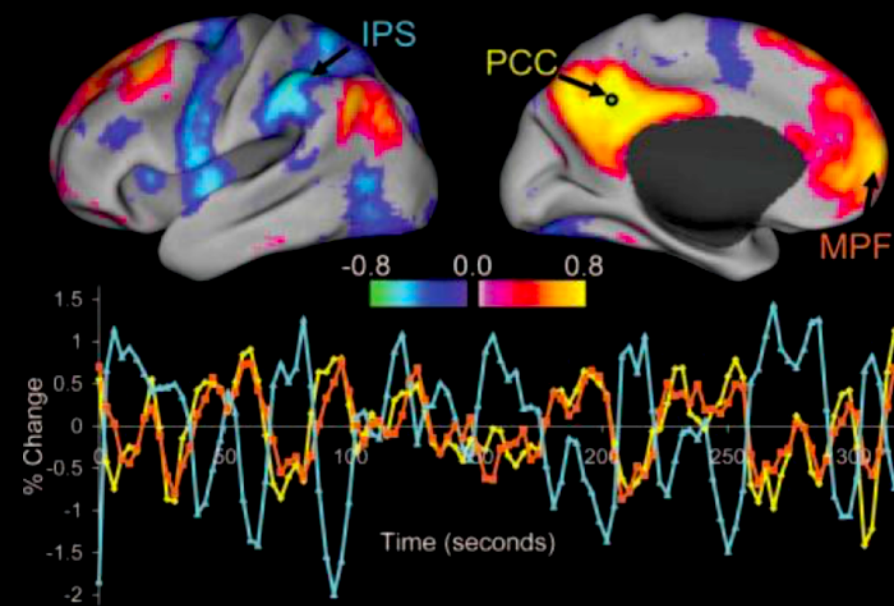


...

MEAN  
Z

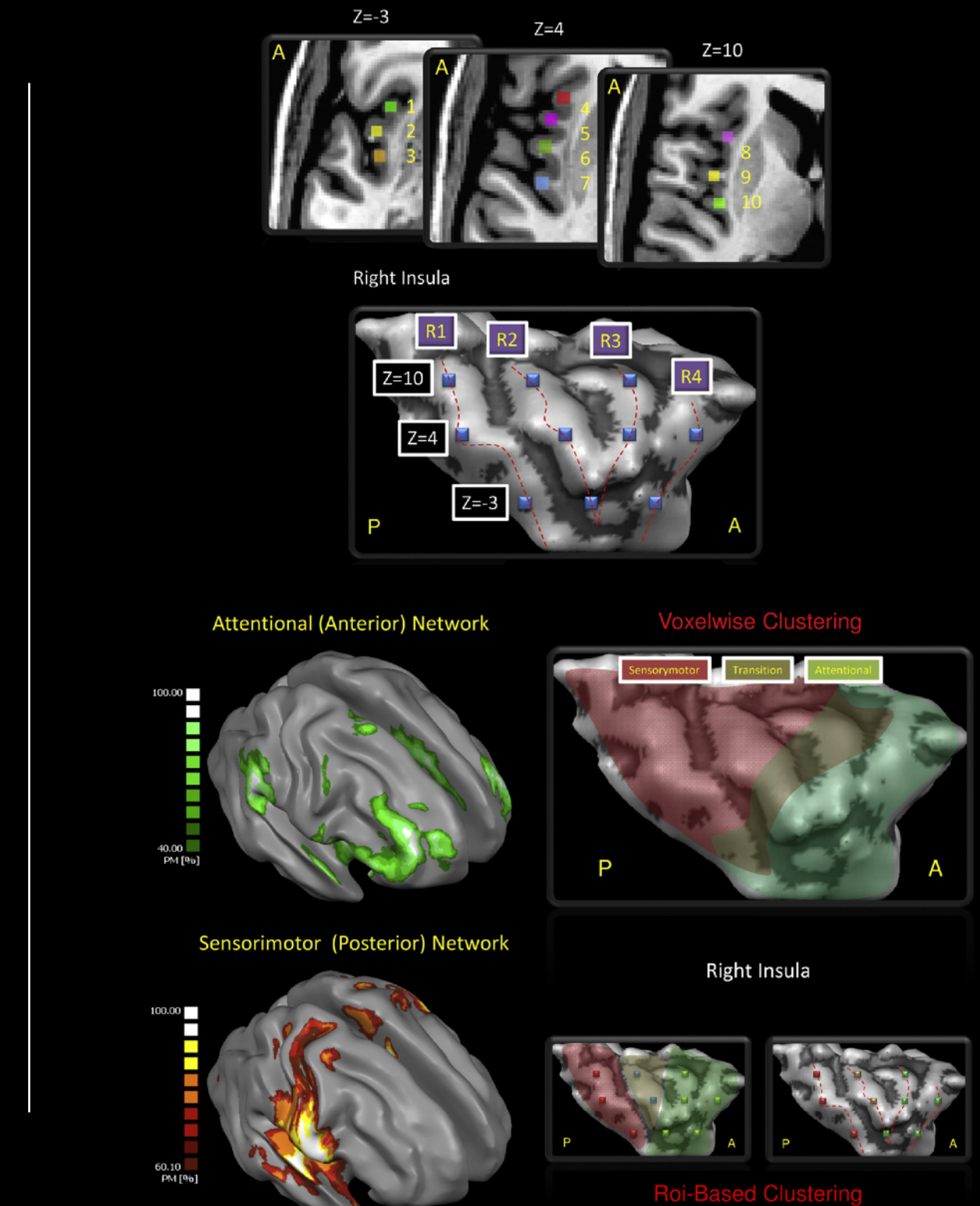
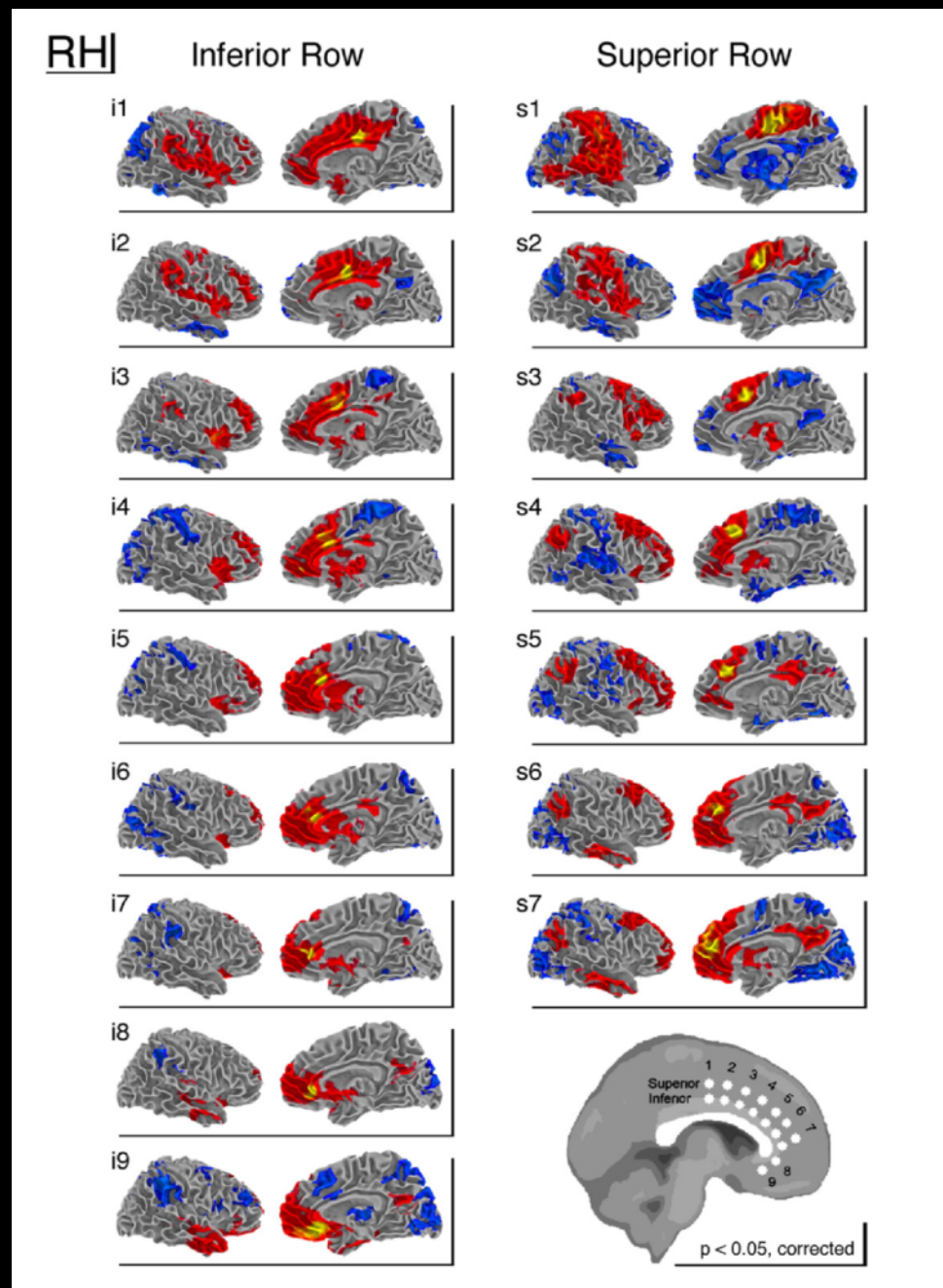


## EXTENSIONS - SEEDING FROM SEVERAL SEEDS



Fox et al 2005 PNAS

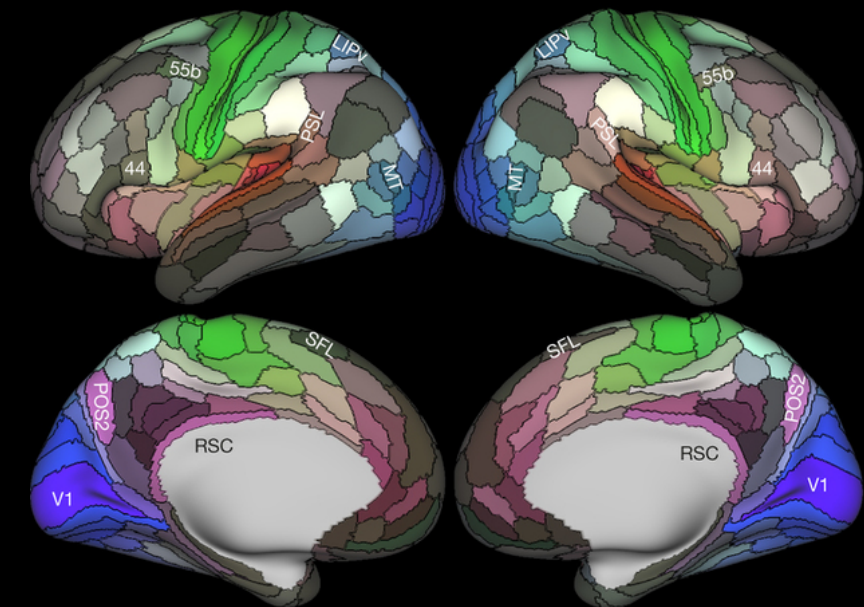
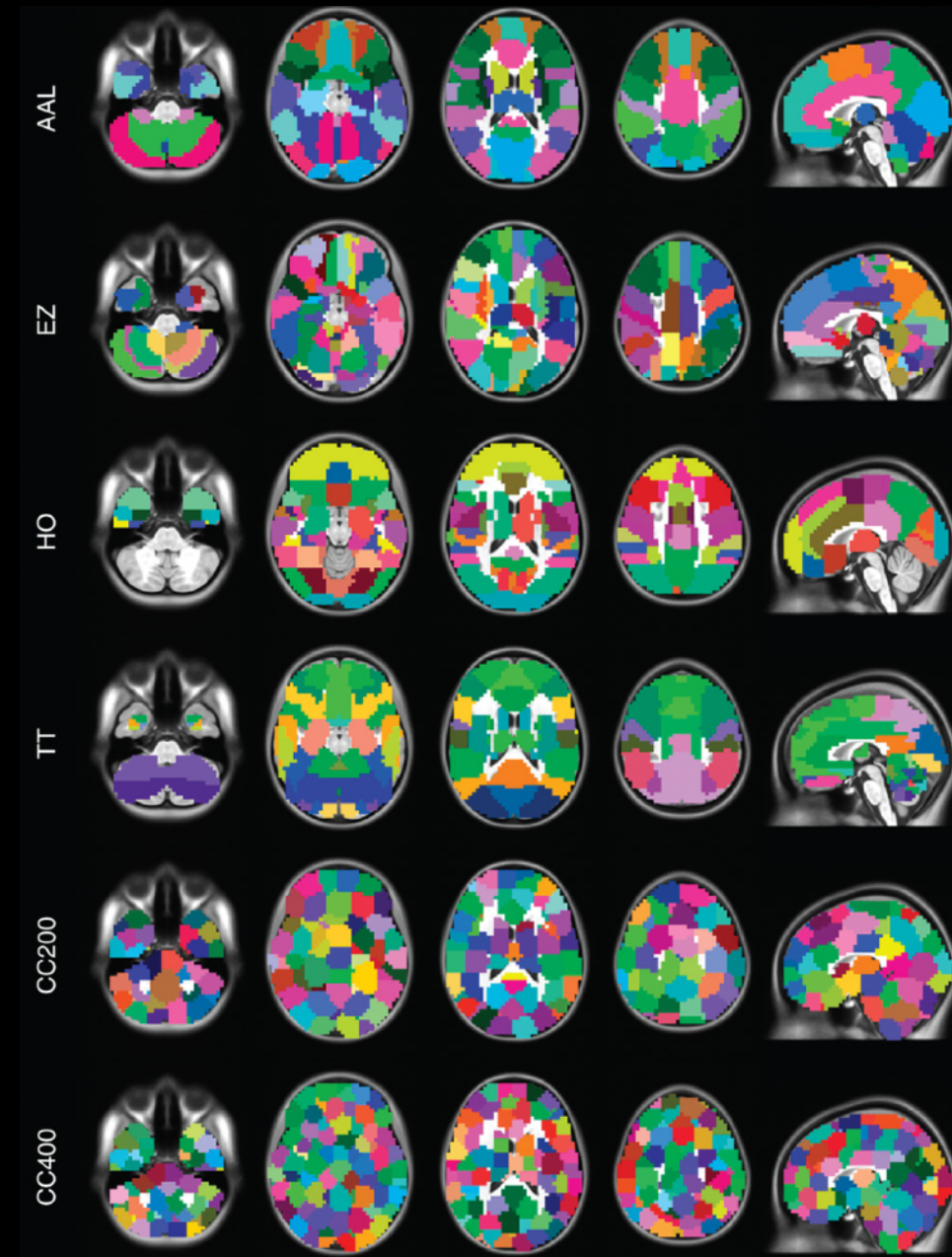
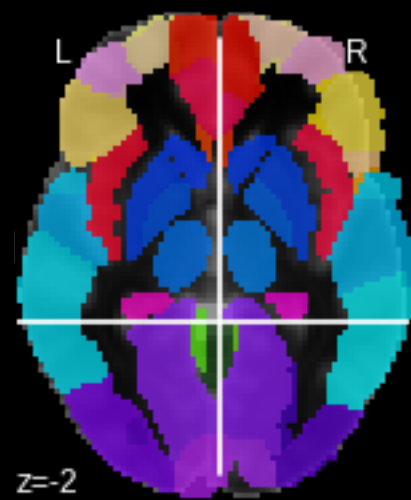
# EXTENSIONS- SYSTEMATIC SCA



Margulies et al 2007 NIMH

Cauda et al 2011 NIMH

## EXTENSIONS - PARCELLATION-BASED SCA

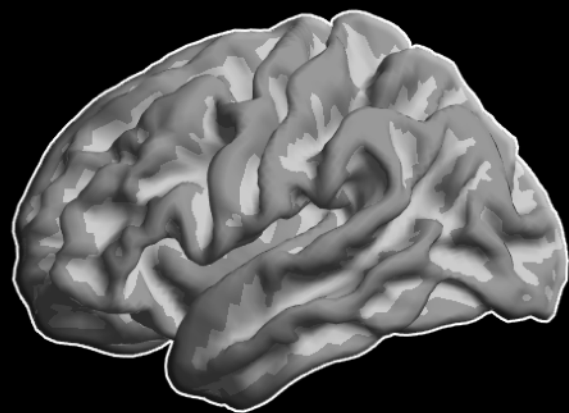


Tzuorio-Mazoyer et al 2002 NIMG

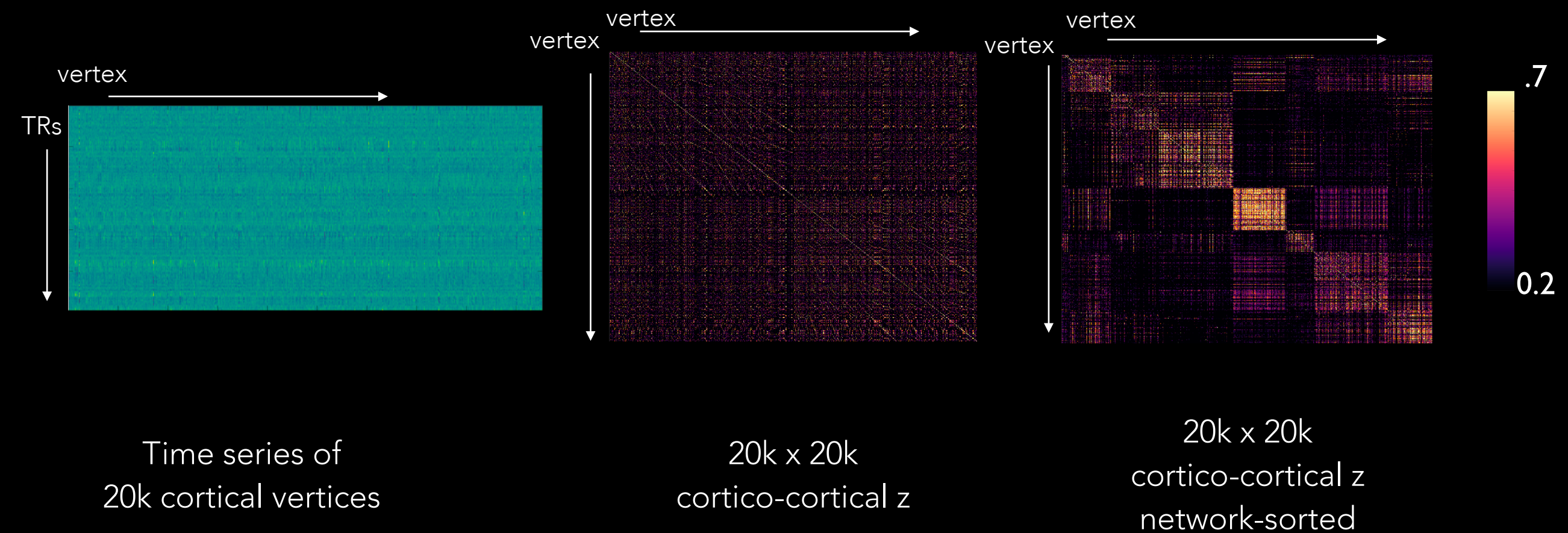
Craddock et al 2013 Nat Meth

Glasser et al 2016 Nature

## EXTENSIONS - WHOLE-BRAIN SCA



# IMAGING DATA: HIGH DIMENSIONAL AND MULTIVARIATE



# HOW TO IDENTIFY NETWORKS HOW TO REDUCE DATA DIMENSIONALITY

COMPRESSION

LINEAR (**PCA, ICA, FA, MDS,...**)

NON-LINEAR (LE, DME,.....)

CLUSTERING

K-MEANS

HIERARCHICAL

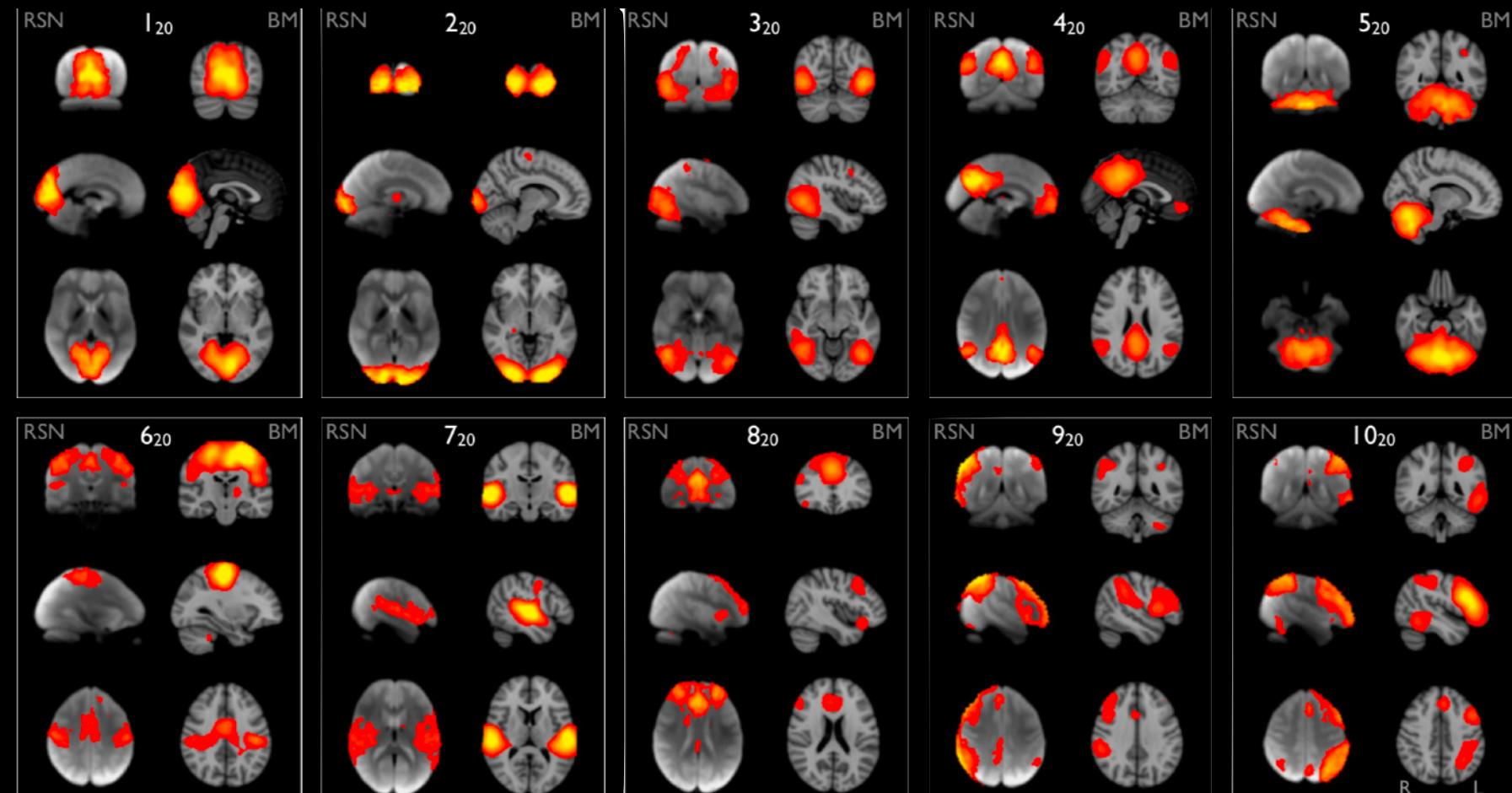
SPECTRAL

WEEK 4

→ WEEK 4

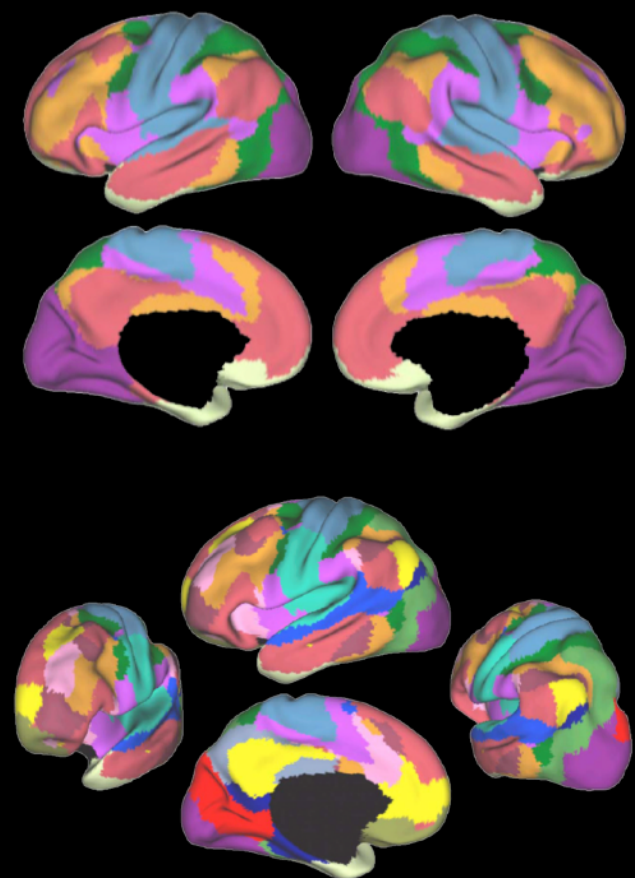
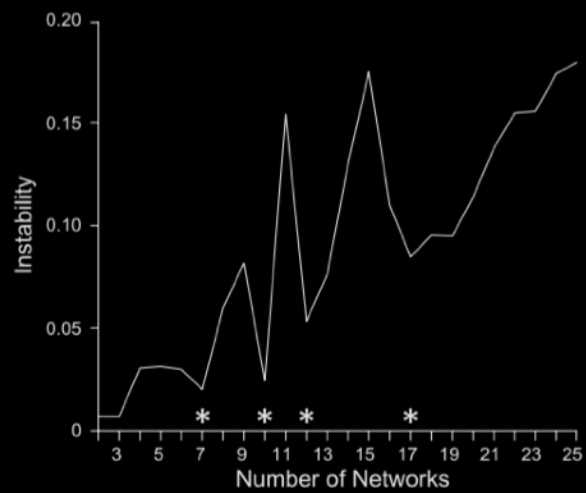
→ WEEK 6

# ICA

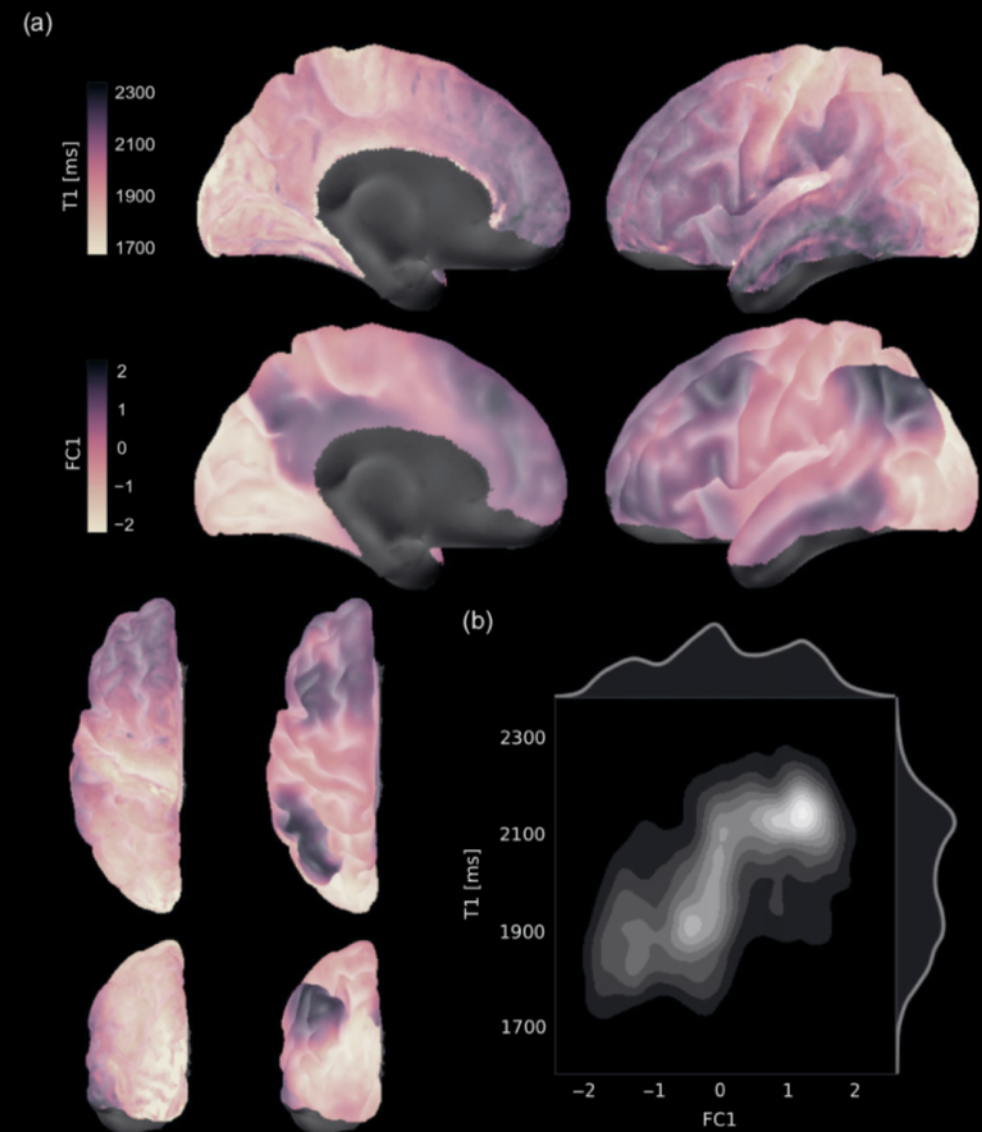
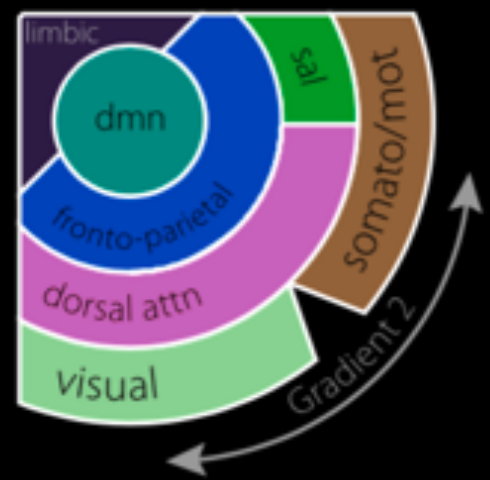
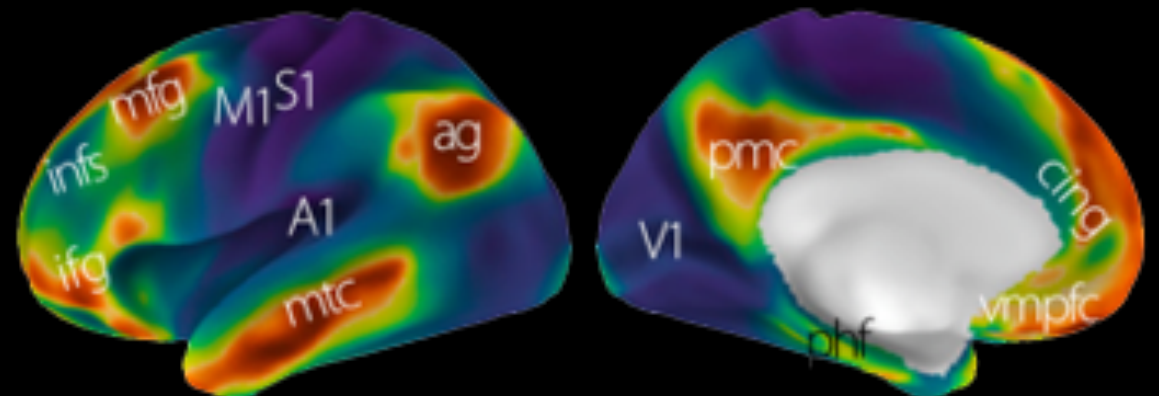


Smith et al 2009 PNAS

## NETWORK CLUSTERING



# CONNECTIVITY GRADIENTS



→ THIS WEEK

# RESTING-STATE fMRI CONNECTIVITY

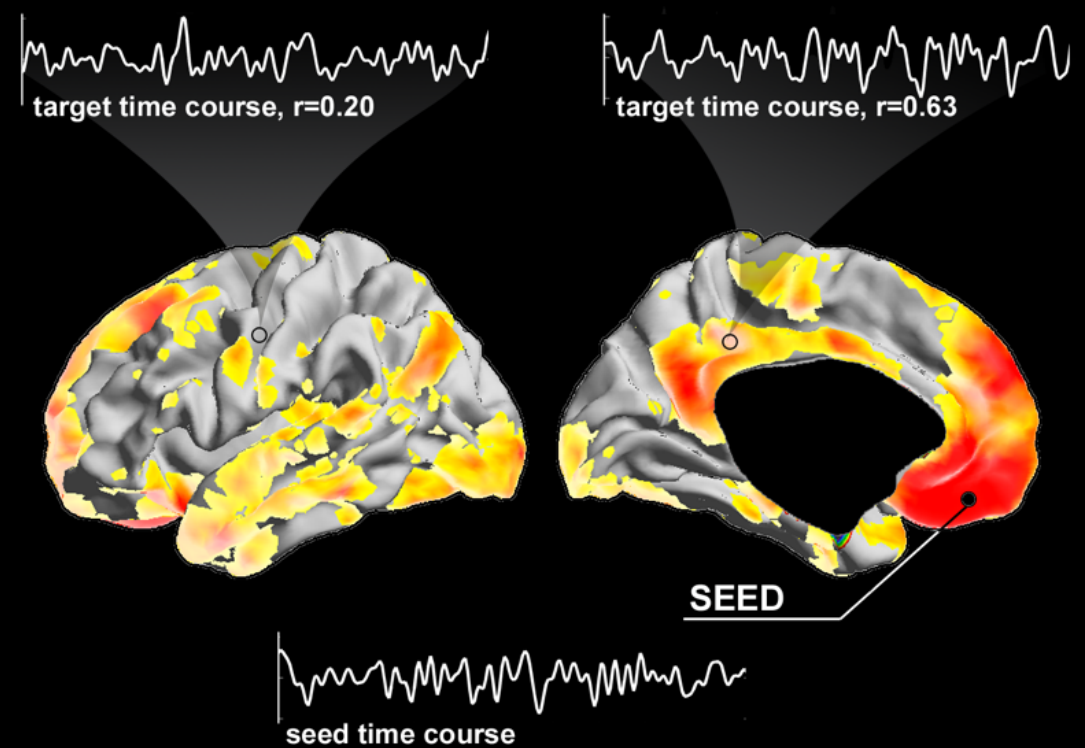
CORRELATION SPONTANEOUS  
BRAIN ACTIVITY

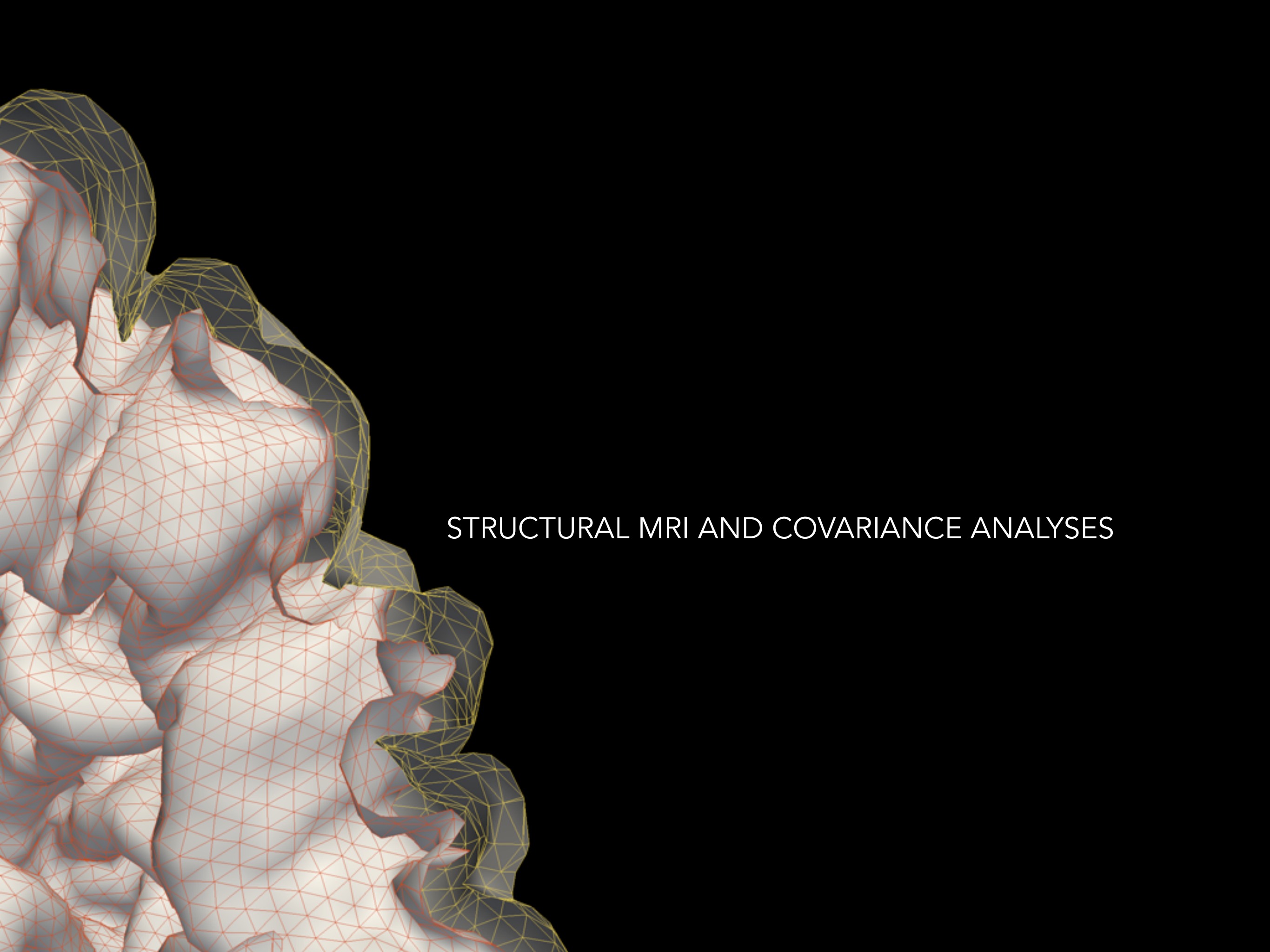
COST-EFFECTIVE & REPRODUCIBLE

INDIVIDUALIZED

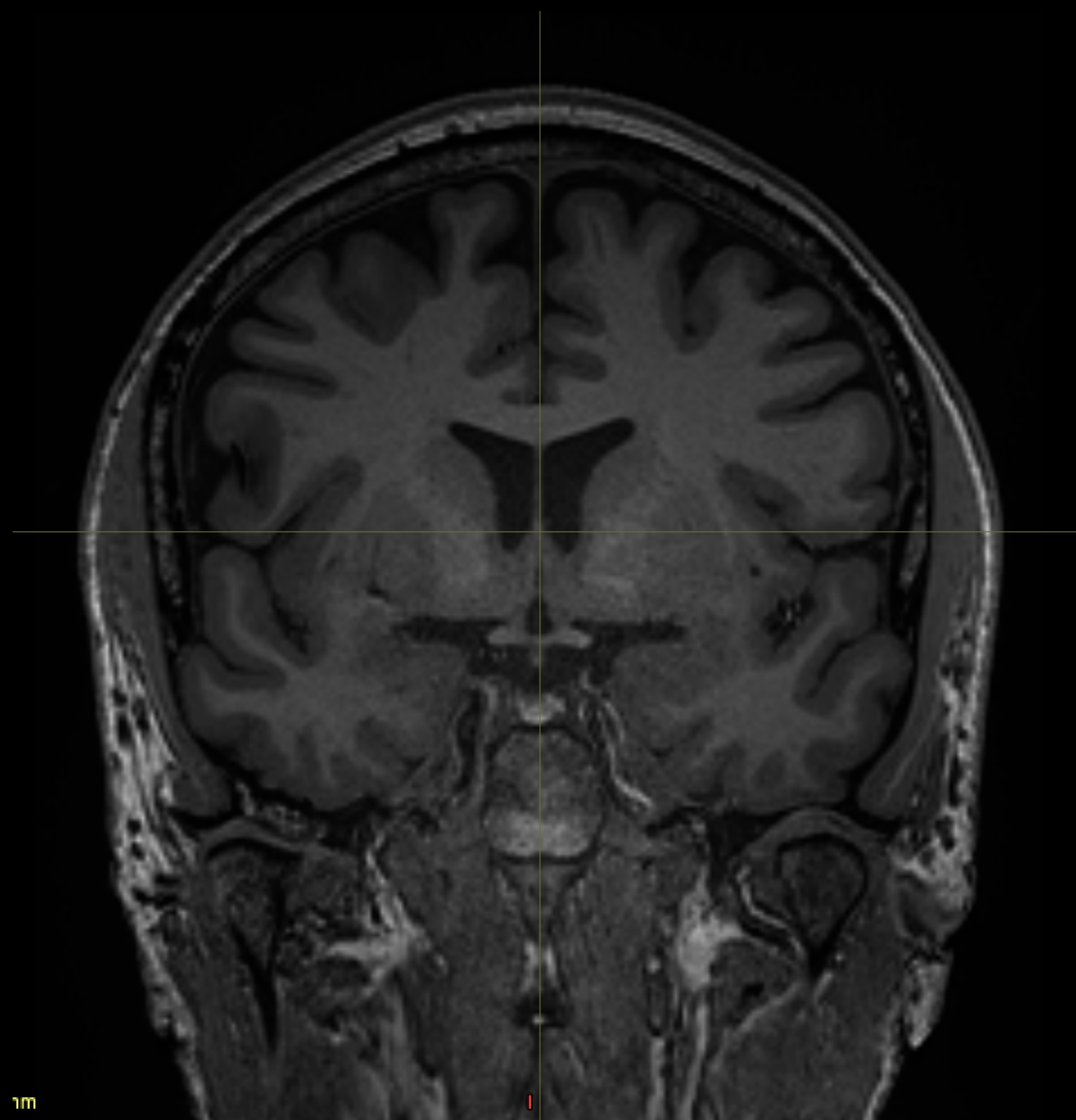
SEEDING FROM GM -  
ALLOWING DIRECT CORRELATIONS  
WITH OTHER CORTICAL FEATURES

CHALLENGES REMAIN:  
EFFECTS OF PHYSIOLOGY,  
MOTION,  
INDIRECT CONNECTIONS,  
CORRELATION WITH MENTAL STATES  
& INDUCTION





STRUCTURAL MRI AND COVARIANCE ANALYSES



1m

some processing...



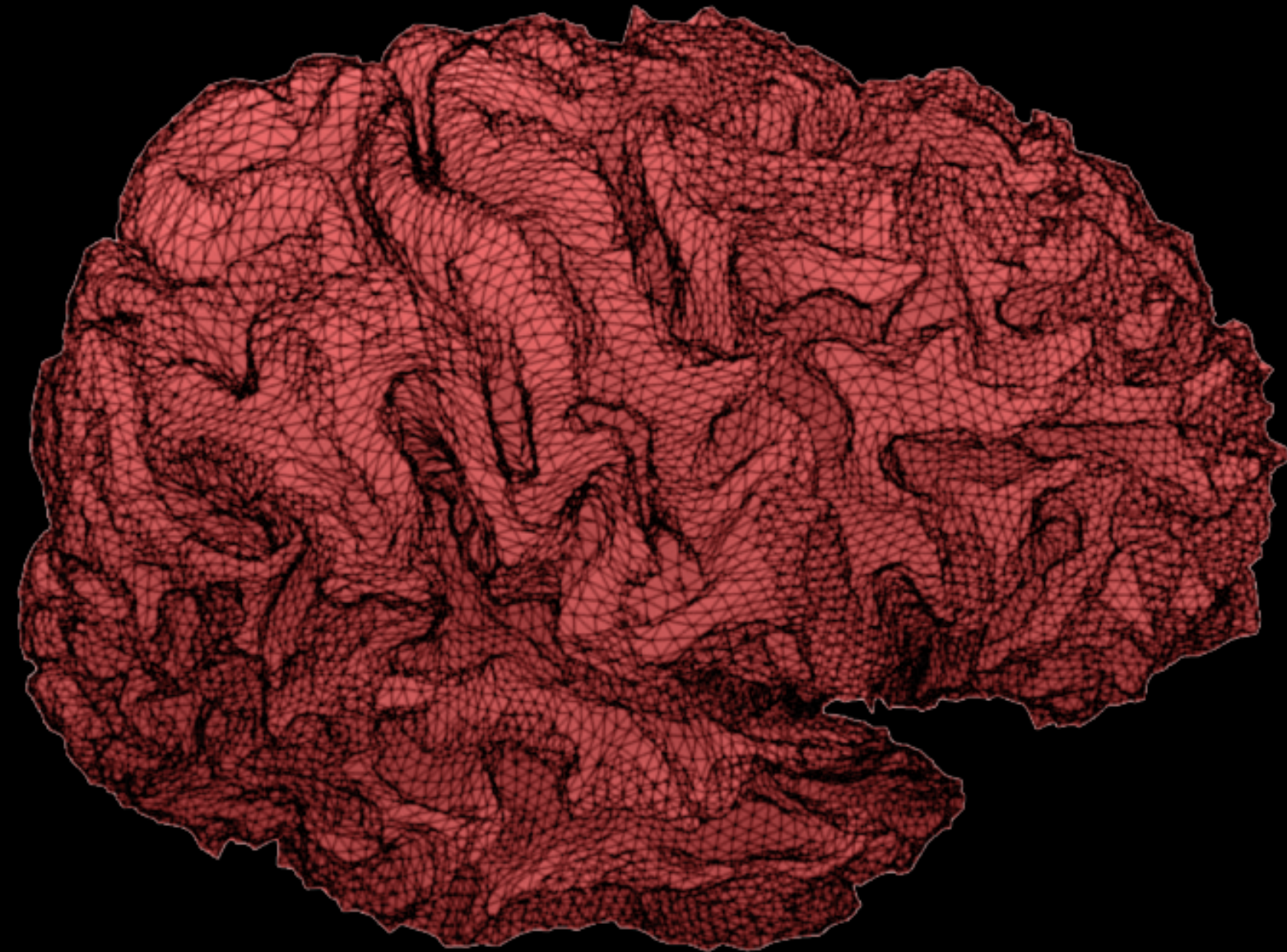
CIVET

OMM: March 17

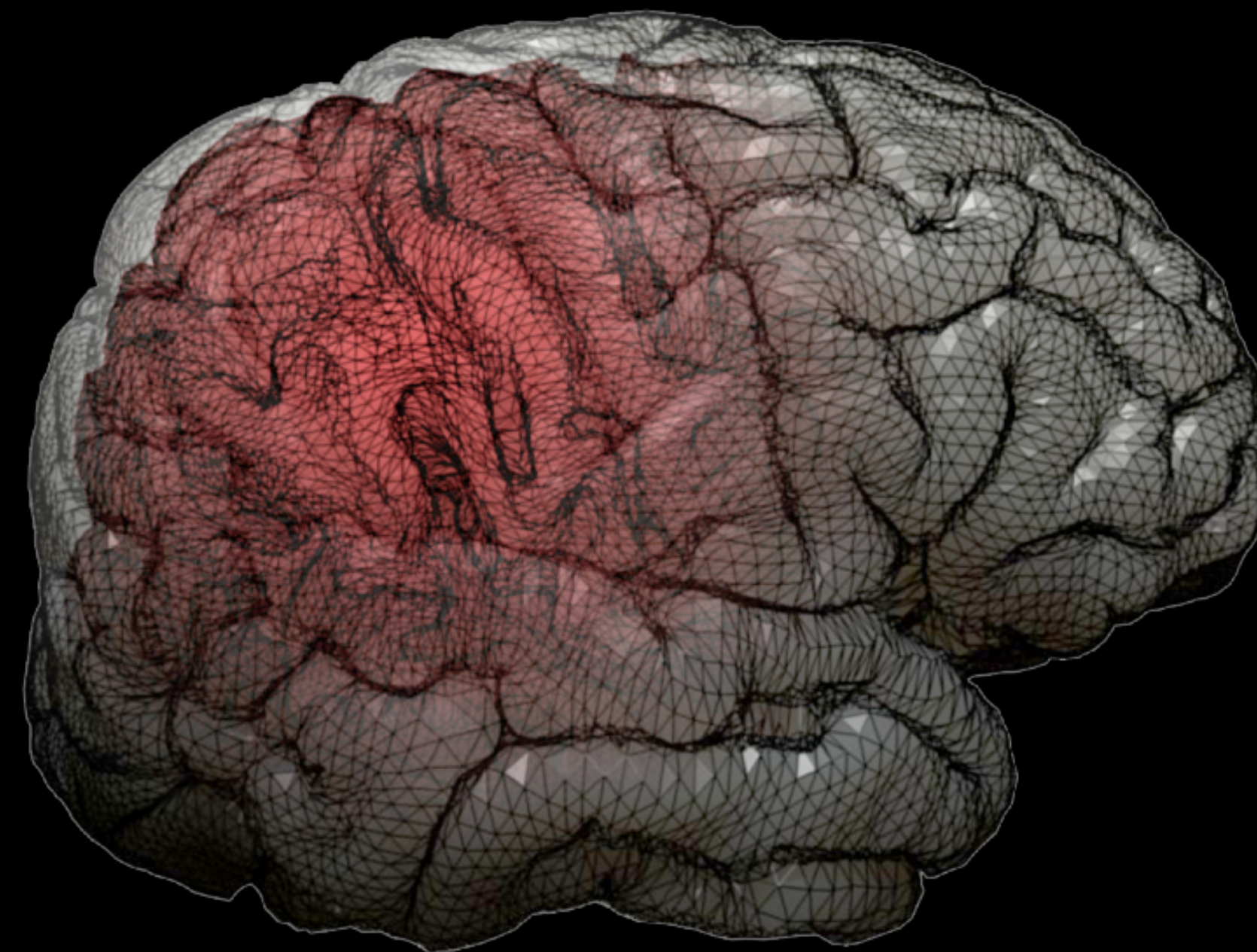
MacDonald et al. (2000) *NeuroImage*

Kim et al. (2005) *NeuroImage*

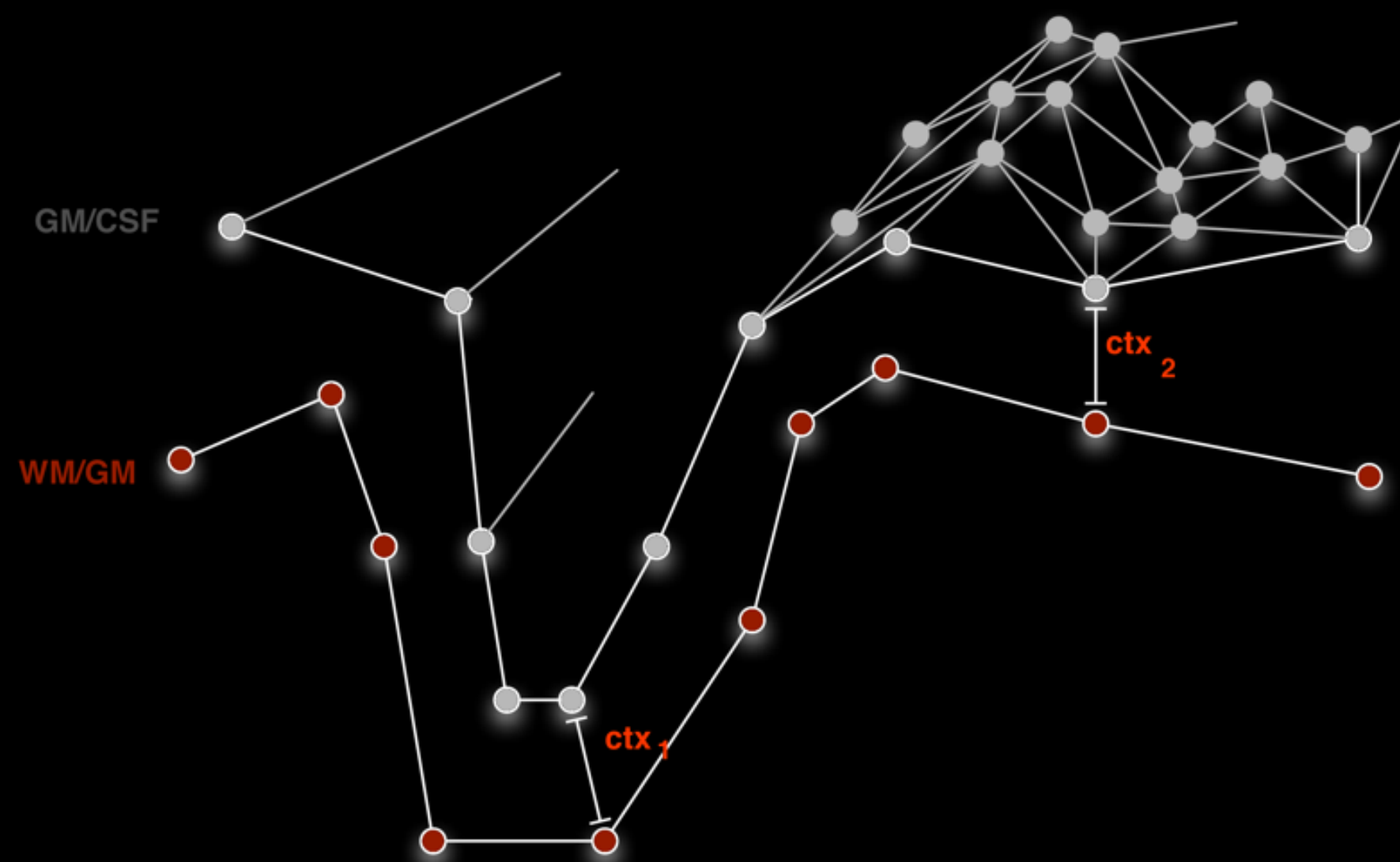
WM surface



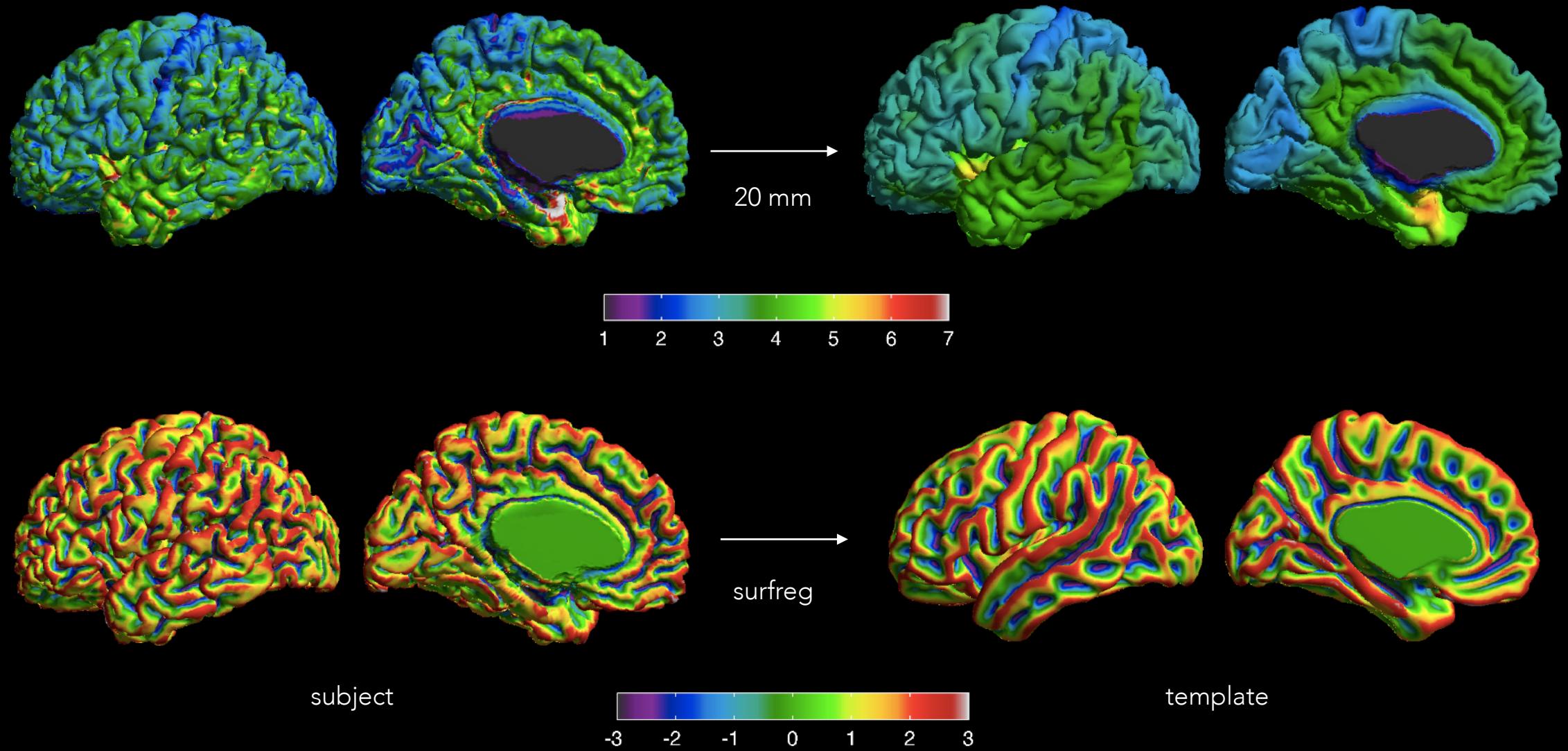
GM surface



# THICKNESS



# SURFACE BASED PROCESSING

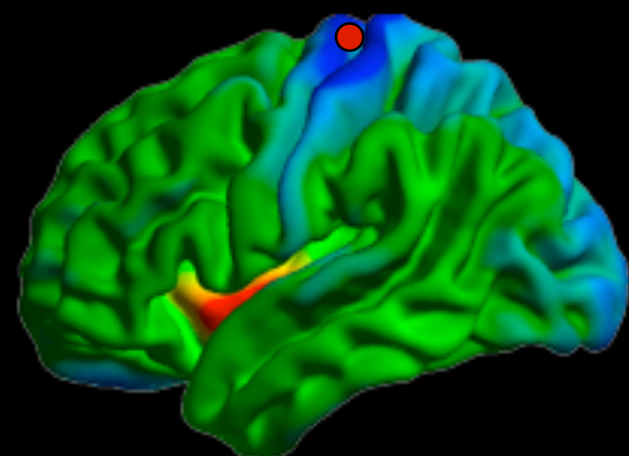


Chung et al. (2003) NeuroImage

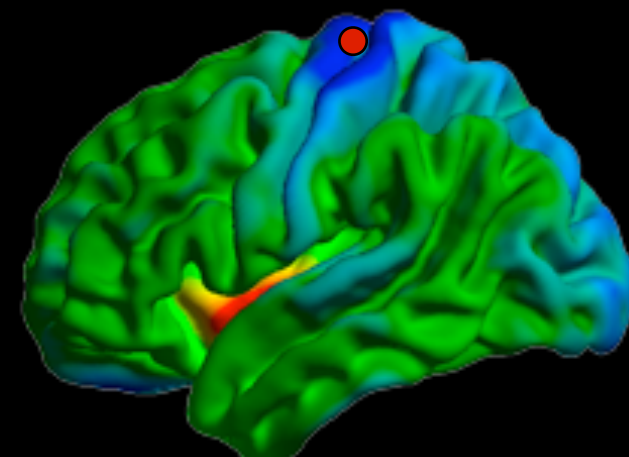
Robbins et al. (2004) MedImaAnalysis

# STATS

Controls



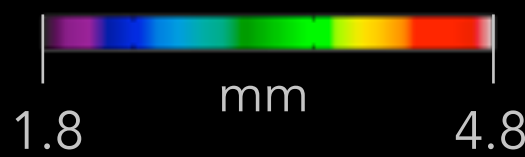
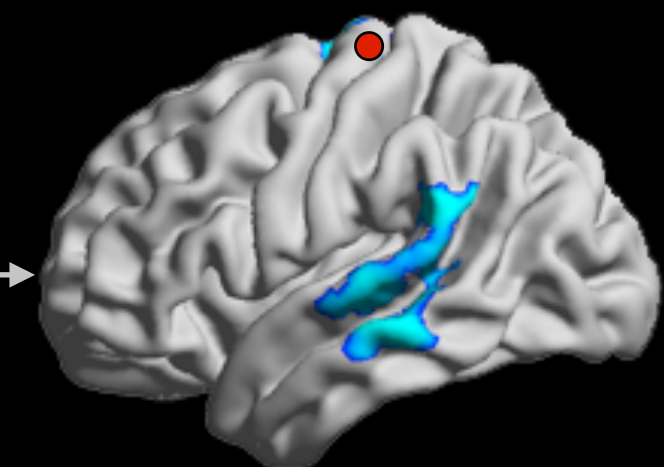
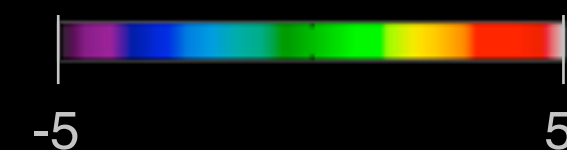
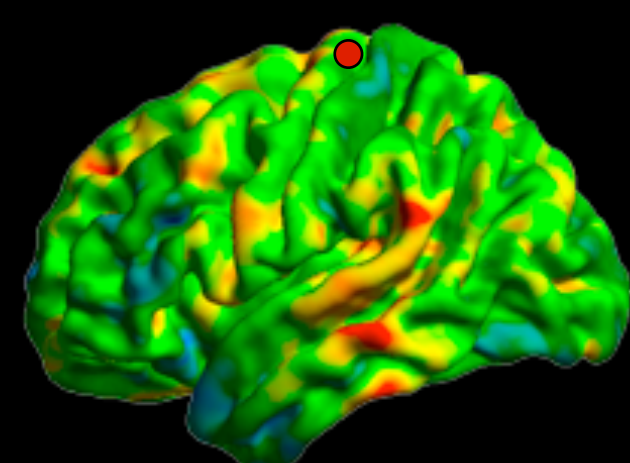
Patients



GLM

t-map

p-values



# MRI COVARIANCE ANALYSIS

IDEA:  
CORRELATE MRI  
INDICES ACROSS SUBJECTS

+

COST-EFFECTIVE, REPRODUCIBLE

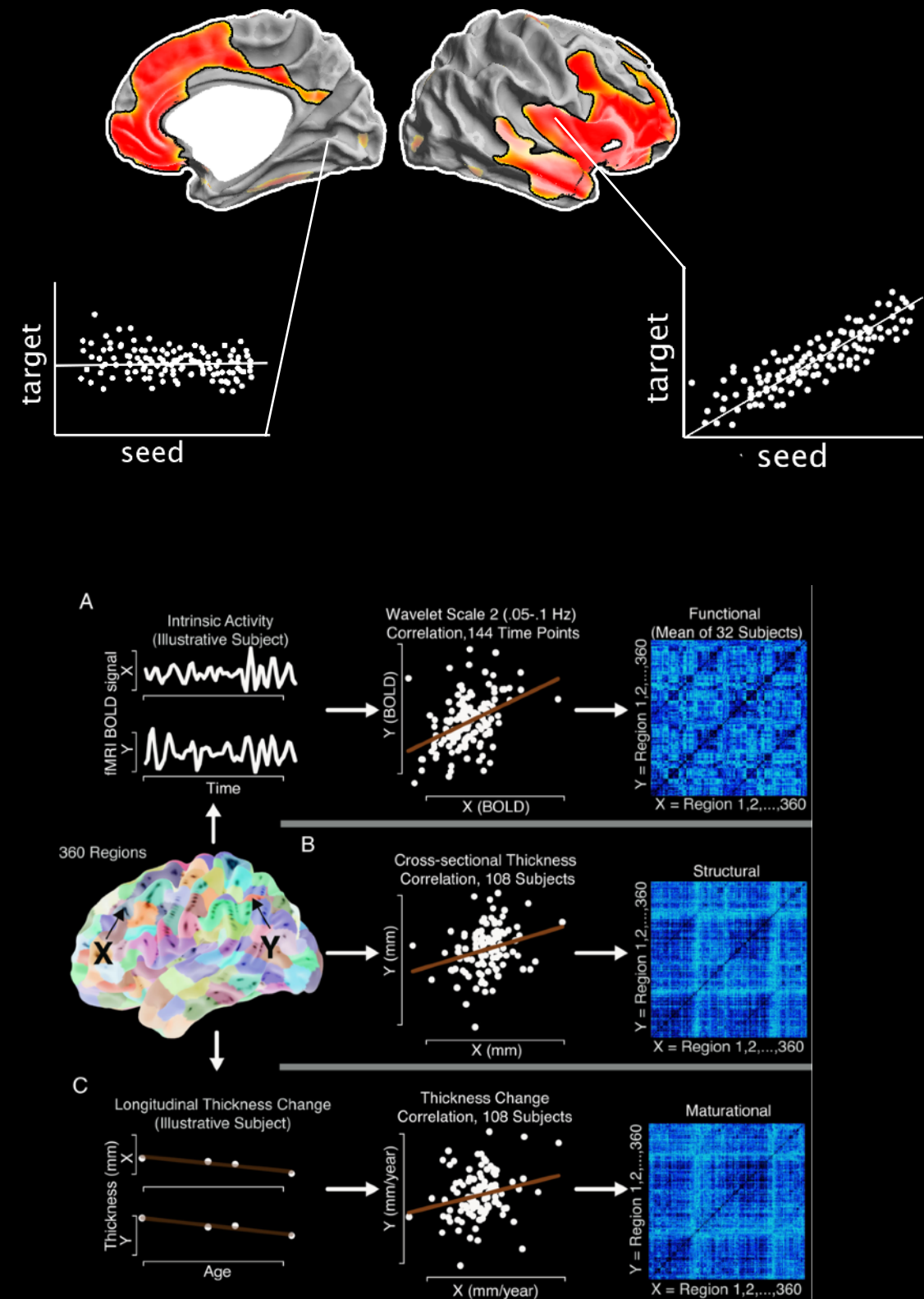
DIRECT SEEDING FROM GREY  
MATTER POSSIBLE

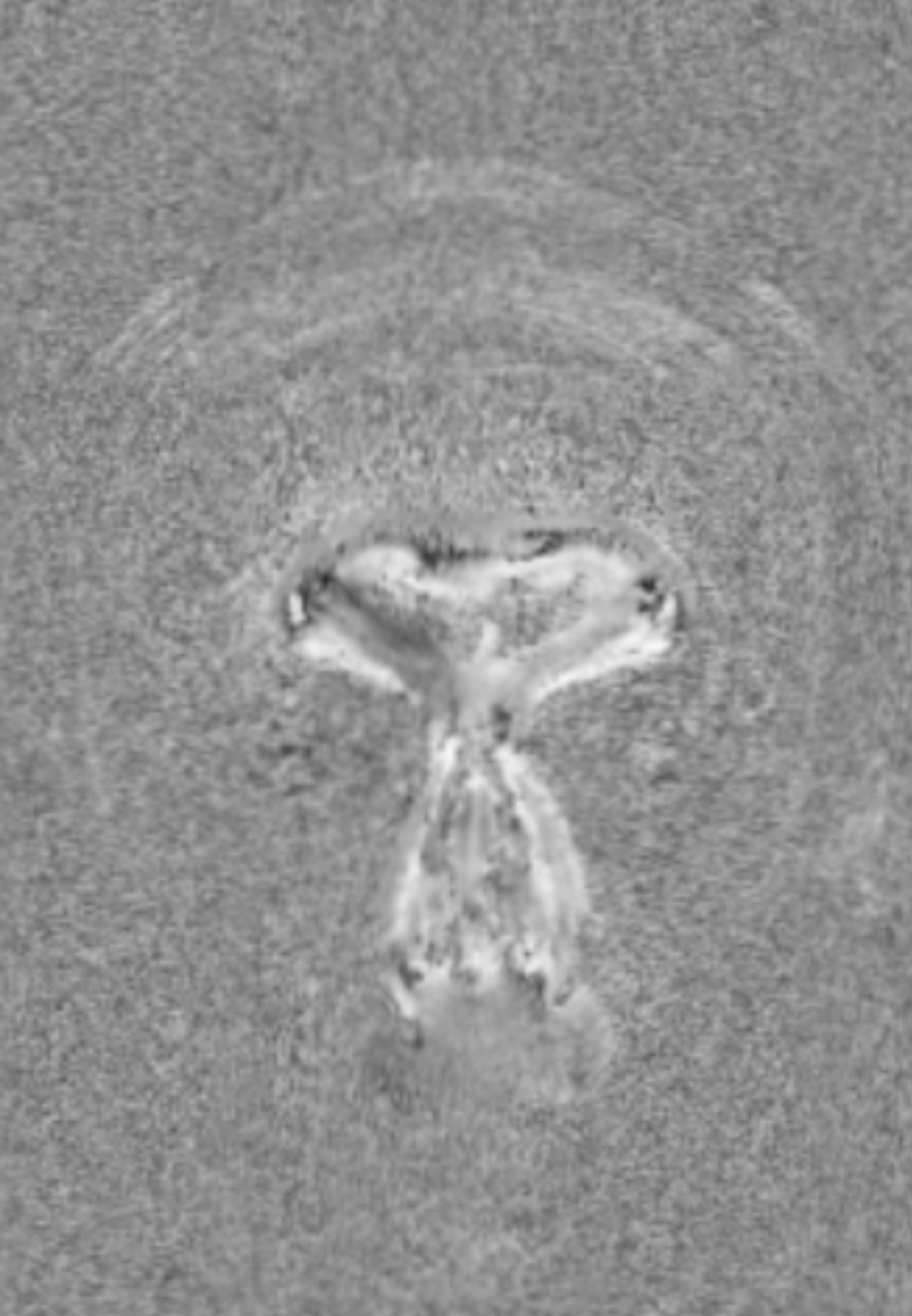
SIMPLE PREPROCESSING AND MODELLING

-

ONLY GROUP-WISE

RELATES RATHER TO PROCESSES  
THAN TO STATES





MICROSTRUCTURE  
AND MICROSTRUCTURAL  
PROFILE COVARIANCE

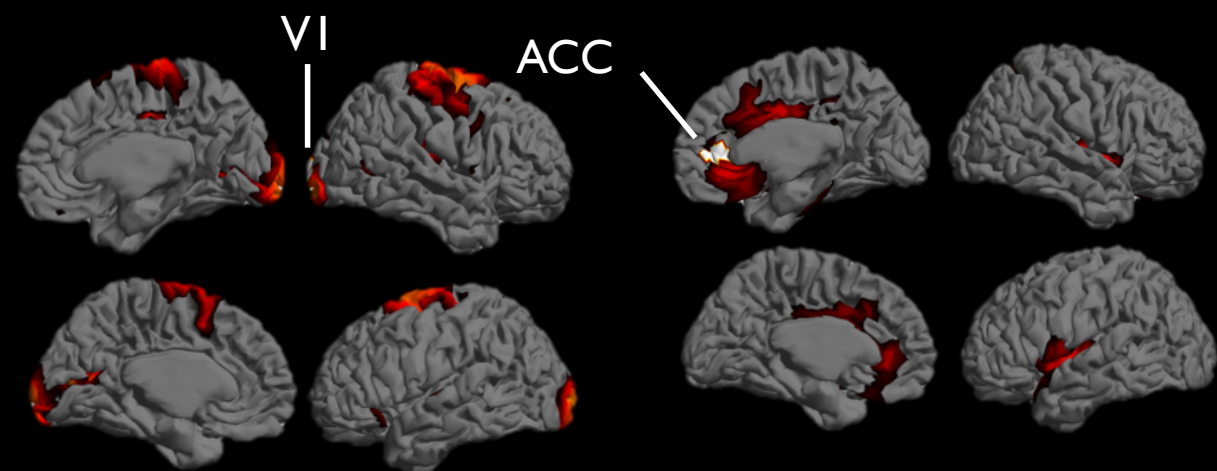
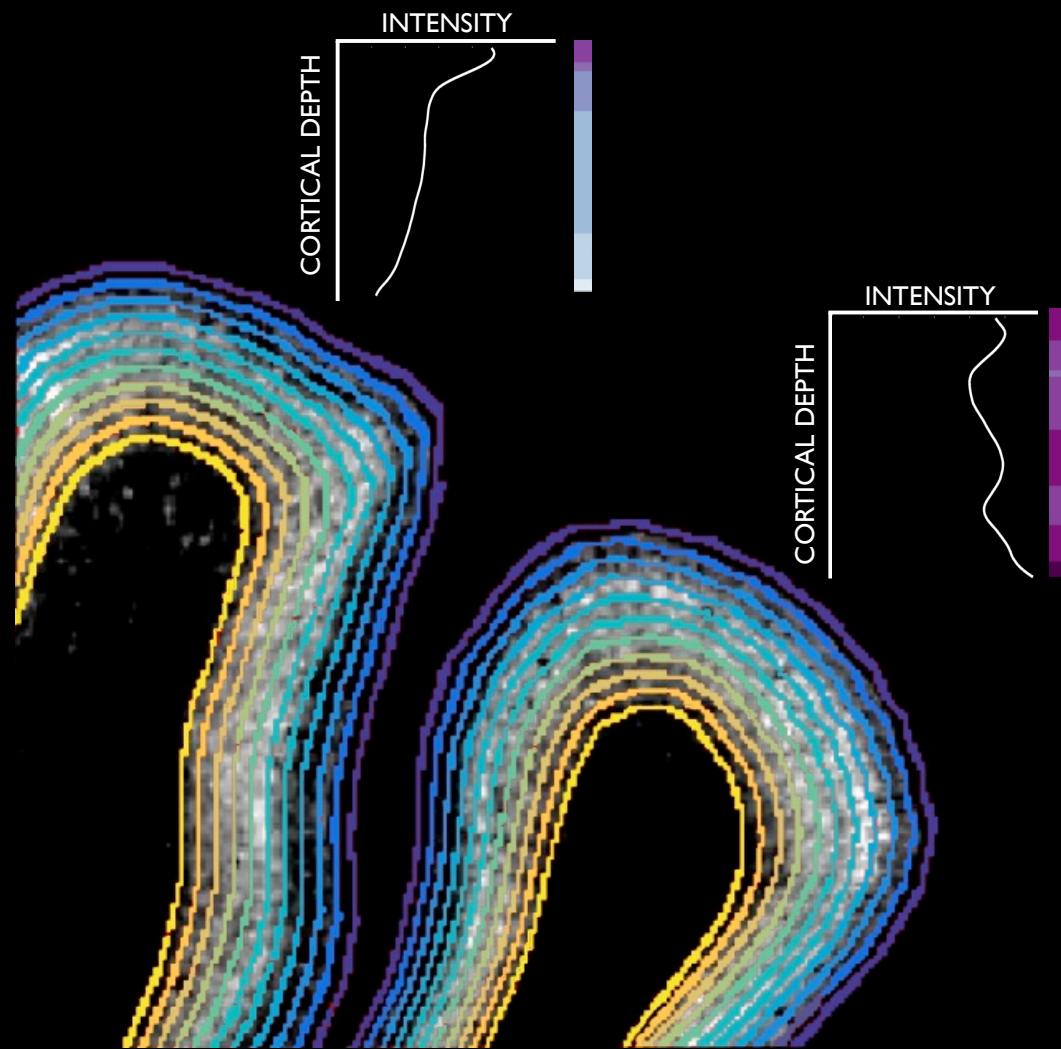
# MICROSTRUCTURAL COVARIANCE ANALYSIS

SINGLE SUBJECT PROFILING OF BRAIN STRUCTURE

MEASUREMENTS OF INTRACORTICAL TISSUE INTENSITY

CORRELATION OF MEASURES BETWEEN AREAS

PROVIDES SINGLE SUBJECT MICROSTRUCTURAL NETWORKS



# MICROSTRUCTURAL COVARIANCE ANALYSIS

SINGLE SUBJECT PROFILING OF BRAIN STRUCTURE

MEASUREMENTS OF INTRACORTICAL TISSUE INTENSITY

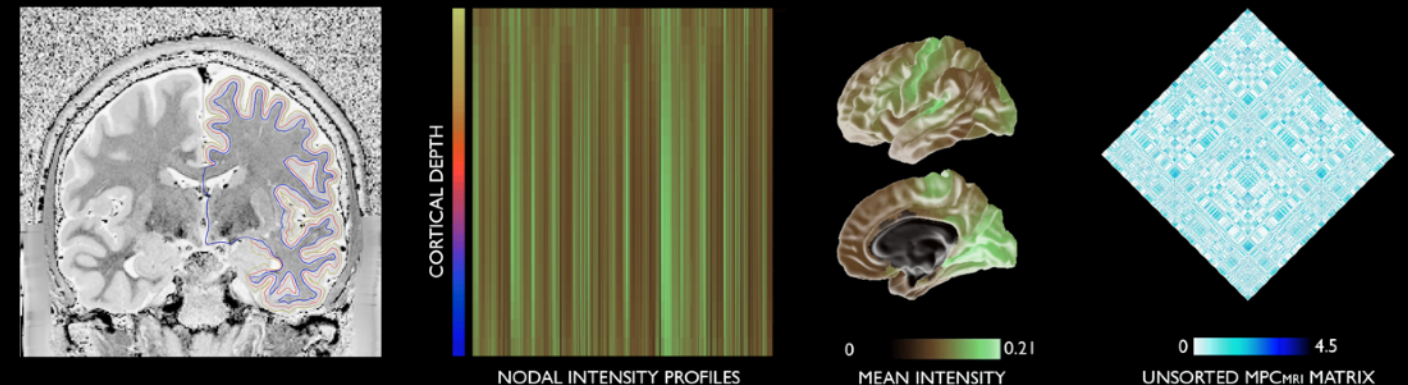
HISTOLOGICALLY VALIDATED

REPRODUCIBLE ACROSS T1W/T2W, QT1, MT

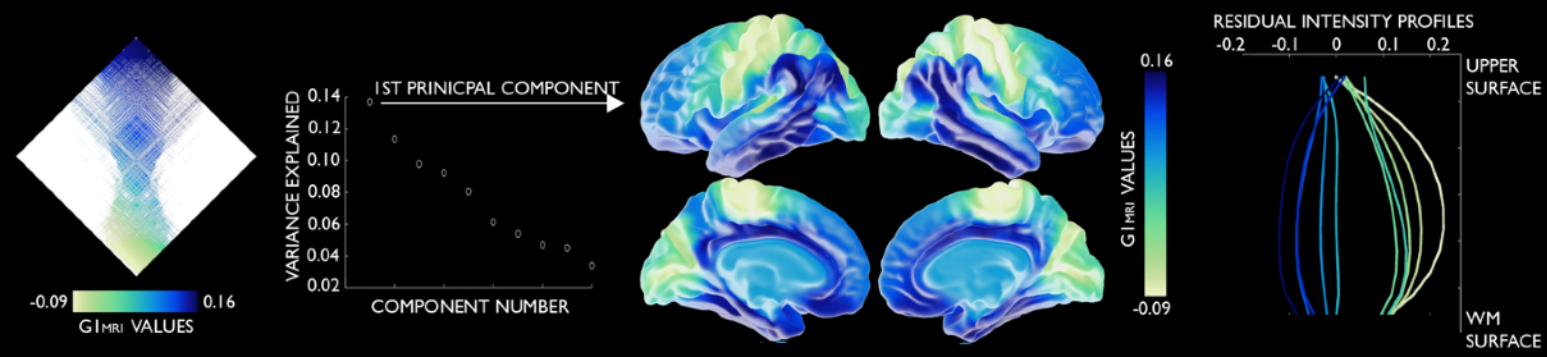
WORKS AT 3T AND 7T

REPLICABLE ACROSS INDIVIDUAL SUBJECTS

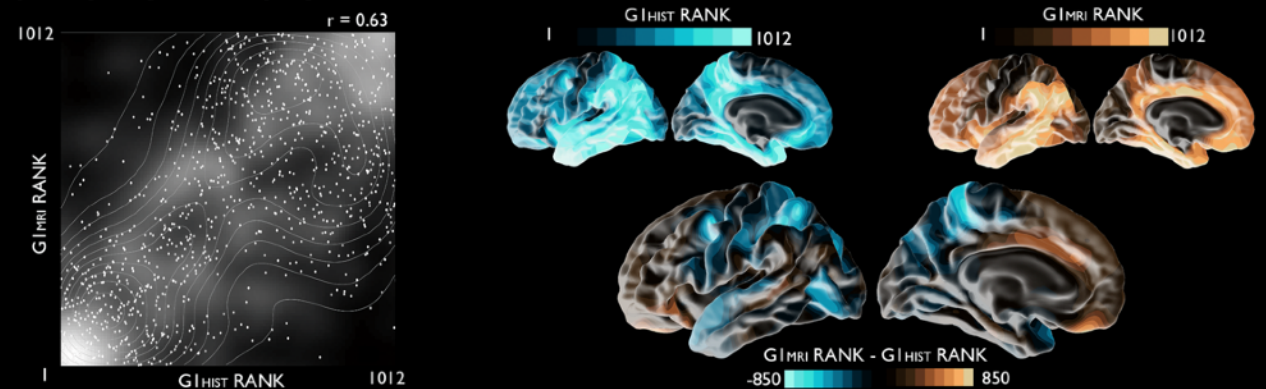
## A) IN-VIVO SURFACE CONSTRUCTION AND SAMPLING



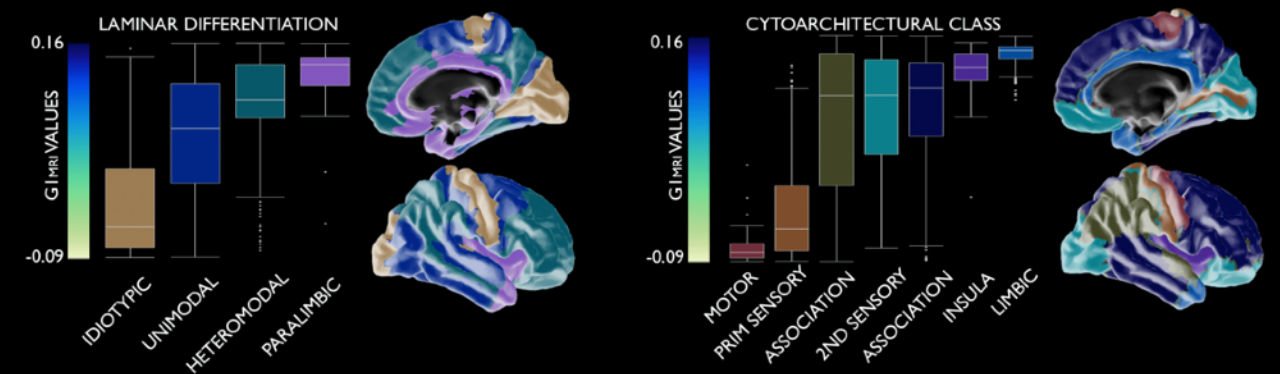
## B) IN VIVO GRADIENT OF MICROSTRUCTURE PROFILE COVARIANCE ( $G_{IMRI}$ )



## C) RELATION OF $G_{IMRI}$ TO $G_{IHIST}$



## D) NEUROSTRUCTURAL CORRELATES OF $G_{IMRI}$



# THIS WEEK

OXFORD

## ORIGINAL ARTICLE

### A Systematic Relationship Between Functional Connectivity and Intracortical Myelin in the Human Cerebral Cortex

Julia M. Huntenburg<sup>1,2</sup>, Pierre-Louis Bazin<sup>3,4</sup>, Alexandros Goulas<sup>5</sup>, Christine L. Tardif<sup>3,6</sup>, Arno Villringer<sup>3</sup> and Daniel S. Margulies<sup>1</sup>

<sup>1</sup>Max Planck Research Group for Neuroanatomy and Connectivity, Max Planck Institute for Human Cognitive and Brain Sciences, 04103 Leipzig, Germany, <sup>2</sup>Neurocomputation and Neuroimaging Unit, Department of Education and Psychology, Free University of Berlin, 14195 Berlin, Germany, <sup>3</sup>Department of Neurology, Max Planck Institute for Human Cognitive and Brain Sciences, 04103 Leipzig, Germany, <sup>4</sup>Department of Neurophysiology, Max Planck Institute for Human Cognitive and Brain Sciences, 04103 Leipzig, Germany, <sup>5</sup>Institute of Computational Neuroscience, University Medical Center Hamburg-Eppendorf, 20246 Hamburg, Germany and <sup>6</sup>Cerebral Imaging Centre, Douglas Mental Health University Institute, McGill University H4H 1R3, Montreal, QC, Canada

Address correspondence to Pierre-Louis Bazin. Email: bazin@cbs.mpg.de; Daniel S. Margulies. Email: margulies@cbs.mpg.de

Cerebral Cortex, February 2017;27: 981–997

doi: 10.1093/cercor/bhw030  
Advance Access Publication Date: 10 February 2017  
Original Article

Downloaded from https://academic.oup.com/cercor/article-abstract/27/2/981/2981988 by guest on 10 February 2017



## ARTICLE

DOI: 10.1038/s41467-017-01285-x

OPEN

### The challenge of mapping the human connectome based on diffusion tractography

Klaus H. Maier-Hein

Tractography based on non-invasive diffusion imaging is central to the study of human brain connectivity. To date, the approach has not been systematically validated in ground truth studies. Based on a simulated human brain data set with ground truth tracts, we organized an open international tractography challenge, which resulted in 96 distinct submissions from 20 research groups. Here, we report the encouraging finding that most state-of-the-art algorithms produce tractograms containing 90% of the ground truth bundles (to at least some extent). However, the same tractograms contain many more invalid than valid bundles, and

HUNTBURG ET AL. 2017 CEREBRAL CORTEX

## Subjects 1-8

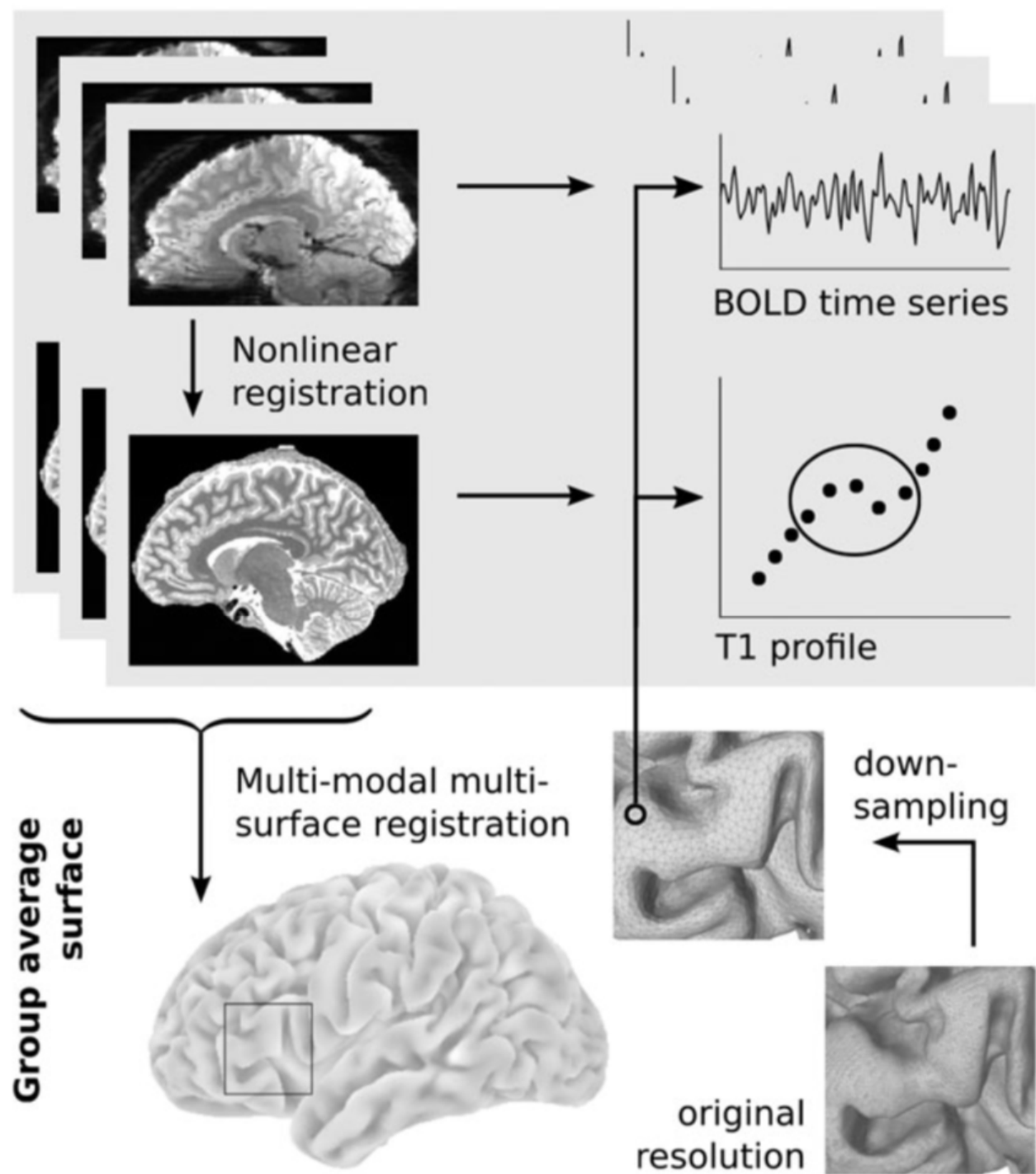
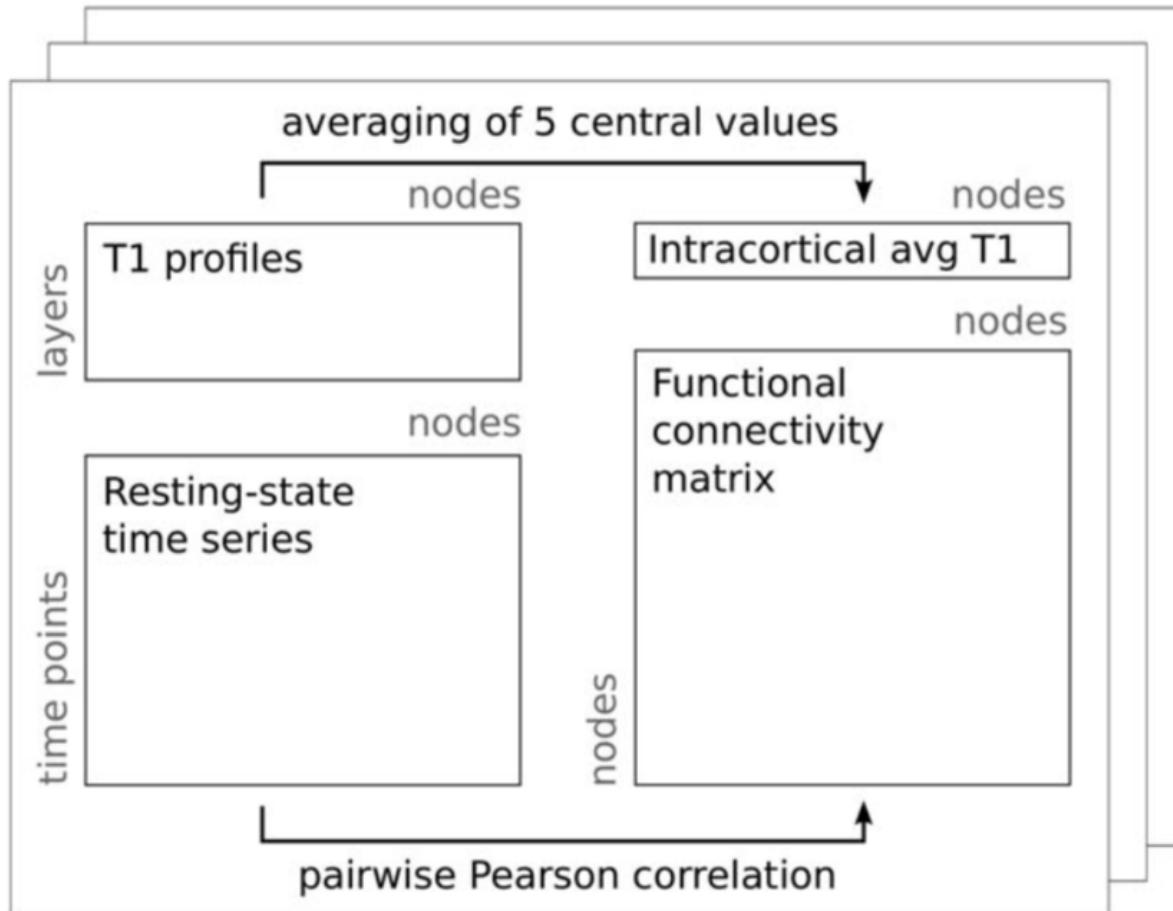
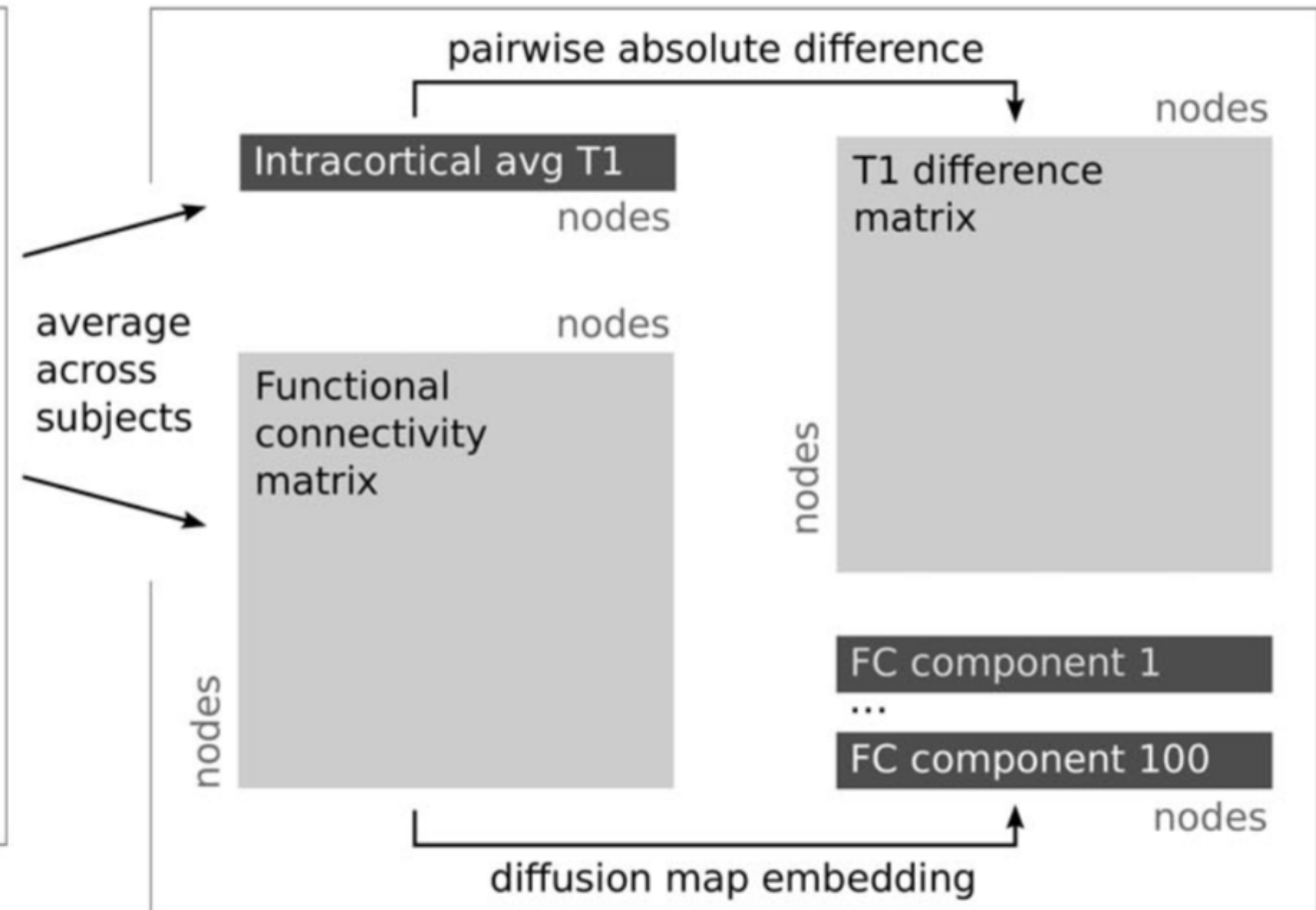


**Figure 1.** Data extraction workflow. Resting-state images were nonlinearly co-registered to the structural space of the same subject. A group-specific surface template was created using midcortical surfaces and intracortical  $T_1$  contrasts of all subjects in a multimodal multisurface registration approach. The group-average surface was downsampled and projected into the space of each subject for sampling of BOLD time series and  $T_1$  profiles. Cortical depth profiles were sampled according to an equi-volumetric principle; only the central values were averaged to minimize partial volume effects.

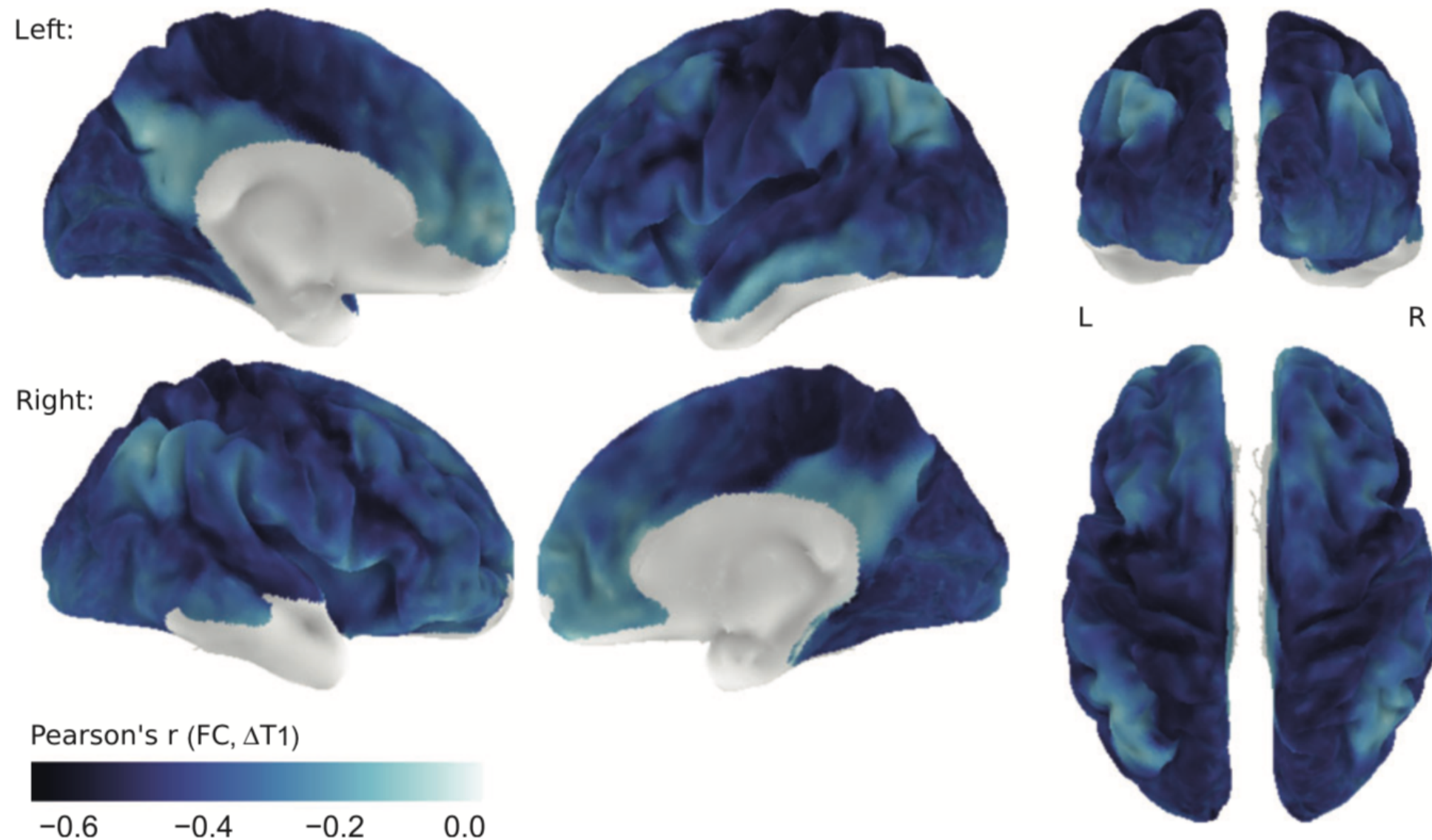
## Subject 1-8



## Group average

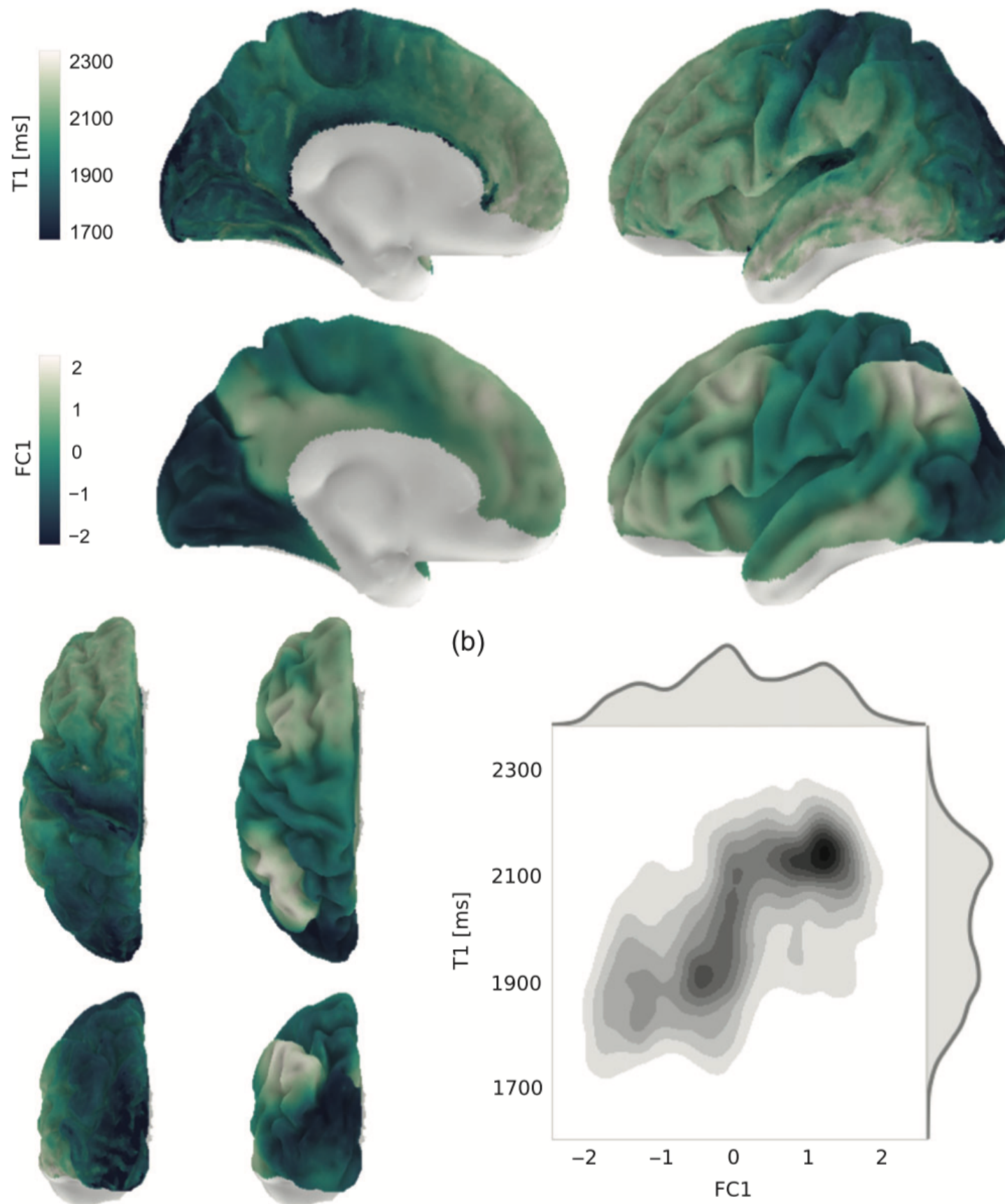


■ Comparing FC matrix and T1 difference matrix  
■ Modelling intracortical avg T1 using FC components

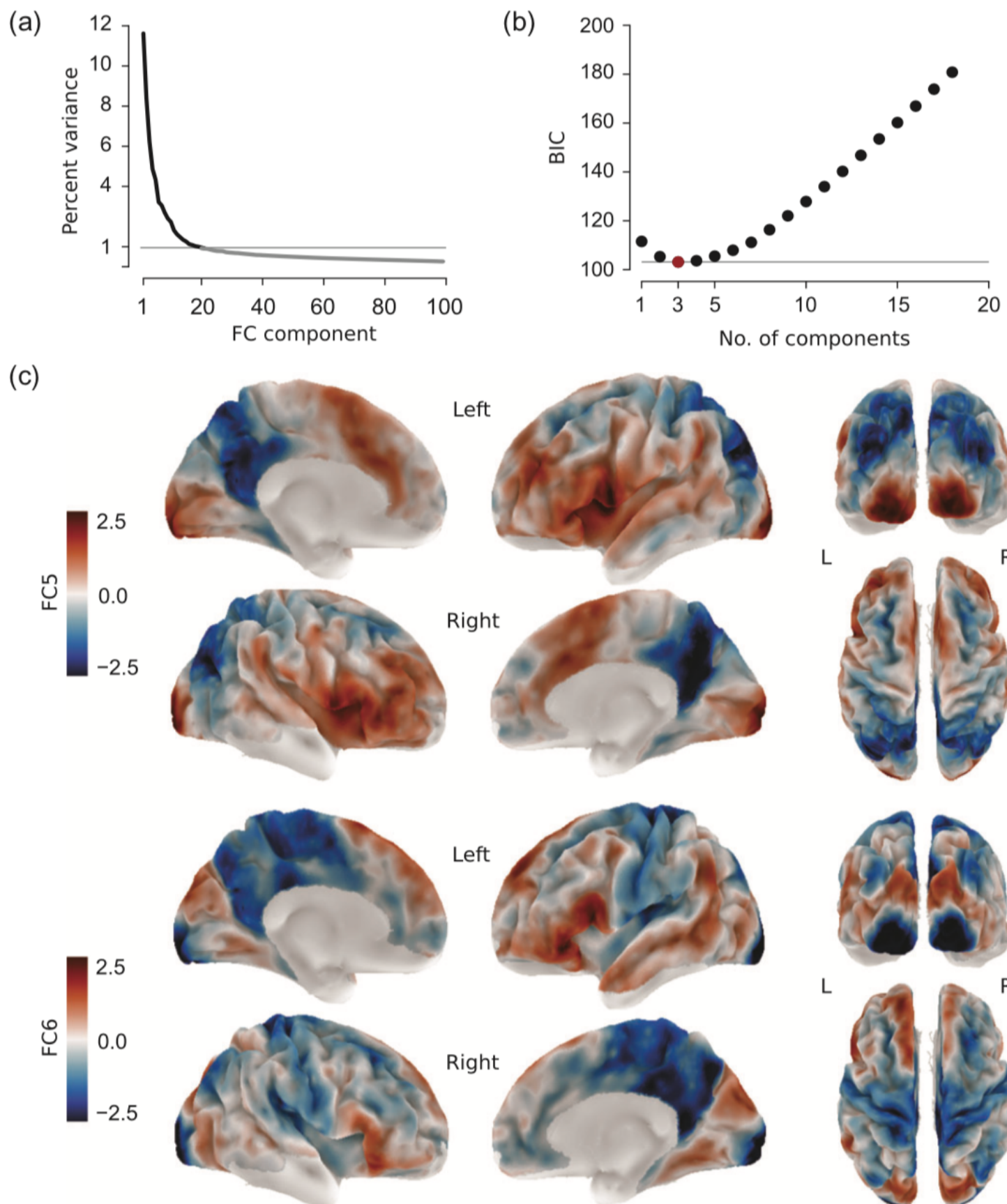


**Figure 3.** Node-wise correlation of functional connectivity and  $T_1$  difference. For each surface node, the correlation between its functional connectivity to all other nodes and its  $T_1$  difference to all other nodes is shown. Values closer to zero (white) indicate a weaker linear relationship between connectivity strengths and  $T_1$  differences. Correlation values are shown on the left (L) and right (R) hemisphere of the group average surface. Nodes with low signal quality in either imaging modality (predominantly in orbitofrontal and ventral temporal areas) were excluded from the analysis.

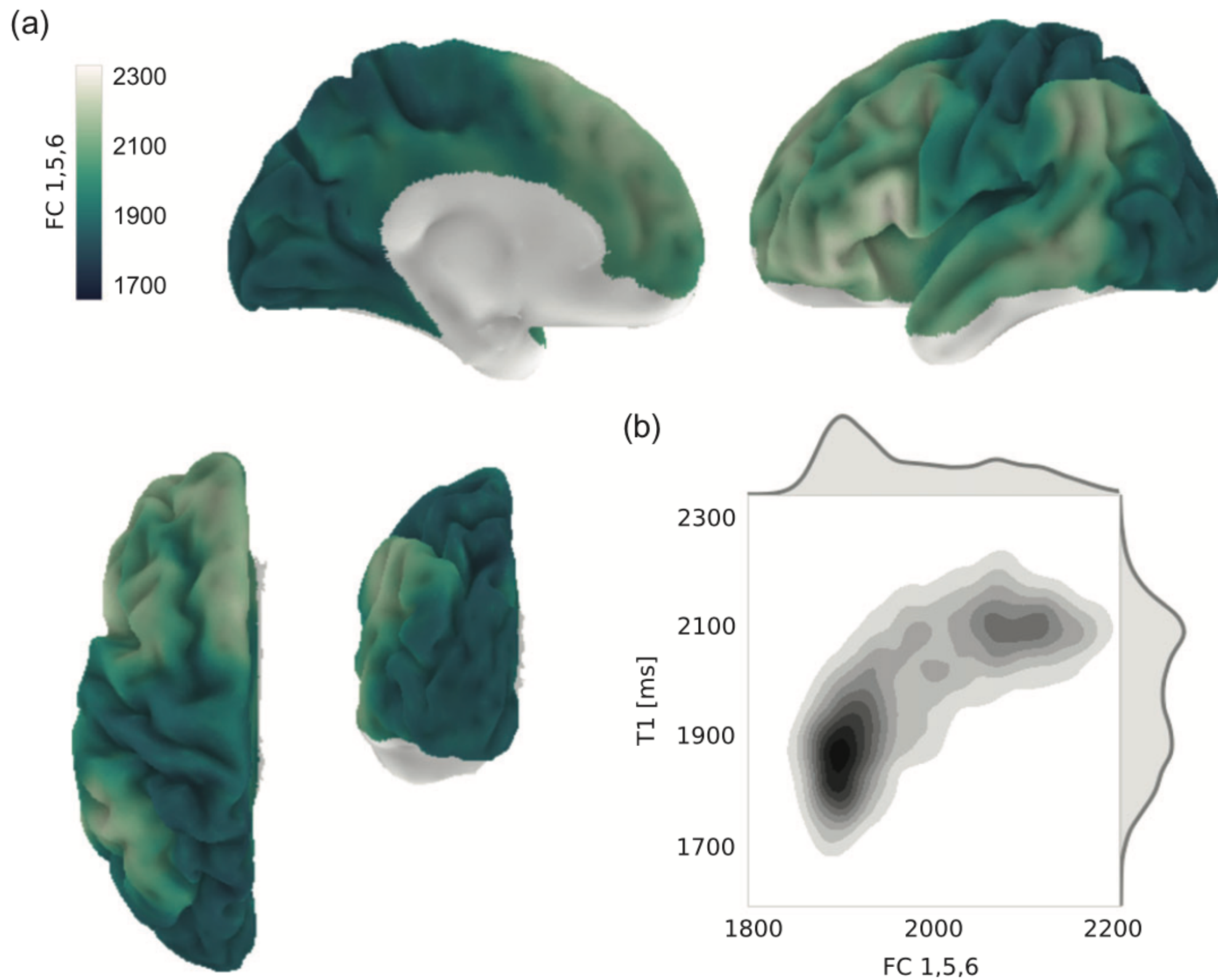
(a)



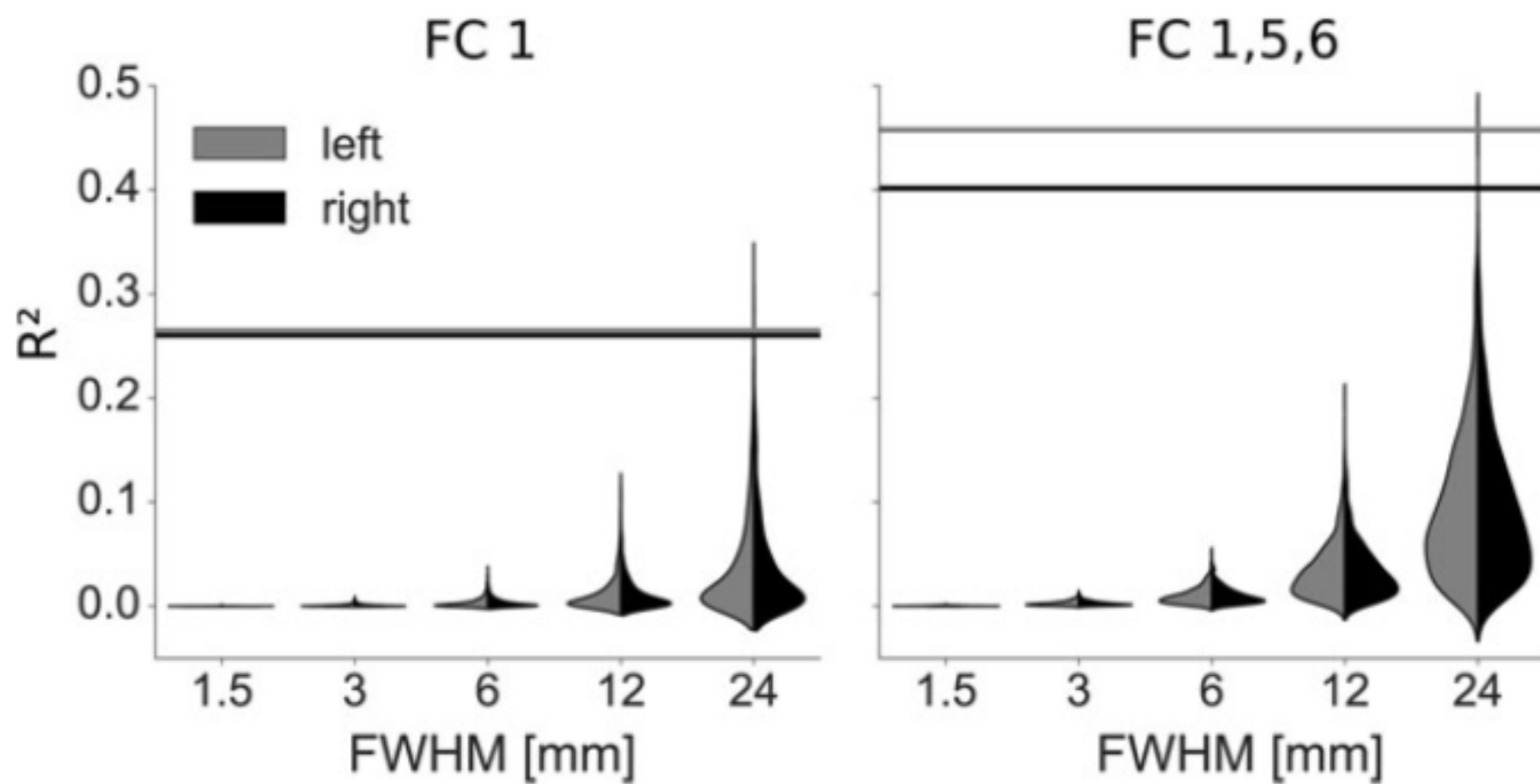
**Figure 4.** Relationship between intracortical  $T_1$  and the principal component of functional connectivity. (a) Intracortical  $T_1$  (top row and left column of bottom row) and the principal component of functional connectivity decomposition (FC1, middle row and right column of bottom row) are shown on the surface of the left hemisphere. Nodes with low signal quality in either imaging modality were excluded from the analysis. The surface plots for the right hemisphere are highly comparable and are shown in Supplementary Figure 5. (b) Bivariate distribution of FC1 and  $T_1$  values across both hemispheres.



**Figure 5.** Using multiple connectivity components to fit intracortical  $T_1$ . (a) Variance in the connectivity transition matrix  $\mathbf{M}$  explained by the different embedding components. (b) BIC values of the best performing model by number of components employed. The best model (FC1, 5, 6) is highlighted in red. (c) Connectivity components FC5 (top row) and FC6 (bottom row), together with FC1 constituting the best performing model, are shown on the left (L) and right (R) hemisphere of the group average surface. Values indicate the relative position of a given surface node along the respective component and have no unit. Nodes with low signal quality in either imaging modality were excluded from the analysis.

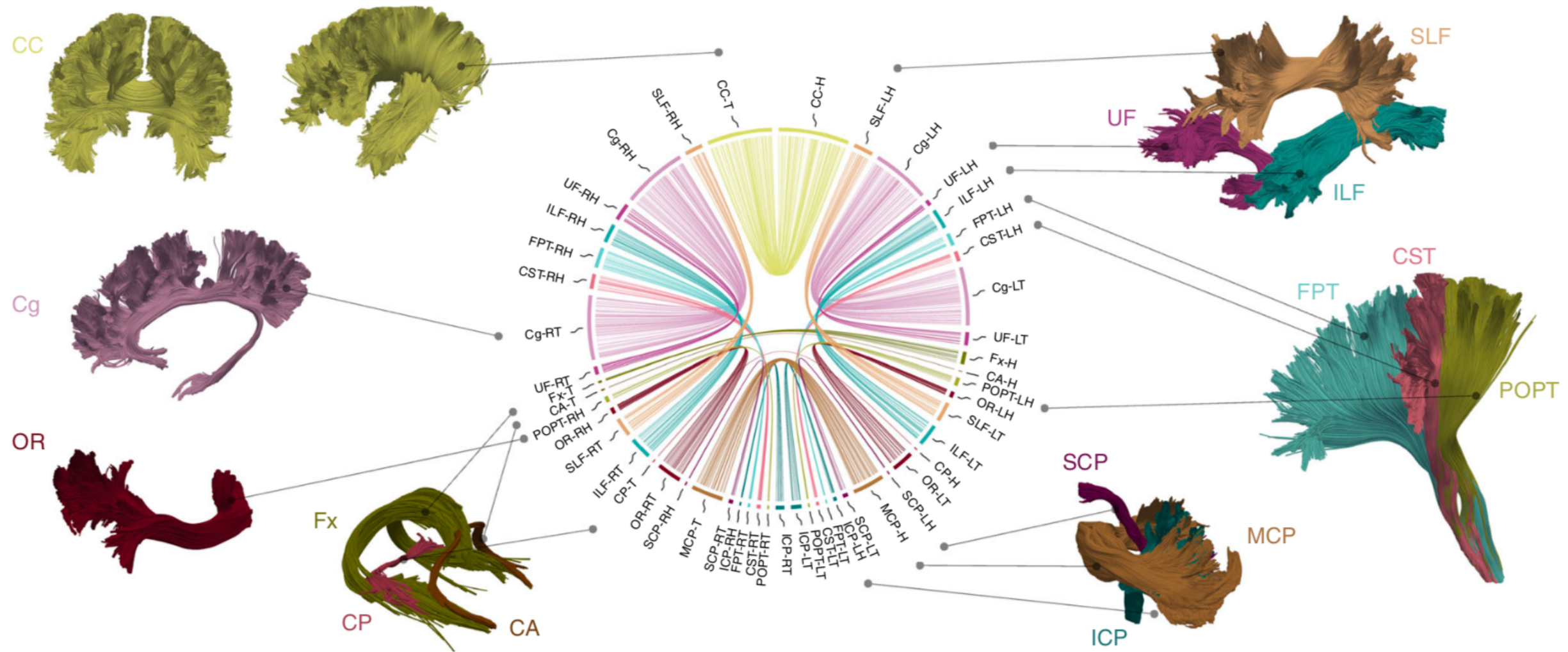
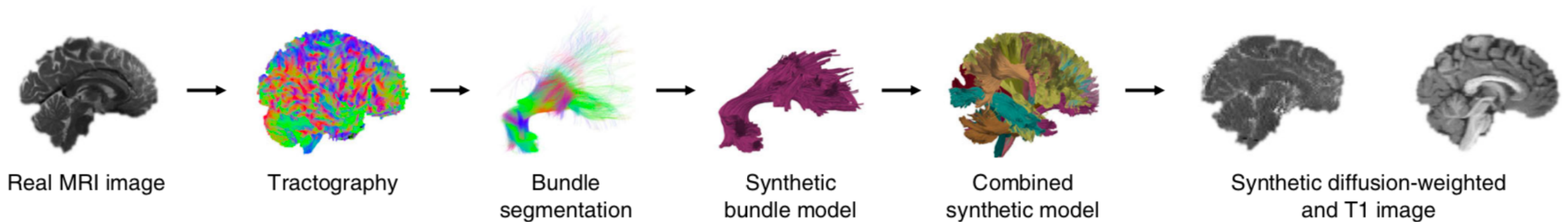


**Figure 6.** Combination of connectivity components providing the best fit to intracortical  $T_1$ . (a) Result of modeling  $T_1$  as a linear combination of connectivity components FC 1, 5, and 6, shown on the left hemisphere. Nodes with low signal quality in either imaging modality were excluded from the analysis. The surface plots for the right hemisphere are highly comparable and are shown in Supplementary Figure 5. (b) Bivariate distribution of modeled and original  $T_1$  values across both hemispheres.



**Figure 7.** Validation of model fit. Random, smoothed data sets were fitted using linear models containing only FC1 (left) or FC1, 5, and 6 (right). The distributions of resulting  $R^2$  values for the left (grey) and right (black) hemisphere are shown as split violin plots. Horizontal lines indicate the values obtained when fitting respective models to the actual map of myelin content (FWHM = 1.5 mm).

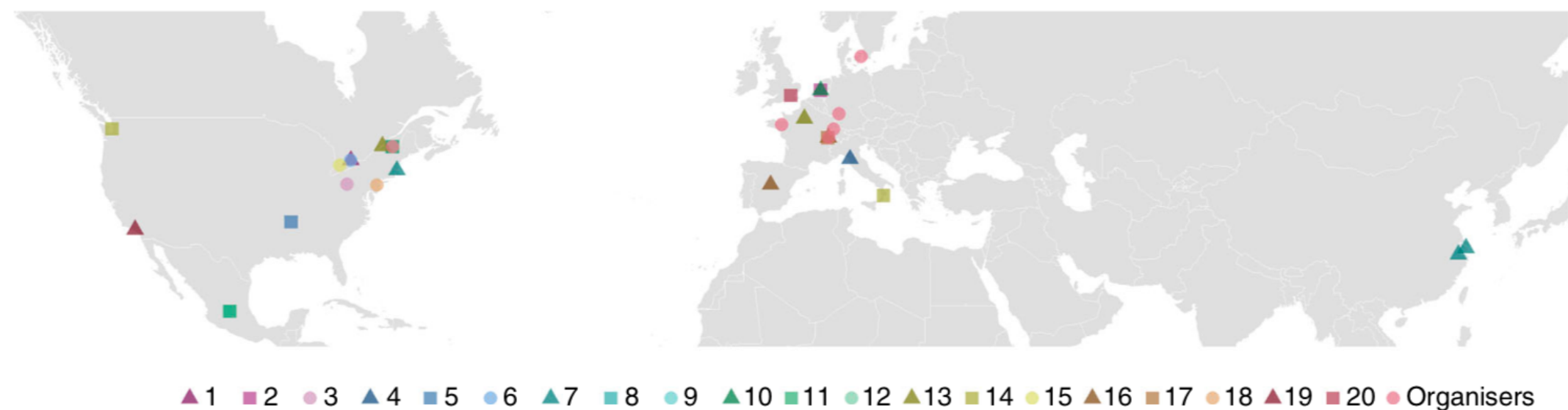
MEYER-KLEIN ET AL. 2018 NAT COMMS



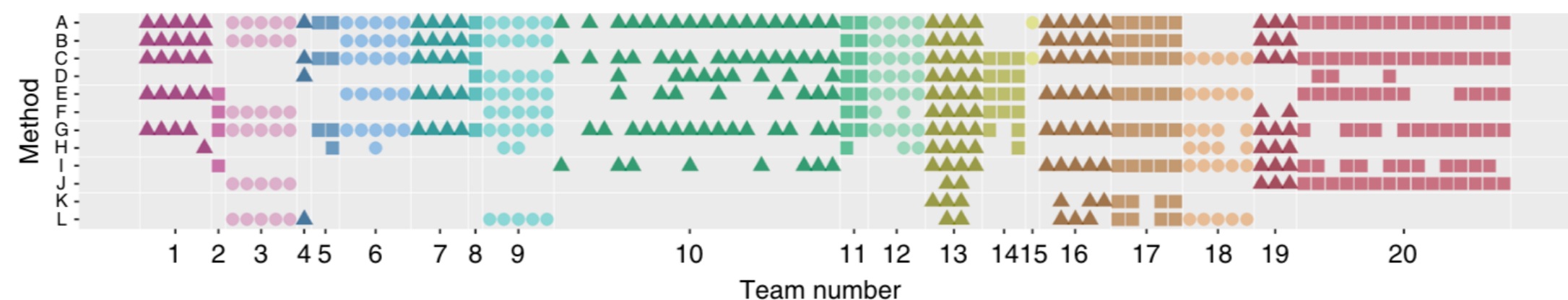
**Fig. 1** Overview of synthetic data set. The top row summarizes the phantom generation process. The simulated images are generated from 25 major bundles, which are shown in the bottom part of the figure. These were manually segmented from a whole-brain tractogram of a HCP subject and include the CC, cingulum (Cg), fornix (Fx), anterior commissure (CA), optic radiation (OR), posterior commissure (CP), inferior cerebellar peduncle (ICP), middle cerebellar peduncle (MCP), superior cerebellar peduncle (SCP), parieto-occipital pontine tract (POPT), cortico-spinal tract (CST), frontopontine tracts (FPT), ILF, UF, and SLF. The connectivity plot in the middle shows the phantom design. The segment positions correspond to the involved endpoint region (from top to bottom: frontal lobe, temporal lobe, parietal lobe, occipital lobe, subcortical region, cerebellum, brain stem). The radial segment length and the connection number in the plot are chosen according to the volume of the respective bundle endpoint region. Abbreviations: right (R) and left (L) hemisphere, head (H) and tail (T) of each respective bundle

**a**

Lab location of teams

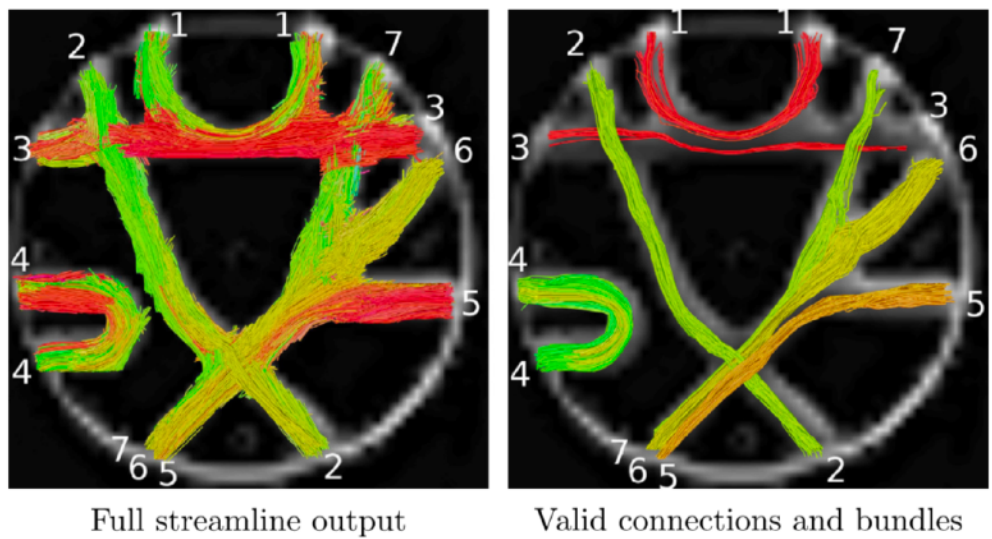
**b**

Pipeline configuration of teams

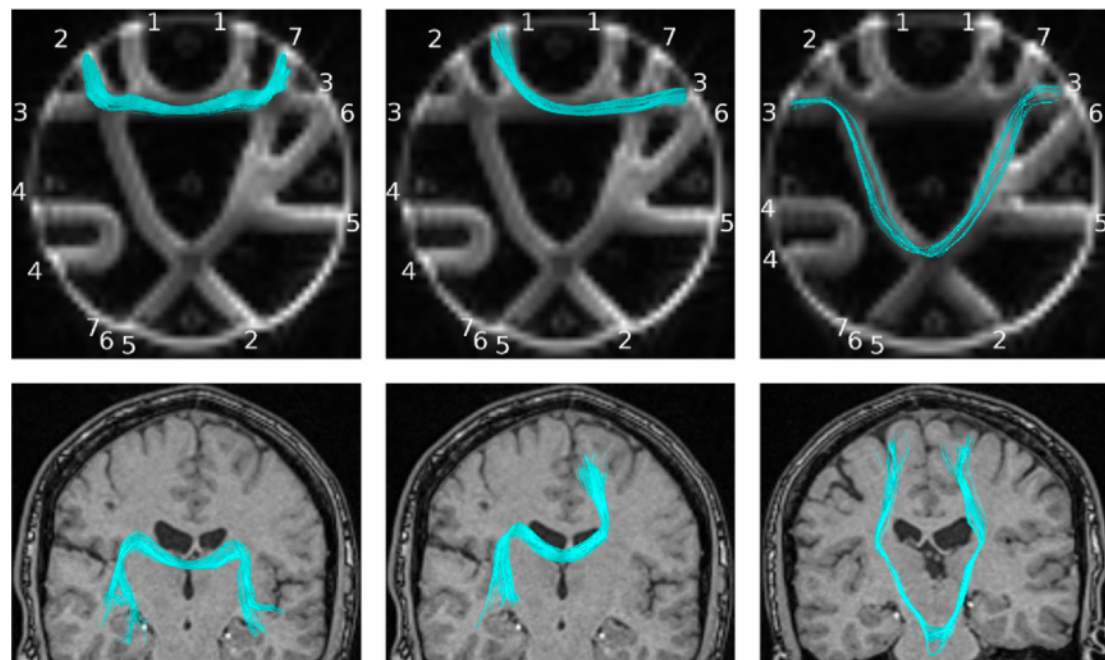


**Fig. 2** Summary of teams and tractography pipeline setups. **a** Location of the teams' affiliated labs. **b** Configuration of the different pipelines used for processing (A: motion correction, B: rotation of b-vectors, C: distortion correction, D: spike correction, E: denoising, F: upsampling, G: diffusion model beyond diffusion tensor imaging (DTI), H: tractography beyond deterministic, I: anatomical priors, J: streamline filtering, K: advanced streamline filtering, L: streamline clustering)

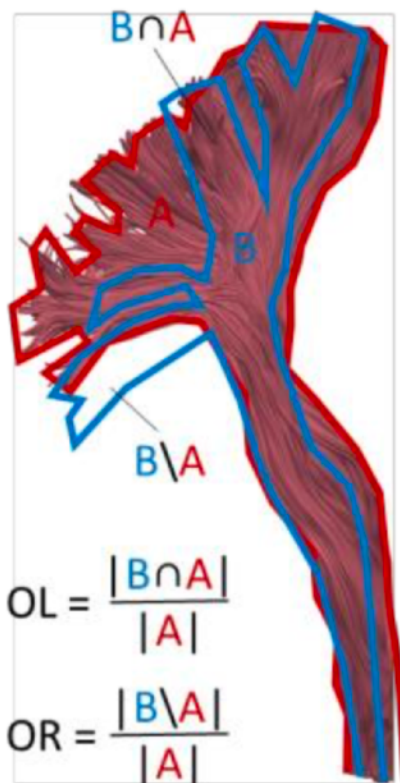
		Ground truth		
		Tract	No tract	
experiment	Tract	True Positives (TP) <b>a</b>	False Positives (FP) <b>b</b> Type 1 error	$\text{PPV} = \frac{\text{TP}}{\text{TP} + \text{FP}}$ Precision
	No tract	<b>c</b> False Negatives (FN) Type 2 error	<b>d</b> True Negatives (TN)	$\text{NPV} = \frac{\text{TN}}{\text{TN} + \text{FN}}$ False omission rate
		<b>Sensitivity</b> $\frac{\text{TP}}{\text{TP} + \text{FN}}$	<b>Specificity</b> $\frac{\text{TN}}{\text{TN} + \text{FP}}$	
Or,		$\frac{\mathbf{a}}{\mathbf{a} + \mathbf{c}}$	$\frac{\mathbf{d}}{\mathbf{d} + \mathbf{b}}$	



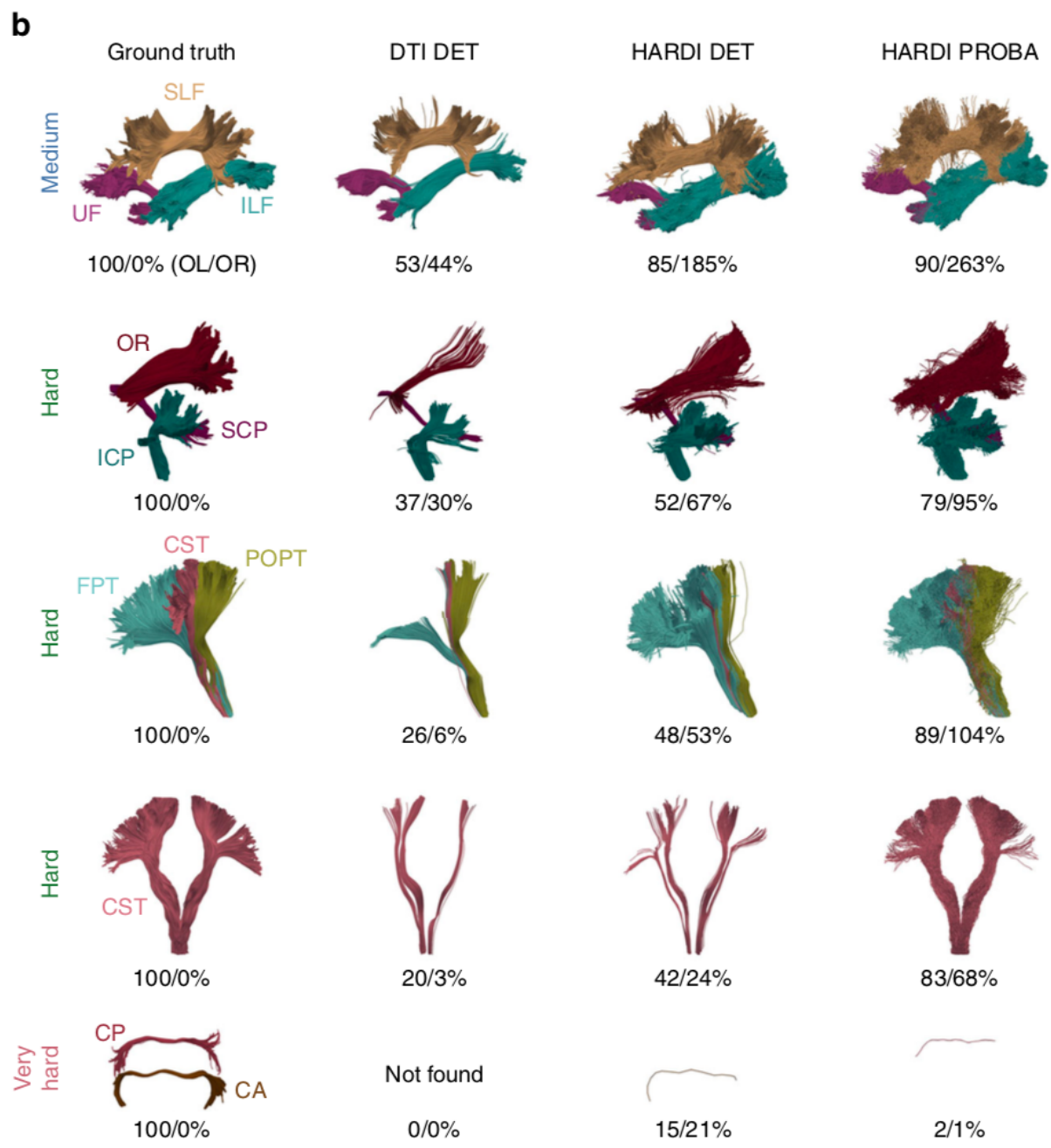
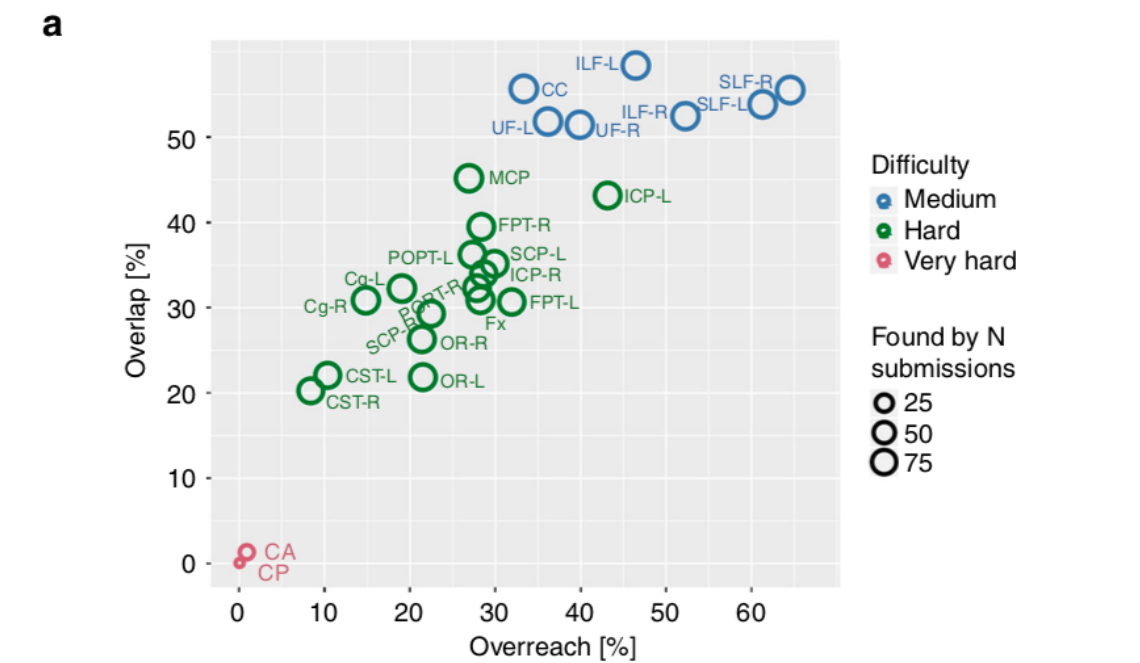
**Fig. 2.** Example of a tractography pipeline output and the resulting valid connections filtered by the ROIs.



**Fig. 3.** Invalid Connections (IC) between 2 ROIs of gray matter on the FiberCup and the real data analogies.



**Supplementary Figure 1.** Schematic illustration of the overlap (OL) and overreach (OR) metrics. OL quantifies the percent overlap of the ground truth bundle A (red) with the evaluated bundle B (blue). OR sets the non-overlapping volume of B into relation with the volume of the ground truth bundle A.



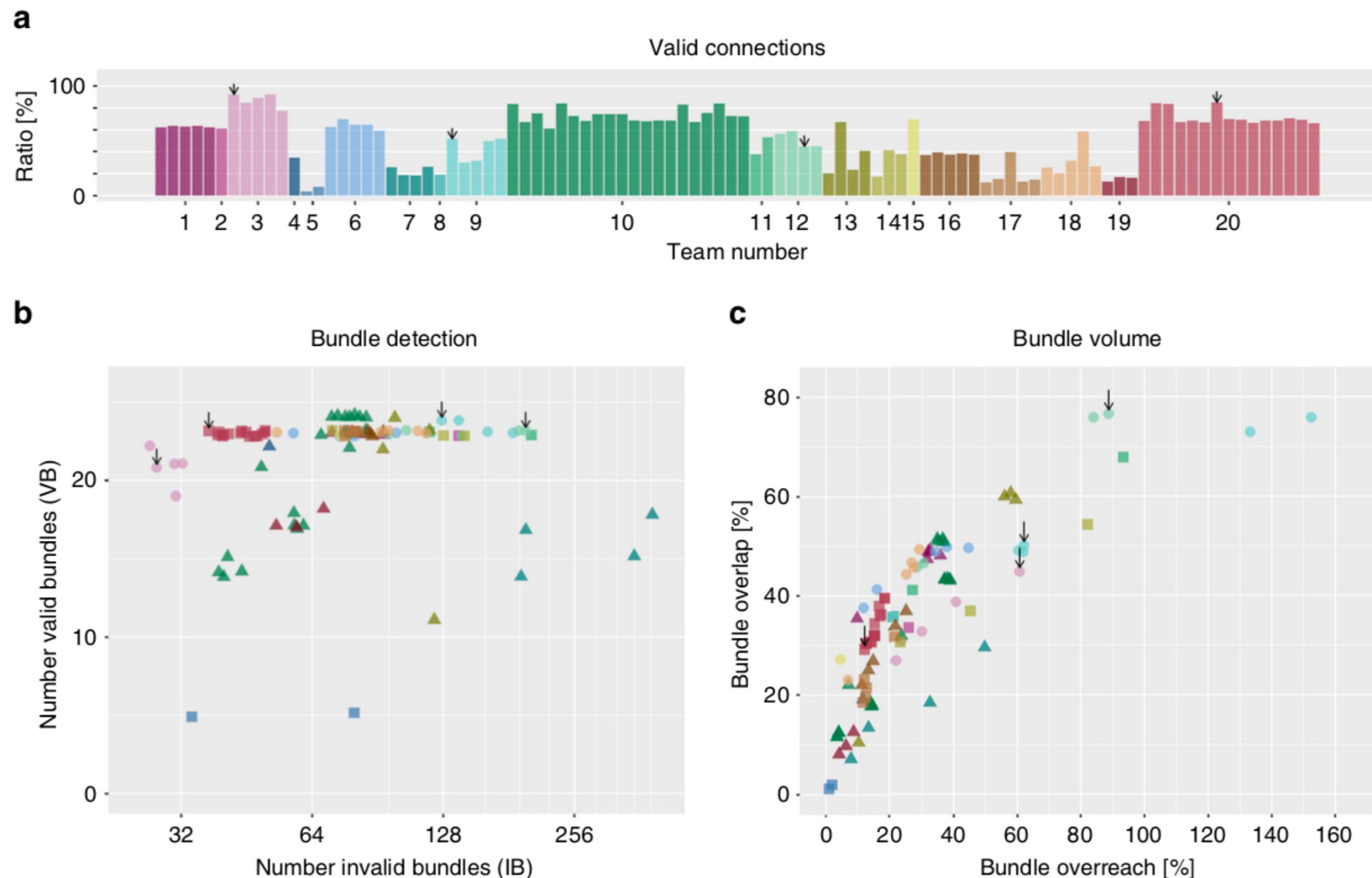


**Fig. 4** Between-group differences in tractography reconstructions of VBs and IBs. Overview of the scores reached by the different teams as **a** percentage of streamlines connecting valid regions, **b** number of detected VBs and IBs (data points are jittered to improve legibility), and **c** volume overlap (OL) and overreach (OR) scores averaged over bundles. Black arrows mark submissions used in the following figures (see Supplementary Note 5 for discussion)

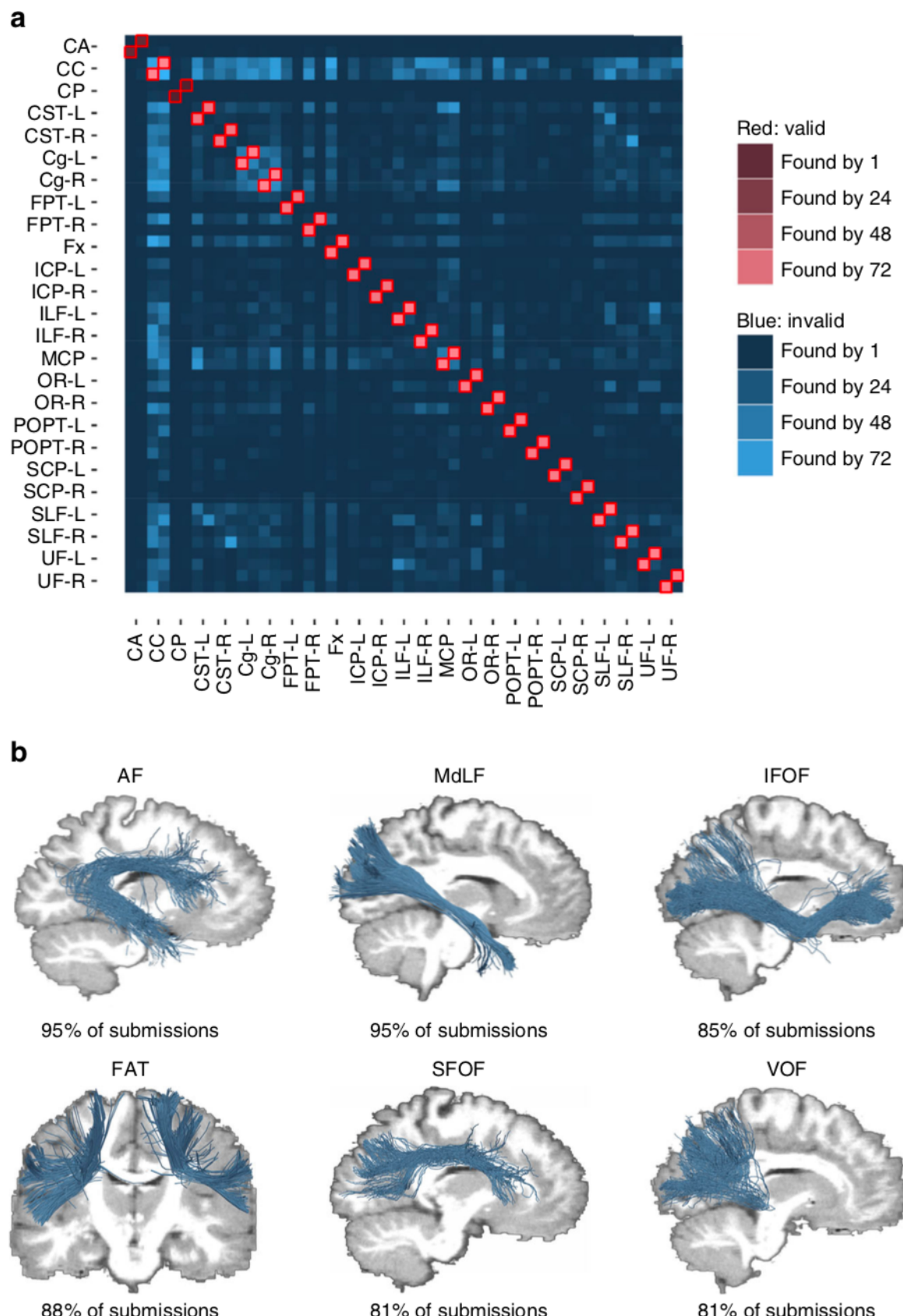


**Fig. 5** Overview of VBs and IBs and examples of invalid streamline clusters. **a** Each entry in the connectivity matrix indicates the number of submissions that have identified the respective bundle. The two rows and columns of each bundle represent the head-endpoint and tail-endpoint regions. The connectivity matrix indicates a high number of existing tracts that were identified by most submissions (red). It also indicates systematic artefactual reconstructions across teams (blue). **b** Examples of IBs that have been consistently identified by more than 80% of the submissions, but do not exist in the ground truth data set. The AF, for example, was generated from ILF and SLF crossing streamlines, whereas the IFOF was generated from by crossing ILF and UF streamlines. The MdLF, FAT, SFOF, and VOF were other examples of highly represented IBs

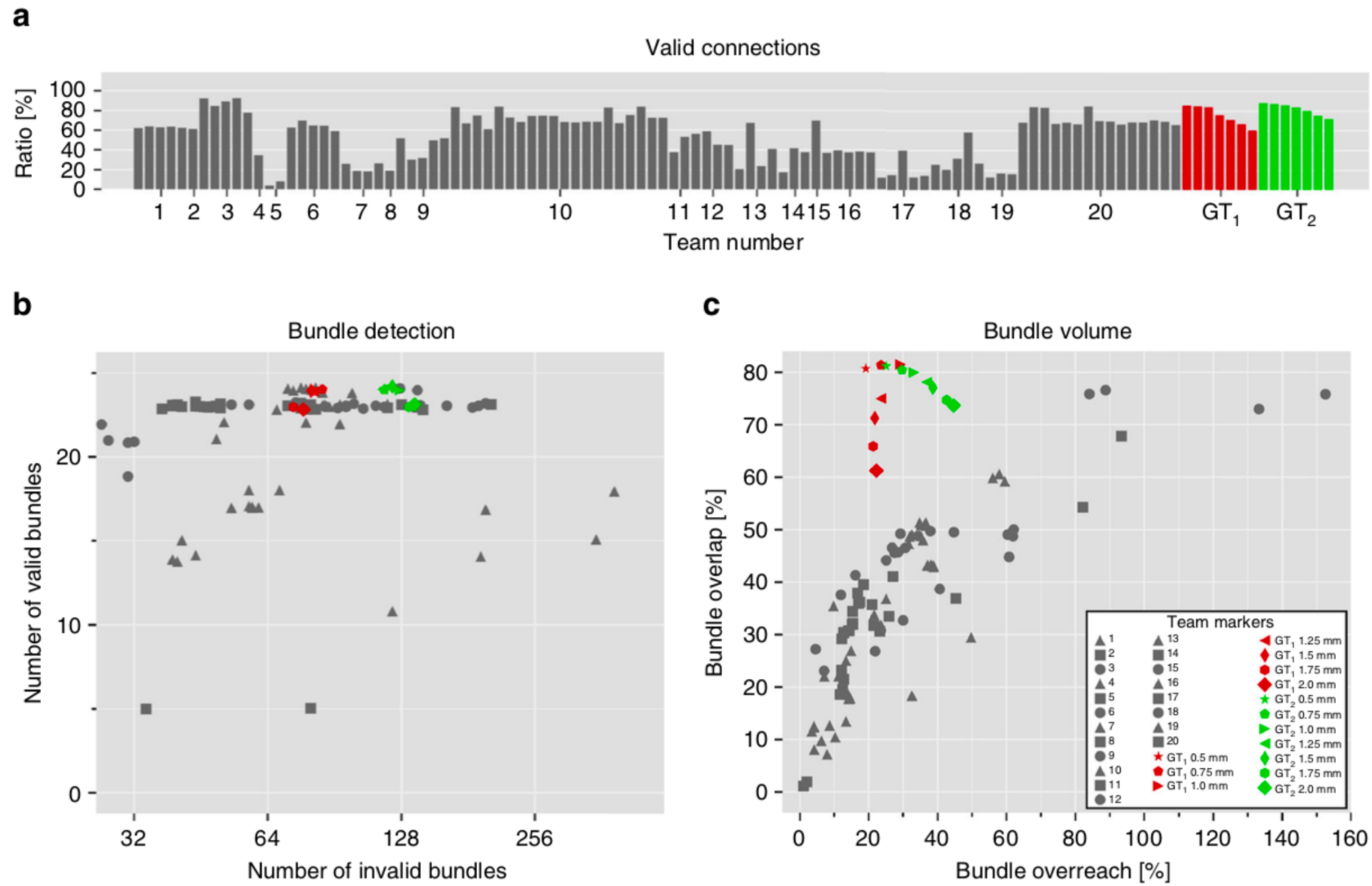


**Fig. 6** Tractography on ground truth directions with no noise still affected by IB problem. We applied deterministic tractography directly to the ground truth vector field with multiple resolutions (2, 1.75, 1.5, 1.25, 1.0, 0.75, and 0.5 mm). Two independent implementations of deterministic tractography methods were used to obtain the results (GT<sub>1</sub> and GT<sub>2</sub>, cf. Supplementary Note 2). **a** Percentage of streamlines connecting valid regions. **b** Number of detected VBs and IBs (data points are jittered to improve legibility). **c** Volume overlap and overreach scores averaged over bundles

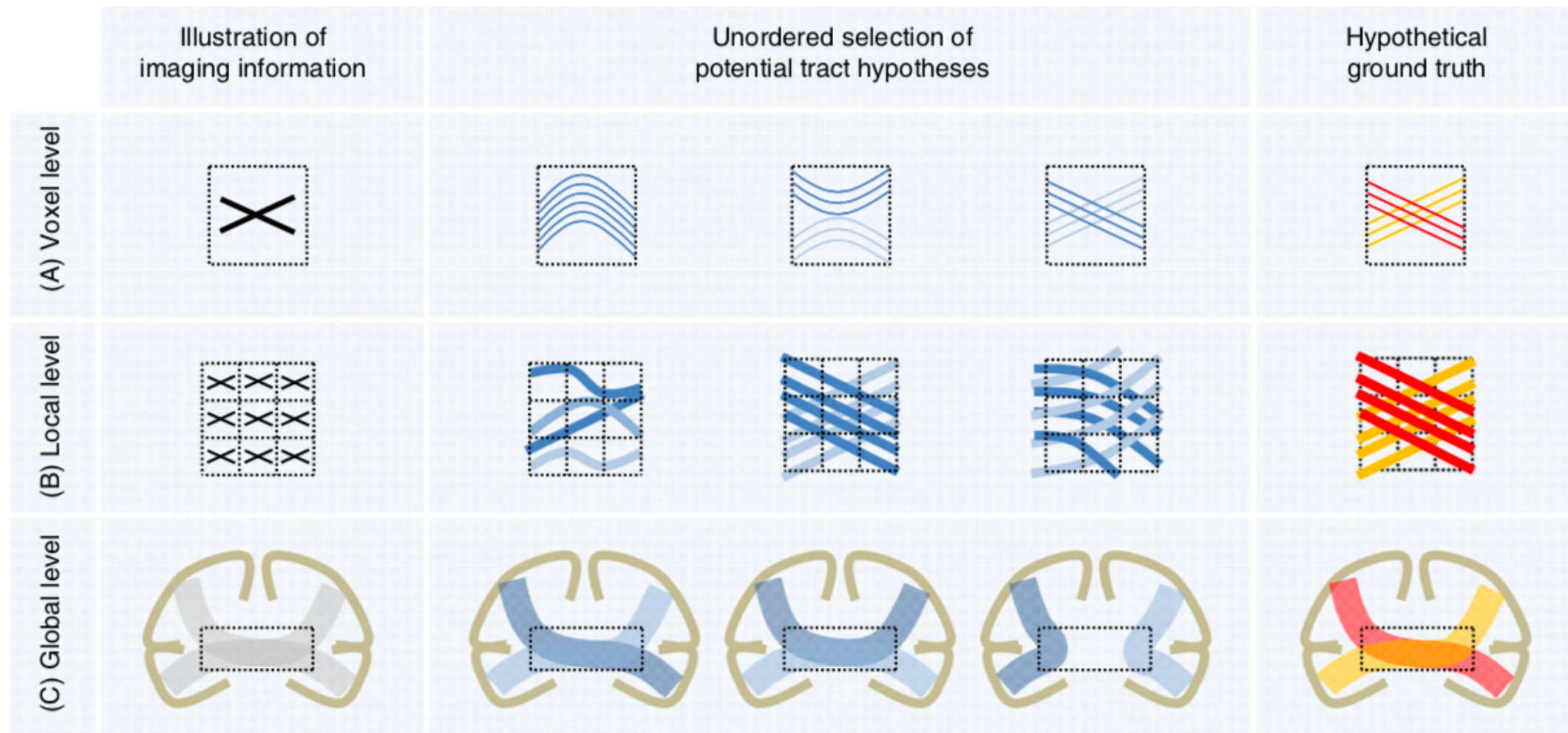


**Fig. 7** Ambiguous correspondences between diffusion directions and fiber geometry. The three illustrations at voxel, local, and global level are used as an example to illustrate the possible ambiguities contained in the diffusion imaging information that may lead to alternative tract reconstructions. (A) The intra-voxel crossing of fibers in the hypothetical ground truth leads to ambiguous imaging information at voxel level<sup>7</sup>. (B) Similarly, the imaging representation of local fiber crossings can be explained by several other configurations<sup>7</sup>. (C) At a global level, white matter regions that are shared by multiple bundles (so-called “bottlenecks”, dotted rectangles)<sup>35</sup> can lead to many spurious tractographic reconstructions<sup>36</sup>. With only two bundles in the hypothetical ground truth (red and yellow bundle), four potential false-positive bundles emerge. Please note that the hypothetical ground truth used in the global-level example is anatomically incorrect as most of the callosal fibers are homotopically distributed (i.e., connect similar regions on both hemispheres)

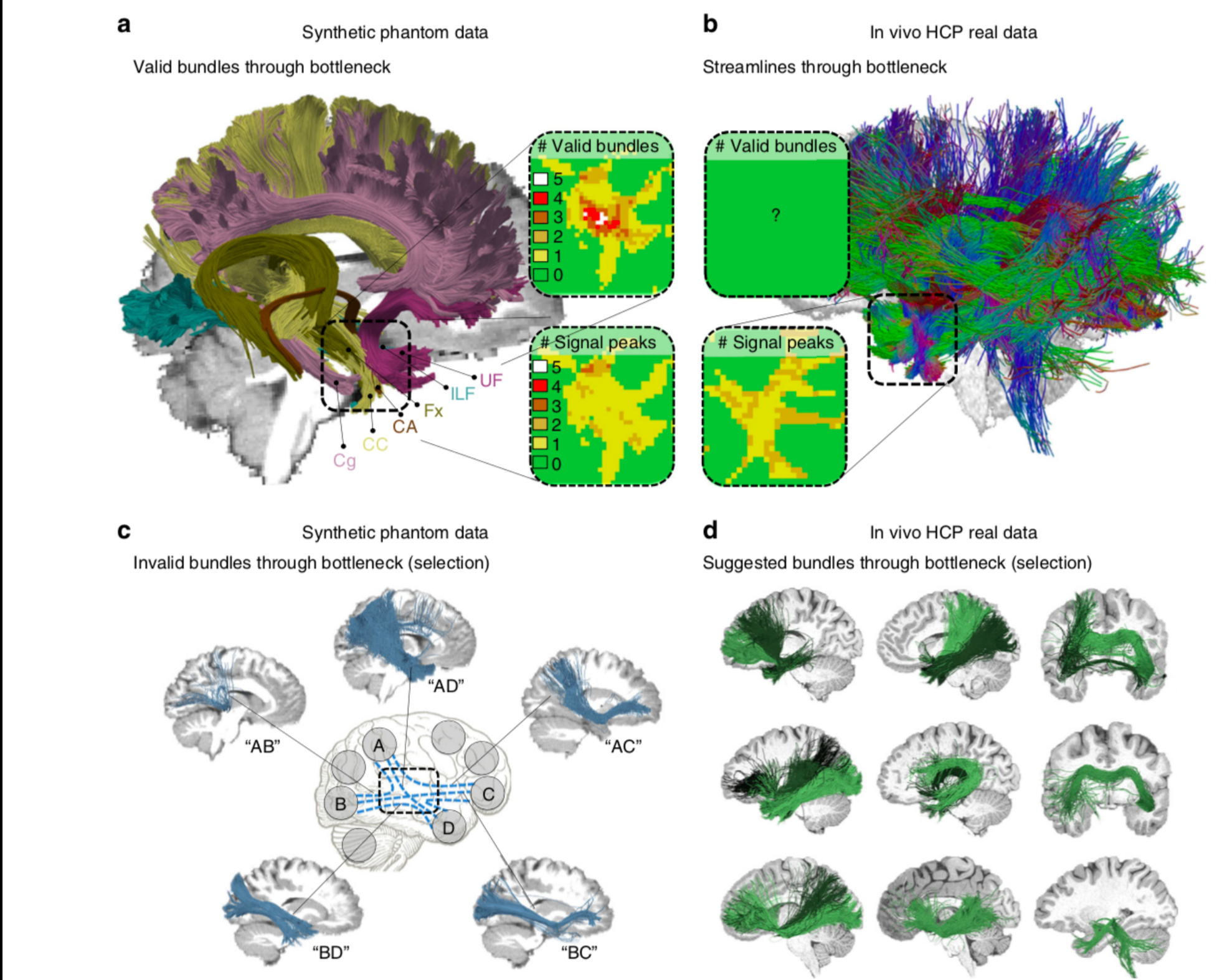


**Fig. 8** Bottlenecks and the fundamental ill-posed nature of tractography. **a** Visualization of six ground truth bundles converging into a nearly parallel funnel in the bottleneck region of the left temporal lobe (indicated by square region). The bundles per voxel (box "# Valid bundles") clearly outnumber the peak directions in the diffusion signal (box "# Signal peaks"). **b** Visualization of streamlines from a HCP in vivo tractogram passing through the same region. **c** Exemplary IBs that have been identified by more than 50% of the submissions, showing that tractography cannot differentiate between the high amount of plausible combinatorial possibilities connecting different endpoint regions (see Supplementary Movie 1). **d** Automatically QuickBundle-clustered streamlines from the in vivo tractogram going through the temporal ROI. The clustered bundles are illustrated in different shades of green. These clusters represent a mixture of true-positive and false-positive bundles going through that bottleneck area of the HCP data set (see Supplementary Movie 2)

**Table 1 Summary of the statistical analysis**

	VC	VB	IB	OL	OR
Motion correction	12% ± 13%	0.3 ± 2.8	-3 ± 38.1	2% ± 12%	7% ± 10%
Rotate b-vecs	-5% ± 14%	-1.2 ± 2.9	20.8 ± 39.6	-6% ± 12%	-8% ± 9%
Distortion correction	-1% ± 13%	-2 ± 2.7	-4 ± 36.8	-2% ± 11%	-11% ± 10%
Spike correction	1% ± 13%	0.9 ± 2.6	4.6 ± 35.2	5% ± 11%	10% ± 9%
Denoising	1% ± 13%	0.6 ± 2.6	3.2 ± 35.2	3% ± 11%	12% ± 9%
Upsampling	1% ± 13%	0.2 ± 2.7	9.3 ± 36.4	4% ± 11%	11% ± 9%
Beyond DTI	-12% ± 13%	2.2 ± 2.6	21.5 ± 35.2	13% ± 11%	15% ± 9%
Beyond deterministic	-10% ± 13%	-0.3 ± 2.6	41 ± 35.3	12% ± 11%	17% ± 9%
Anatomical priors	1% ± 13%	-3.8 ± 2.6	-11.6 ± 35.2	-15% ± 11%	-16% ± 9%
Streamline filtering	21% ± 13%	2.9 ± 2.8	-41.6 ± 38.1	8% ± 12%	-4% ± 9%
Adv. streamline filtering	-11% ± 13%	2.8 ± 2.7	0.9 ± 36.5	11% ± 11%	4% ± 10%
Clustering	-3% ± 13%	0.2 ± 2.7	-1.1 ± 36.4	-4% ± 11%	2% ± 9%

Green cells indicate a significant positive influence ( $p < 0.05$ ) and red cells indicate a significant negative impact ( $p < 0.05$ ). Numbers indicate the estimated mean effect on the metric and its standard deviation. The first column of the table represents the different parts of the processing pipeline that we have grouped into categories. The other columns represent the metrics: VC valid connections, VB valid bundles, IB invalid bundles, OL overlap, OR overreach

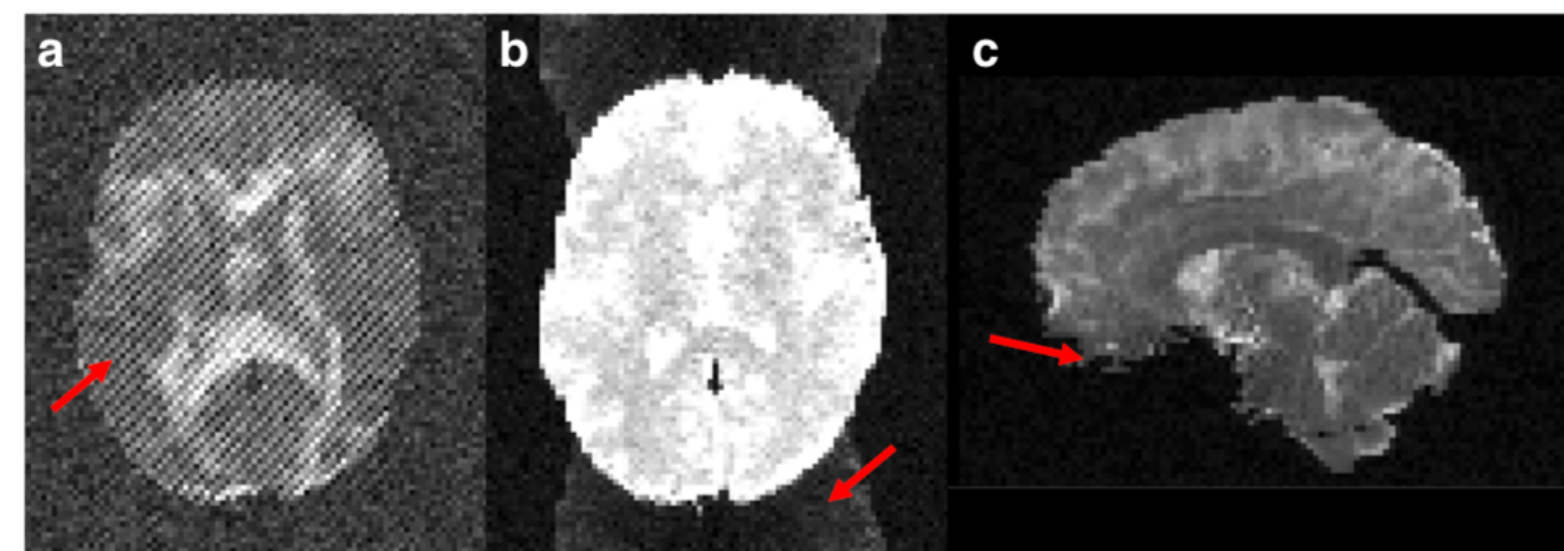


**Fig. 9** Illustration of artifacts included in the synthetic data set. Exemplary illustration of the spike (a), N/2 ghost (b), and distortion artifacts (c) contained in the final diffusion-weighted data set. Supplementary Movie 3 gives an impression of the complete synthetic data set provided